UNIVERSITÀ DEGLI STUDI
DI TRENTO

DEPARTMENT OF INFORMATION ENGINEERING AND COMPUTER SCIENCE
ICT International Doctoral School

Exploring the interplay between the human brain and the mind: a complex systems approach

Barbara Benigni

Advisor

Prof. Manlio De Domenico

Università degli Studi di Padova

Fondazione Bruno Kessler

Co-Advisor

Prof. Stefano Merler

Fondazione Bruno Kessler

June 2022

Abstract

The understanding of human brain mechanisms has captured the imagination of scientists for ages. From the quantitative perspective, there is evidence that damages to brain structure affect brain function and, as a consequence, cognitive aspects. As there is evidence that brain structure might be affected by altered cognition. However, the complex interplay between the human brain and the mind remains still poorly understood. This fact has important clinical consequences, limiting applications devoted to the prevention and treatment of brain diseases. In the present thesis, we aim to enhance our understanding of human brain mechanisms by means of an integrated and data-driven approach, by adopting a systemic perspective and leveraging on tools from computational and network neuroscience. We successfully enhance the state of the art of computational neuroscience in several manners. Firstly, we inspect human cognition by focusing on the geometric exploration of concepts in the human mind to build new data-driven metrics to complement the neurological assessment and to confirm Alzheimer's disease diagnosis. We formalize a new stochastic process, the potential-driven random walk, able to model the trade-off between exploitation and exploration of network structure, by accounting for local and global information, providing a flexible tool to span from random walk to shortest-path based navigation. Probing the interplay between brain structure and dynamics by means of its Von Neumann entropy, we develop a new framework for the multiscale analysis of the human connectome, which is effective for discerning between healthy conditions and Alzheimer's disease. Finally, by integrating data from the human brain structural connectivity, its functional response errors as measured by Direct Electrical Stimulation and semantic selectivity, we propose a new procedure for mapping the human brain triadic nature, thus providing a model-oriented bridge between

the human brain and mind. Besides shedding more light on human brain functioning, our findings offer original and promising clues to develop integrated biomarkers for Alzheimer's disease detection, with the potential of extension for applications to other neurodegenerative diseases and psychiatric disorders.

Keywords [Complex systems, Computational neuroscience, Network neuroscience, Alzheimer's disease]

Acknowledgments

Every doctoral path is a unique journey. To me, these have been challenging years on both the professional and personal side. Several times I had the feeling of having lost my way, but now I can peacefully confirm that only "when it is dark enough, you can see the stars". I couldn't have seen these stars without all the invaluable people that have walked by me during my unforgettable journey.

Professionally, the first I would like to thank is my Supervisor, Prof. Manlio De Domenico, he has been the giant on whose shoulders I was dwarf, for real. He has always encouraged and believed in me from the very beginning. He has never been afraid to spend his time discussing with me on our findings and possible new ideas, even lively but always finalized to improve the quality of my research activity: thanks for the endless energy and patience. Besides his unbridled passion for the scientific research, Prof. Manlio De Domenico has transmitted to me his personal approach to problem solving and his successful rules on how to share and spread a new idea around the world. These have been probably the greatest soft skills learned during my Ph.D. Finally and mostly, I want to thank Prof. M. De Domenico for not having been the "boss" but the *primus inter pares* of his research Lab, the CoMuNe Lab, where I had the honor of being hosted.

Together with my Supervisor, I would like to thank my Co-Advisor, Stefano Merler, although very committed to his researches and to his collaboration with the national health agency due to COVID-19, his co-advisory has always been timely, pragmatic and precious. A special thanks goes also to Monica Dallabona, neuropsychologist of the Azienda Provinciale per i Servizi Sanitari (APSS) in Trento, for our genuine and fruitful collaboration.

A sincere thanks is for Prof. Jordi Soriano-Fradera and Prof. Daniele Marinazzo who reviewed this work, dedicating me their precious time and providing me with insightful comments.

Of course, I can not miss to thank all the "CoMuNers": Giulia, Valeria, Oriol, Riccardo, Arsham, Sebastiano, Nicola and Sebastian. They were not just colleagues, who offered me invaluable advices and time, but friends and I am sure our research fraternity will last forever.

Here I would like to mention also the "Catalans", a kind of Spanish side of the "CoMuNers", supervised by the uniquely sparkling Prof. Alex Arenas. A heartfelt thanks goes to Benjamin, Lluís and Giulio, international conferences would not have been the same without them. In the same vein, I just want to thank all those people that I met in Salina island – where I had the opportunity to attend a dreamy school on Complex Systems – such as Gabriele, Blas and Kim.

On the personal side, the greatest thanks go to my mother, Caterina, and to my father, Andrea, simply for their existence and for being the most important people of my life. Without their infinite love, support and the proper education, I would have never been able to undertake a Ph.D. career. Of course, a heartfelt thanks is also for the rest of my family.

I can never thank enough all my friends, from Bergamo, from Polimi, from Fondazione Bruno Kessler, from Trento and from around the world, to be among the most precious treasures of this life and for always holding my hands, even from miles away.

A virtual thanks is for Pier Giorgio Caselli, for his meditations towards the *knowledge of self* and for the esoteric lectures which have contributed to open my mind towards a possible dialogue between science and spirit. Also, I would like to thank Bonobo and Thievery Corporation, their music has inspired me to write tons of words during my Ph.D. journey.

I would like to acknowledge the immeasurable value of the Trentino's

mountains, the Dolomites and the alpine lakes – especially il lago di Lamar – that together have contributed to recharge my soul, making me gain balance and calm during my years spent in Trento. A existential thanks is for The Horse in the Vine, for being there at the right moment and for being my certainty when I was on the bus.

Finally, my thanks goes to Sebastian, who has been my special person during these years, always by my side and more than just a colleague in this adventure. With him I have always shared the passion for complex systems and together we dream about a *New Renaissance*, as he likes to define it. Sebastian's genius, flow and love have shaken me up but also supported and lulled me during these years, taking me closer to a renewed and deep awareness on the Universe we are living in.

I am full of gratitude to all people and natural entities mentioned here.

To the collective consciousness,
eventually emerging from this universe

Contents

List of Tables

List of Figures

Chapter 1

Introduction

How does the brain work? This is probably one of the most fascinating – still unsolved – issues human beings have been facing for long. Coupling with this wondering, a further more unrevealed issue arises: how do brain architecture and activity concur in creating the mind? And finally, is it possible to answer these questions with current tools from neuroscience?

While keeping the curiosity of scholars from several fields alive, a complete knowledge on the brain-mind interplay still eludes us, posing serious challenges in both the scientific and clinical field. Particularly, the unawareness on this matter prevents us from identifying neurodegenerative diseases or psychiatric disorders on time, with obvious limitations to prevention and treatment thereof.

In this thesis, we approach the human brain functioning, and its underlying mechanisms giving rise to the mind, from the core framework of computational neuroscience. Specifically, we will consider the brain as a complex system and by leveraging on tools from network neuroscience – a field at the edge of computational neuroscience and network science – we aim to enhance our understanding of human brain in a more integrated, mathematical and data-driven manner. Hence, we provide potentially important implications for brain diseases, especially the neurodegenerative

one of Alzheimer, which constitutes the motivation and the case study of our work.

In this sense, conceptual and mathematical principles from network neuroscience will be our guides along the journey of this thesis, towards a systemic understanding of the human brain and mind. Such a journey will begin with the analysis of cognitive capacities in both healthy and non-healthy brains. Specifically, we will show how the exploration of concepts in the human mind unravels its plausible latent geometry. In this first stage, neuropsychological data and concepts expressed by human beings will be our fuel, geometry and network science our means of transport. The trade-off between exploitation of what is known and exploration of what is unknown in space and mind will lead us to more theoretical lands where we formulate a new stochastic process for routing strategies: the potential-driven random walk. Our journey will continue in the direction of information theory. By considering the persistence of information flow, we will provide a multiscale characterization of both healthy and non-healthy brains. As the ultimate goal, according to a complex system perspective, we will define a new framework for bridging between the physical brain and the human mind.

In the next sections of this opening chapter, we provide the readers with the main ingredients to understand the research activity conducted during these doctoral years. To facilitate the lecture, this introduction is divided following the rule of 5 Ws, replacing when with how. Like in any respectable story, *Who* is the protagonist, *Why* is the reason motivating the story, *Where* defines the context, *What* is what the story is about, and *How* are the tools to understand the whole story.

In Sec.1.1, we define the subject (*Who*), the macro context (*Where*) and the motivation (*Why*) of the thesis. Specifically, *Who* is the human brain. *Where* is computational neuroscience, which constitutes the positioning of

this thesis in the study of human brain and mind and in the main research areas of ICT. *Why* constitutes the motivation of our work, i.e. the burden of Alzheimer's disease.

In Sec.1.2, we introduce the complexity paradigm, a successful cutting-edge framework to unravel human brain complex mechanisms, including the emergence of the mind. Finally, we describe network science as the proper manner to model the human brain when regarded as a complex system (*What*), and the relatively new research field of Network Neuroscience (*How*).

In Sec.1.3, we conclude the chapter with the thesis overview, highlighting, point by point, the innovative aspects of our work for each tackled issue.

1.1 Context and motivation

In this section, we introduce the essential notions about the human brain, the real protagonist of our research, then the motivation of our work and finally, its positioning in the context of computational neuroscience.

1.1.1 Who: The human brain

The human brain, and its complexity, are the main protagonists of this thesis. The brain is probably the most complex organ of human body. It is the control center of sensory response, motor skills, breathing, temperature, hunger, memory, thoughts, emotions and every process that regulates our being. Anatomically, the brain is divided in two hemispheres, and each hemisphere has four lobes (frontal, parietal, occipital and temporal). Normally, a healthy brain has about 100 billion neurons along with 100 trillion synapses. These latter enable the signaling throughout the neuronal circuits of the brain, forming the cellular basis of the entire realm of human

activities, from movement to emotions and memories [23]. It is interesting to notice that the number of brain cells does not considerably change in a lifespan, remaining almost the same in children and adults [102] since it is super rare for neurogenesis to continue during adulthood [258]. Therefore, what distinguishes the abilities of children from those of adults is not in the number of neurons itself, but it is mostly determined by *how* these cells are connected with each other [102]. Thus, the secret of human brain firstly lies in its *connections*. At the time of birth, the brain network is sparse with neurons largely unconnected. During the first two years of life, brain cells start connecting rapidly, reaching one hundred trillion synapses, double than the ones of an adult [102]. At the end of age two, we have a peak in the number of human synapses and the strategic "neural pruning" begins. In this way, only connections that are actively used in brain circuits are maintained, and the rest is eventually discarded [102]. Our brain connections will dynamically modify for the whole lifetime, with synapses changing their pattern according to the external conditions, but also to learn new skills and to recover from brain injuries. This dynamical modification of neuronal patterns is possible because of a phenomenon known as neuroplasticity [173, 219]. This means, for example, that brain routing strategies are flexible and not fixed to one optimal path [218]. Thanks to this flexibility, pattern of cortical activation can change over time allowing for new skills and abilities to be learnt. This aspect will be considered in chapter 3, where neuroplasticity is taken as one of the real world scenario representing the result of a particular routing strategy, *driven* by some external factors. Specifically, we will see how to define a (new) stochastic process to model such a kind of routing strategies, fundamentally driven by the objective of minimizing distances but also by exogenous conditions.

The human brain has a complex multiscale organization, in both spatial and temporal domain [38]. In fact, the brain exhibits a spatial and

temporal scaling, or in other words, a peculiar organizational principle or phenomenon across multiple resolutions. In the spatial domain, the scaling principles include a heterogeneous and hierarchical organization of brain components coupled with a sparse connection pattern [142, 34]. This means that not only the spatial distribution of components is heterogeneous but also their connectivity pattern. In addition, within each scale, the structure is organized into modules [38]. Topologically, a module is defined as a group of highly interconnected components which are poorly connected to the components in other modules. Such an organization guarantees robustness, adaptivity and evolvability to the brain networks and is crucial for the global communication within the entire brain cortex [195]. For what concerns temporal scaling, the brain dynamically changes its organization over time enabling different cognitive functions and capacities [6]. Such a complex evolving structure gives rise to elaborate neuronal phenomena which are the physical and biological fundamentals of cognition [38]. In chapter 4, we will present a new way to characterize the multiscale nature of human brain from an information-theoretic perspective, by providing a new framework based on spectral entropy.

One of the main mysteries of human brain, crucial for our research, is how the apparently static neuronal anatomy – and its architecture – gives rise to functional activities, enabling, in turn, a myriad of vital tasks from the most automatic actions and reactions to perception, and ultimately cognition [217].

In this thesis, we attempt to make a step further towards a possible mapping of such a mystery, using a systemic perspective and by leveraging on powerful tools from networks science. In the next section of this chapter (Sec.1.2), we present the paradigm shift needed to address the brain complexity issue and the formal approaches to tackle the inner relation between brain structure, function and mind. Specifically, we will benefit

from the new paradigm of complexity science to investigate cognition in healthy and non-healthy brains, for example by focusing on the exploration of concepts within the human mind (in chapter 2). Finally, as the ultimate goal of this thesis, we will provide a new framework for coupling structural brain networks with functional brain areas and cognitive semantic tiles, thus providing a novel promising way for bridging the triadic nature of the human brain (in chapter 5).

1.1.2 Why: The burden of Alzheimer's disease

Alzheimer' disease represents the motivation of the present research. In the following lines, we give an overview of Alzheimer's disease, highlighting the global magnitude of this burden.

In the last decades, extraordinary successes in medicine together with the socio-economic development all over the world have fostered a global rising in life expectancy. While the ageing of population represents a significant achievement in science and healthcare, it also presents new important challenges, that need to be addressed by the society. Such challenges include direct and indirect public ageing costs, which in the euro area are projected to increase by 28.2% of GDP in 2040 [205]. Along with the cost increase due to rising longevity, new priorities have emerged for the global public health [269]. First of all, the need to reduce the significant increase in mortality due to non-communicable diseases (NCD), i.e. diseases that are not directly transmissible from person to person [159, 301]. Reducing premature mortality due to non-communicable diseases has become imperative in global development policies, to the point that in 2015 United Nations General Assembly included precisely this issue in the Sustainable Development Goal (SDG) 3.4, as shown in Fig.1.1 [210].

Furthermore, this goal will have a drop-down role for the success of other SDGs such as the reduction of poverty, the improvement of work quality

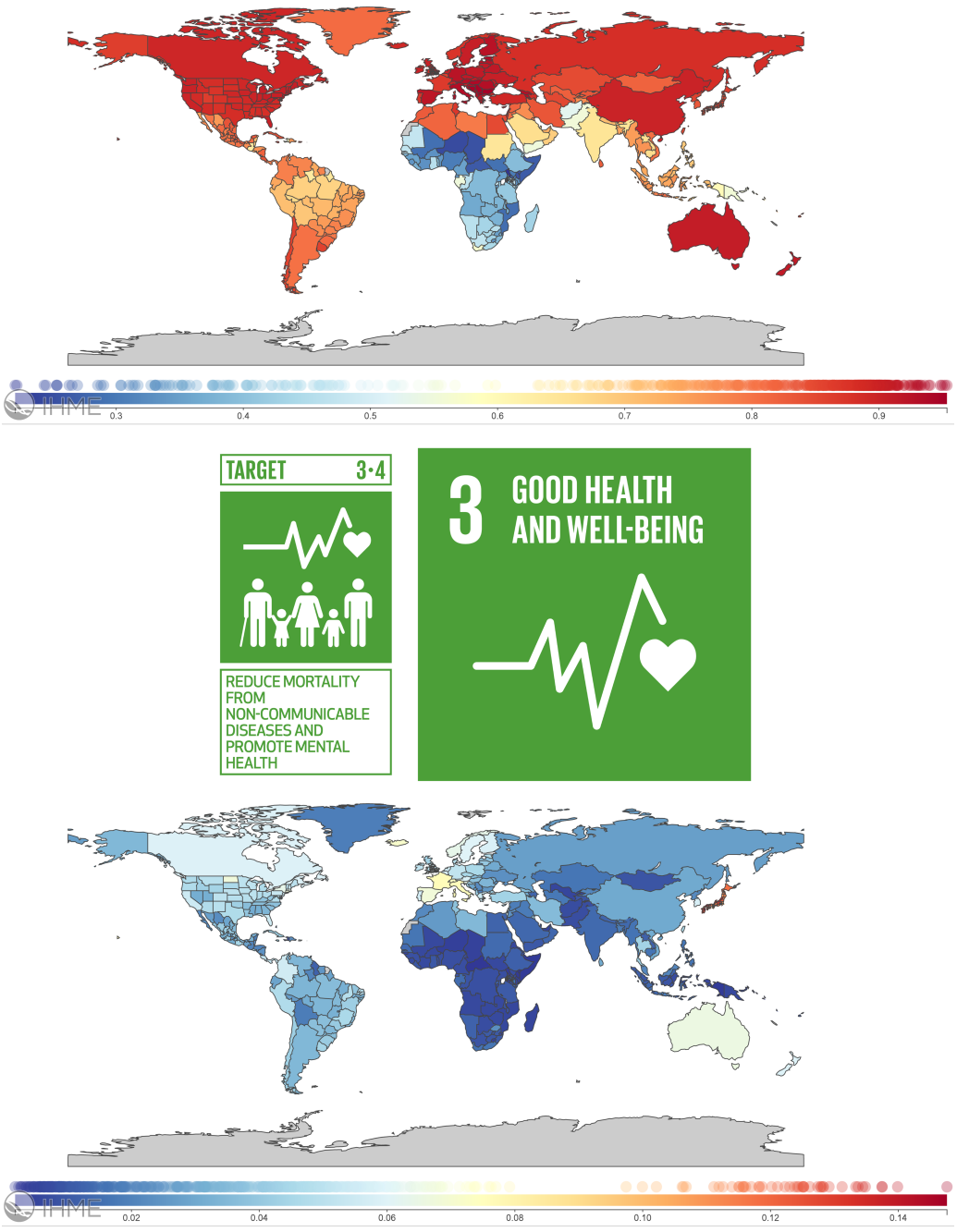

Figure 1.1: **SDG 3.4 and non-communicable diseases.** Top plot: percent of total deaths in 2019 due to non-communicable diseases (both sexes, all ages); bottom plot: percent of total deaths in 2019 due to Alzheimer's diseases and other dementias (both sexes, all ages). Figure composed from https://vizhub.healthdata.org/gbd-compare/ and https://sdgs.un.org/goals/goal3.

and economic growth [210].

Among NCD is dementia (see bottom plot in Fig.1.1), that has become a global burden, having impact not only on the people with dementia but also on their caregivers [297]. Nowadays, Alzheimer's disease (AD) is the most common type of dementia, representing a public priority in the healthcare system [297]. According to the last World Alzheimer Report, nowadays 55 million people are living with dementia all over the world and this community is expected to reach 78 million by 2030, and 139 million in 2050. Every three seconds, there is a new case of dementia, but still there is no cure [220]. Moreover, this neurodegenerative disease entails different costs: the ones for the formal cares, and the ones for the so called "informal" cares. The former are about a trillion US dollars a year, and are forecast to double by 2030, while the latter can be estimated in terms of hours per year spent by the caregivers and amount to approximately 82 billion [220]. It is thus of utmost importance to enhance our understanding of Alzheimer's disease from both the scientific and the clinical perspective to eventually improve the diagnosis and identify its early-warning signals, useful for the prevention and treatment thereof. This thesis represents an effort in making a step further towards a data-driven understanding of Alzheimer's disease from a computational and network neuroscience perspective.

Typically, people with Alzheimer's disease [14] exhibit a progressive loss of episodic memory (e.g. what happened two days before) [133, 27] and disorientation (e.g. getting lost in familiar places) [146, 202]. Other characteristic symptoms are related to functional apraxia and aphasia [104], i.e. the inability to accomplish everyday activities (e.g make coffee) [23] together with difficulties in finding the right word in the right moment. Remarkably, Alzheimer's disease patients have deficits in verbal fluency tasks whether phonemic or semantic [18, 63, 204, 167, 254, 270, 172, 53].

This aspect, linked to speech disorder and language alteration in neurodegenerative diseases, will be central for the second chapter of this thesis (chapter 2). In fact, it will represent our starting point to provide new indicators to investigate the ability of healthy and non-healthy brains in navigating concepts. Specifically, we will show that such a navigation is measurable, proving that an underlying, latent, geometry characterizing the human mind is plausible [50].

Alzheimer's disease affects the brain with several abnormalities. Particularly, two main brain changes occur in Alzheimer's disease, one outside neurons and one inside neurons. Outside neurons, the protein fragments beta-amyloid accumulate, generating the so-called beta-amyloid plaques; while inside neurons, the storage of an anomalous form of the protein tau originates the so-called tau tangles or neurofibrillary tangles [23]. There is evidence that beta-amyloid plaques affect neuron-to-neuron communication at synapses eventually provoking the cell death [23]. As there is evidence that tau tangles prevent the neurons from the transport of nutrients and all vital substances [23]. How these proteins relate with each other, or what causes them to reach such damaging levels remains still poorly understood [164, 23]. Eventually, the beta-amyloid plaques and neurofibrillary tangles lead to loss of both synapses and neurons, resulting in the atrophy of brain areas which cannot be reversed [23]. Concomitantly, Alzheimer's disease patients present an efficiency loss in the information exchange between brain areas [93]. Based on the idea that information exchange in the human brain is crucial for vital tasks and that such an exchange is compromised in Alzheimer's disease, in chapter 4 we propose an information-theoretic approach to assess connectome's information capacity at different stages of dementia. Specifically, by investigating the persistence of the information flow across the whole brain state, we provide a multiresolution analysis of the human brain [51].

Nowadays, it is not possible to diagnose Alzheimer's disease with 100% certainty, unless examining post-mortem brain cells [202]. In living patients, the diagnosis combines multiple factors and methods, encompassing neuropsychological tests and neuroimaging techniques [164]. Meanwhile we live longer life, medicine and the healthcare system are evolving towards more technological and data-driven approaches trying to make prognosis and diagnosis more and more accurate [211]. Among others, deep learning approaches are widely used for image processing and have been used for the classification of Alzheimer's Disease (AD) pathophysiology in magnetic resonance and positron emission tomography (PET) [184, 274]. Nevertheless, while being machine learning good at predicting outcomes and indispensable to handle enormous amount of data, they do not return information about the causes.

From the quantitative perspective, there is evidence that damages to brain structure affects its function and, as a consequence, cognition. As there is evidence that brain structure might be affected by altered cognition [80]. However, the mechanisms behind the interplay between structure, function and cognition are fundamentally still unknown. This lack of knowledge makes difficult to identify which disease is affecting a patient or going to affect a healthy individual, with obvious limitations to prevention and treatment of neurodegenerative diseases and psychiatric disorders. The incomplete knowledge about the complex interplay between structure, function and cognitive capacity within the human brain constitutes the research problem of this thesis. The generation of second-order gaps due to such an incomplete knowledge, for example the failure to identify neurodegenerative diseases on time, represents the motivation of the present research, and its intrinsic case study.

1.1.3 Where: Computational Neuroscience

Computational neuroscience constitutes the research positioning of this thesis. In the following lines, we provide some hystorical highlights that led to the birth of this research field.

The study of the brain and nervous system has far origins dating back to ancient Egypt, but it is only in the second half of the twentieth century that the term "neuroscience" firstly appears in the scientific field [264]. In particular, the mid-1960s signed the beginning of an era where neuroanatomy, neurochemistry, neurophysiology and neuropsychology start cooperating all together for a single common goal: unravel the brain structure and functioning of both normal and abnormal brain. In this sense, neuroscience is a multidisciplinary science, whose aim is especially to understand the physical and biological basis of human behavior [264]. In 1985, about fifteen years later, a step forward was made in such a field with the rise of *computational neuroscience*, which combined the mathematical counterpart and the theoretical analysis to the traditional study of nervous system. Nowadays, computational neuroscience is defined as the branch of neuroscience which investigates how the nervous system is organized, develops and processes information, as well as how mental abilities originates within this system [278]. The major focus in computational neuroscience is the development and evaluation of *models* for inquiring into these specific aspects. The broad range of studies within computational neuroscience spans from advanced analysis of brain-imaging data to more technical applications using brain-like computations or helping the development of better treatments for patients with neurodegenerative diseases, brain damages and other brain-related disorders in general [278]. This discipline explores the mechanisms of the brain on multiple levels, spanning from single-neuron modeling to consciousness, posing the focus on neurons,

circuits, systems, and the whole brain. The 21st century has seen the arrival of big data and a consequent cultural shift in neuroscience, as in many other research fields. In fact, the study of brain and nervous systems transitioned from a vertical dimension where specific techniques were applied to single problems and species to a horizontal dimension able to integrate data from a variety of different techniques to solve problems in different species [245]. Specifically, brain imaging techniques, such as functional Magnetic Resonance Imaging (fMRI) or Positron Emission Tomography (PET), analytical advances, such as the ones in network theory and machine learning, and the availability of large computing resources, gave us the possibility to collect and analyse large sets of data with an unprecedented rate [108]. Of particular interest for this work, is the revolution that big data have generated in the healthcare system but mostly the application of network theory to neuroscience (this aspect will be discussed in subsection 1.2.2). Despite the challenges of using big data as a healthcare resource, the benefits they could bring in understanding diseases, reducing times and uncertainties, and thus in formulating diagnosis to eventually establish suitable therapies, are potentially uncountable [249]. Availability of new data means new opportunities to be exploited. Commonly, the main tasks addressed by data can be resumed as description, prediction, and counterfactual prediction [149]. Specifically, description means using data to resume some salient features of the world and identifying meaningful variables, i.e. variables that are statistically significant in a given context. Prediction is finding a relationship between the various features to inform about future outputs. Finally, counterfactual prediction is used to understand how certain features would unfold if the world had been different in some given aspects. In principle, within this thesis, data will be used in the light of a descriptive goal, for gaining insights about brain functioning in health and diseases, from different perspective.

1.2 The new paradigm of complexity science

The ultimate goal of neuroscience is to unravel how the brain works and how it relates to the mind, as discussed in section 1.1. However, traditional neuroscientific studies most of the time refer to very specific questions relying on more and more detailed data sets [38]. To comprehensively address the complexity of the human brain and the wide issue of brain-mind interplay, the sole neuroscientific perspective might not be enough. Rather, a fruitful approach would be the one that investigates the brain-mind interplay in a multidisciplinary fashion, especially by complementing findings from neuroscience with concepts and principles from physics but even philosophy [38]. In this regard, the complexity paradigm – a worldview in the opposite of traditional reductionism – is proving to be the ideal candidate to reveal the multifaceted nature of the human brain, and eventually to bridge the gap between brain and mind [38].

In the following lines, we introduce the main concepts of the complexity paradigm, allowing the reader to understand the perspective of this thesis while studying the human brain.

The paradigm of *complexity* does not refer to a single specific discipline, instead it provides an approach to study a myriad of complex phenomena in the most diverse research fields [129] and real-world scenarios. Historically, complexity science has mutlidisciplinary roots. In fact, it has evolved from a collection of theories and conceptual tools of cybernetics, social sciences, systems theory, artificial intelligence, non-linear dynamics, fractal geometry, chaos theory, etc.

Complexity theory is not itself a scientific discover or advance but rather it is a framework standing at the basis of new scientific theories aiming, for example, to explain non-linear phenomena [72]. What especially unifies all fields relying on complexity paradigm, is a common "way of thinking" [151].

Essentially, the paradigm of complexity [292] endorses and reflects a holistic view of the world we live in. According to holism, the study of a particular system or phenomenon should put the emphasis on the system as a whole and not as a mere collection of its parts [253]. Because of this emphasis on the system as a whole, holism became known as "systemic perspective" at the beginning of twentieth-century [72]. The pioneers of system thinking were the biologists of the twenties, who began stressing the idea of living organisms as integrated wholes. Shortly after, also other disciplines such as Gestalt psychology and ecology adopted and fostered the system thinking [72]. This was sowing the seeds of a new revolution in the Western science: a revolution walking away from Decartes' reductionism and turning its gaze at connectedness, inter-relation, openness, networks, patterns, context [72] and again, considering dynamics, unpredictability, multidimensionality, in one word: *complexity*. In this vein, Ludwig von Bertalanffy in 1973 observed that some systems, such as the living one, had to interact with each other but also with their environment to stay alive, a principle coming from the General System Theory [291]. Such a concept of interaction between the parts of a system and the environment, required to consider the system as intrinsically open (holism) and not closed (reductionism). The behavior of an open system indeed, is affected by larger and complex conditions outside the system itself, making it difficult to be predicted or controlled [151]. In this perspective, entities *per se* are not sufficient to understand the reality surrounding us, neither is their content, whether material or mechanistic. What really matters are the *inter-relations* between such entities (and with their environment), and consequently the complexity they give rise to. In other word, relations between things, and not the thing itself, are the building blocks of reality [151]. This is especially true for the human brain, whose secret lies in the dynamical inter-connection between brain cells rather than in

the number of brain cells themselves, that moreover does not significantly change in a life span, as stated in Sec.1.1.

Systems where the properties of the whole cannot be inferred from the properties of single constituents, are known as "complex systems". The human brain is a complex system [261, 275, 38]. Other examples are organisms, society, ecosystems, the climate system, the world wide web, the social networks and ultimately the universe. Although belonging to the most disparate research fields, all these systems share important properties. In fact, while being quantitatively different at the microscale they exhibit qualitatively similar behavior and patterns at the macroscale.

Without further ado, let's see the characteristics that are common to this ubiquitous complex systems, including the human brain, plumbed within this thesis.

Firstly, a complex system is composed of inter-connected entities, interacting in multiple ways with each other and with the surrounding environment, giving rise to an overall behavior – or whole – which is, to use the words of Aristotle, greater than the sum of its parts. This overall behavior is called emergence [48] and constitutes the ultimate hallmark of complexity [20]. In a complex system, non-trivial unpredictable behaviours emerge globally from the local interaction between entities [17]. Thereby, life emerges from the interactions between particles as revolutions emerge from the interactions between people. In the animal kingdom, emergent behaviors span from birds flocking and school fishing, to fireflies synchronization, ants colonies organization and many more. Most of the time, emergent behaviors occur spontaneously, without any external input, leaders or central control [200]. For this reason, complex systems are regarded as decentralized systems, where decentralization ultimately occurs on the control.

Strongly related with emergence, self-organization is a peculiar fea-

ture of systems which exhibits complexity [30, 70]. According to self-organization principle, a spontaneous order emerges starting from the component interactions of a disordered system. Curiously, complex systems self-organize into a state that is often "critical", resulting from a misty balance between regularity and randomness [89, 70]. Further, complex systems dynamically change over time, usually by manifesting a non-linear and chaotic nature, leading to the unpredictability of the system in the long run [267]. Finally, it is worth mentioning the great ability of complex systems to adapt themselves to external conditions and changes [199, 147]. In this regard, it may happen that after adapting to a new state of being, due to a damage or a stressor, a system can evolve towards better conditions than before. In other words, a complex system can benefit from a shock. This property is called antifragility [272], and denotes the characteristic of a system to improve and thrive as a result of stress factors. To use the same words of the statistician N. N. Taleb: "And antifragility determines the boundary between what is living and organic (or complex), say, the human body, and what is inert, say, a physical object like the stapler on your desk" [271].

Since interactions matter and since they are especially what most characterizes a complex system, the proper modeling framework is provided by network science. In fact, a complex system can be modeled as a network of interacting components. Specifically, a network is represented as a graph formed by nodes – the components – and links – the interactions among components. Network theory is the modeling framework that we use in this work to investigate the brain as a complex system. This discipline was born from the intersection of different field of study as mathematics, statistical physics, computer science and social science and has been applied to systems of various nature, from gene-gene interactions to food web, from social networks to human brain [38]. From the application of network

theory to the study of the human brain, it stems network neuroscience, a cutting-edge discipline established in the last decade [259].

It is in the complexity paradigm that we intend to frame the study of the human brain and mind within this thesis. In the next subsections, we describe the human brain in the light of a complex system perspective, highlighting all features that make the human brain (and its relation to the mind) an excellent candidate to be understood with the tools from complex system science (in Subsec.1.2.1) and thus network science (in Subsec.1.2.2).

1.2.1 What: The brain as a complex system and the mind as an emergent process

In this subsection we characterize the human brain as a complex system. Specifically, we list how, and to what extent, human brains share important properties with complex systems such as interactions, dynamics, adaptation, emergence and self-organization.

Fundamentally, the human brain is composed of neurons. However, trying to understand the complex global behavior of the human brain from the sole understanding of its neurons is unfeasible. In fact, the human brain is no just a collection of neurons but it is a whole of **interacting** neurons. As anticipated in Sec.1.1, what makes the difference between a new born brain and an adult brain are precisely the number and the kind of **inter-connections** between brain cells. During the whole life span, brain structure and connections continue to change, **dynamically**, to guarantee adaptation to external condition, to learn new skills or to recover from brain injuries. This **adaptability** pertaining the human brain is possible thanks to neuroplasticity. It is interesting to notice that not only the brain structure can change (structural plasticity) but also its functions (functional plasticity). In fact, certain brain functions can move from one specific area to another within the brain, for example if that specific area is

a damaged one [114]. However, even in absence of external input, neuronal dynamics exist within cerebral cortex, exhibiting spatially and temporally complex patterns [157].

Finding a suitable relation between brain structure and dynamical functions on top of it, is a central topic in network neuroscience. In turn, unveiling how mind originates from this relation is even more focal and still remains something that eludes us. But what is the mind? Or at least, what is the mind from a systemic perspective? Before answering this question – and to entirely appreciate the answer – let us review the historical and conceptual milestones concerning the perennial problem related to the origin of mind.

One of the most important effects of the new systemic perspective was the rising of a new understanding of the mind nature, finally overcoming the body-mind dualism of Descartes. The famous philosopher of the seventeenth century, in fact, fundamentally divided nature in two independent realms: that of matter or "extended thing" (*res extensa*) and that of mind or "thinking thing" (*res cogitans*). This division has perpetuated for more than 300 in both Western science and philosophy. Thanks to the revolution that the systemic perspective induced within the study of life, a novel understanding of the mind bloomed from biology in 1960s, pioneered by Gregory Bateson concomitantly with Humberto Maturana and Francisco Varela. Precisely, the novel understanding of the mind eventually abandoned the Cartesian idea of the mind as a (thinking) "thing", to embrace the concept of the mind as a *process* [43]. According to the anthropologist Gregory Bateson, the living world is permeated of an organizing activity which is essentially mental, to use his words: "mind is the essence of being alive" [72]. Substantially, he was claiming that the inter-relation between organisms and their environment were essentially cognitive – or mental – inter-relations. For this reason, mind would not be something exclusive

to organisms themselves, but it would also manifest in ecosystems or social systems [71] (although very fascinating, this extension to ecosystems and social systems is outside the purpose of this thesis, and we refer the curious reader to [72]). This claim carries the typical universal flavor of complex systems. Although brilliant and groundbreaking, the idea of Bateson of the mind as a process was essentially an intuition. Independently and simultaneously, a very similar and consistent concept arises from the studies of two biologists in Latin America. These biologist were Humberto Maturana and Francisco Varela, that contrary to Bateson, felt the need to formalize somehow the idea of mental process, which eventually they developed in the Santiago Theory of cognition [194, 72]. Conceptually, the idea of Santiago theory and that of Bateson were strikingly similar: life and mind are inherently connected. Specifically, the mental process permeates matter, whatever the degree of complexity of the living matter. In this sense, the mental process only differs in the *kind* of interaction that living beings can have and not in the nature of the process itself. In humans, linguistic interactions are among the most complex ones, allowing human beings to create sophisticated societies [72]. The main focus of this new theory of cognition, the Santiago theory, was on development, learning and mostly adaptation. In this regard, Maturana and Varela observed that we cannot drive or direct a living system but we can only disturb it. Such a system, in response, can autonomously react to the external disturbance with a *structural* change (autopoiesis) [194]. Besides specifying a structural change, living systems can also specify which among external perturbations is able to trigger them [194, 72]. From the moment that a living system responds to a disturbance according to its structure and that such a structure continues evolving precisely because of this response, the response itself will be different over time. But changing response according to past experience is what we mean by learning. Hence, according to

Maturana and Varela, structural changes are cognitive acts. In this sense, the Santiago theory claims that mind and matter are two complementary aspects of life: process and structure [194], where the brain is the structure through which the mental process operates [72]. As Maturana and Varela clarify, cognition is an immanent "bringing forth of a world through the process of living" [194, 72].

At the end the 1990s, on the basis of these pioneering studies on the mind and by increasingly adopting a systemic view, a growing consensus began to spread among biologists and neuroscientists: the mind is a cognitive process, *emerging* from the complex neural interactions [288, 277, 103, 85]. Nowadays, network neuroscientists agree that cognition *emerges* from the spatially and temporally complex multiscale structure of the human brain [38]. Specifically, the complex architecture of brain network is responsible for the physical and biological fundamental of cognition [38]. As already explained before in this section, emergence occurs when a system exhibits special properties that its parts do not have on their own. Hence, we can speculate, in the same way of Peter Dodds [89], that no emotion, intelligence or willingness to dream exists in a single neuron, but there it is in the human brain... Therefore, thoughts, emotions, intelligence and ultimately the mind are **emergent** behavior of the human brain, rising from neurons interactions and in general from brain sub-systems exchanges [122]. Comprehending emergent properties is vital to understand the brain functioning, in a complex system perspective [38]. Together with emergence, self-organization is a peculiar feature of the human brain [166], occurring spontaneously at the level of neural circuits, without external control. Hypotheses that Alzheimer's disease might be caused by disruption in structural brain self-organization has been proposed [19], fostering the concept of a fundamental spontaneous order enabling the human brain to function properly [166]. While being emergence and self-organization

intimately related [144], they are formally different processes, especially in terms of our understanding thereof. If for the self-organization process we have models and mechanistic rules that explain how order originates from noise, the same cannot be said for (strong) emergence, that still remains an obscure process. In fact, there is still no consensus on a rigorous definition of emergent phenomena nor on a defined outline of core conditions from which emergence emerges. A plethora of studies has ventured in the endeavor to explain emergence, contributing little by little to define a slice of it, but not yet exhaustively nor definitively [155, 81, 96, 144, 59].

In this thesis, the human brain and mind are considered in the light of complex systems perspective, where the mind naturally emerges from the interaction between brain structure and function [67, 123, 38, 275, 39].

In the very next subsection we present the suitable framework to model the human brain when regarded as a complex system.

1.2.2 How: Network Neuroscience

At this point, it should be clear what are the main characteristics of the human brain, those that identify it as a complex system and what is meant by mind from a systemic perspective. However, a complete understanding of the principles and mechanisms underlying complex brain structure, function and cognition is still eluding us. In this regard, network neuroscience can help tackle this challenging purpose [39], by providing a new integrative framework to record, map, model and analyze components and their interactions, within the human brain. It is interesting to notice that network neuroscience blossomed from the intersection of two parallel drivers [39], established at the beginning of this century, i.e. i) the the availability of new powerful tools to collect brain data and to create comprehensive maps thereof; and ii) the rise of modern network science. Especially groundbreaking it has been the introduction of particular network models, the

multilayer networks [92, 225, 91], enabling the conceptualization and the modeling of the evolving, multifaceted nature of human brains [87]. The availability of data makes tools of networks usable and useful at different spatial and temporal scale, enabling a more intergrated mapping – and thus understanding and modeling – of the brain as a multiscale networked system (see Fig.1.2).

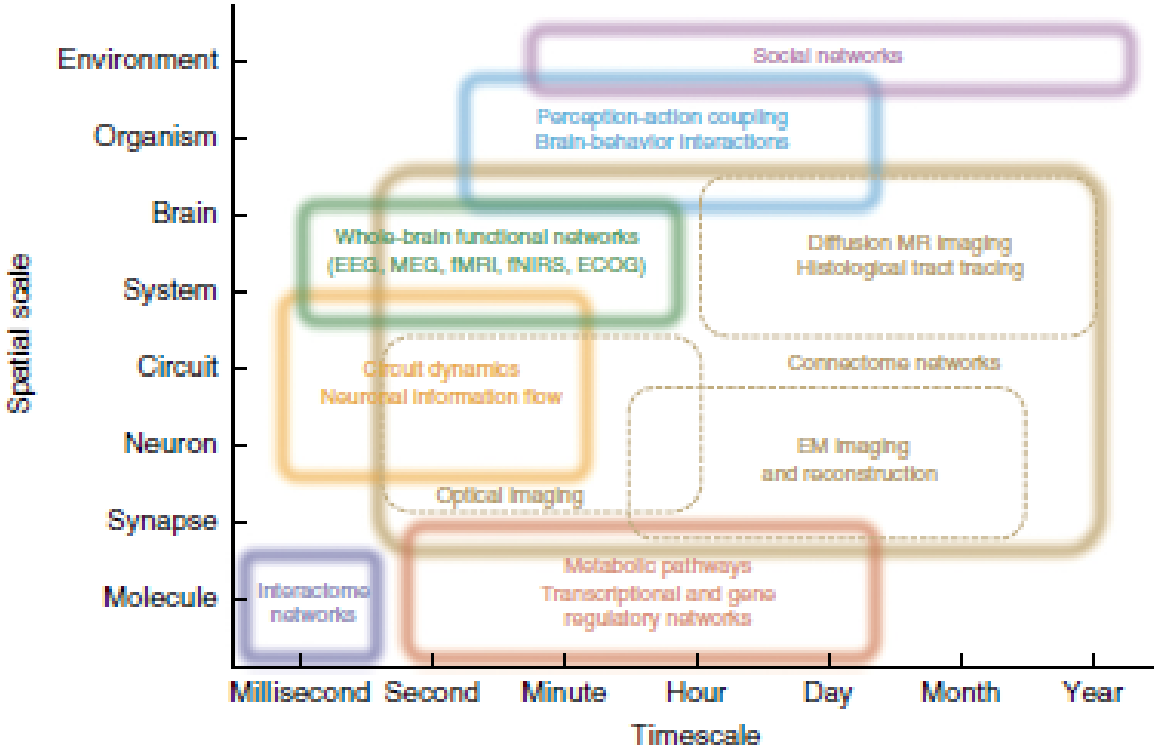

Figure 1.2: **The scales of network neuroscience analysis of the human brain.** Figure from [39].

Essentially, network neuroscience investigates the human brain as an interconnected system, having structural and functional properties. Mainly, three consecutive phases characterize the study of human brain in network neuroscience [39]:

1. Network measurement: this first step consists in collecting relational

data among structural, functional or behavioral elements within the human brain. Here neuroimaging techniques are widely use to record, for example, pattern of brain activation, the magnetic fields produced by electrical activity or the blood oxygenation level in different brain regions;

2. Network reconstruction: in this second phase collected relational data are used to infer patterns of connectivity, in turn used to investigate the brain organization on multiple scales of space and time. Specifically, the connectivity can be structural or functional (see Fig.1.3) but also behavioral. The result is a network, whose nodes are brain sub-units and links are their relations. Such a network can represent transcriptome, interactome, connectomes, networks of functional and effective connectivity...

3. Network analysis: once the network is reconstructed, network science provides a large set of tools for the network analysis, from the most classical centrality measures and statistical properties of the networks to more sophisticated models, such as generative models useful for highlighting topological peculiarities of human brain networks.

It is worth noticing that within the human brain there exists an interdependence in the organization of structural and functional networks, as there is evidence that structural properties are correlated with cognitive performance [67], such as verbal fluency [38]. Also, impaired functions due to diseases like dementia have been correlated with underlying structural properties [36].

To conclude, network science applied to brain data, and giving rise to network neuroscience, can tremendously enhance the integrated neuroscientific inquiry. Within this thesis, tools from network neuroscience will

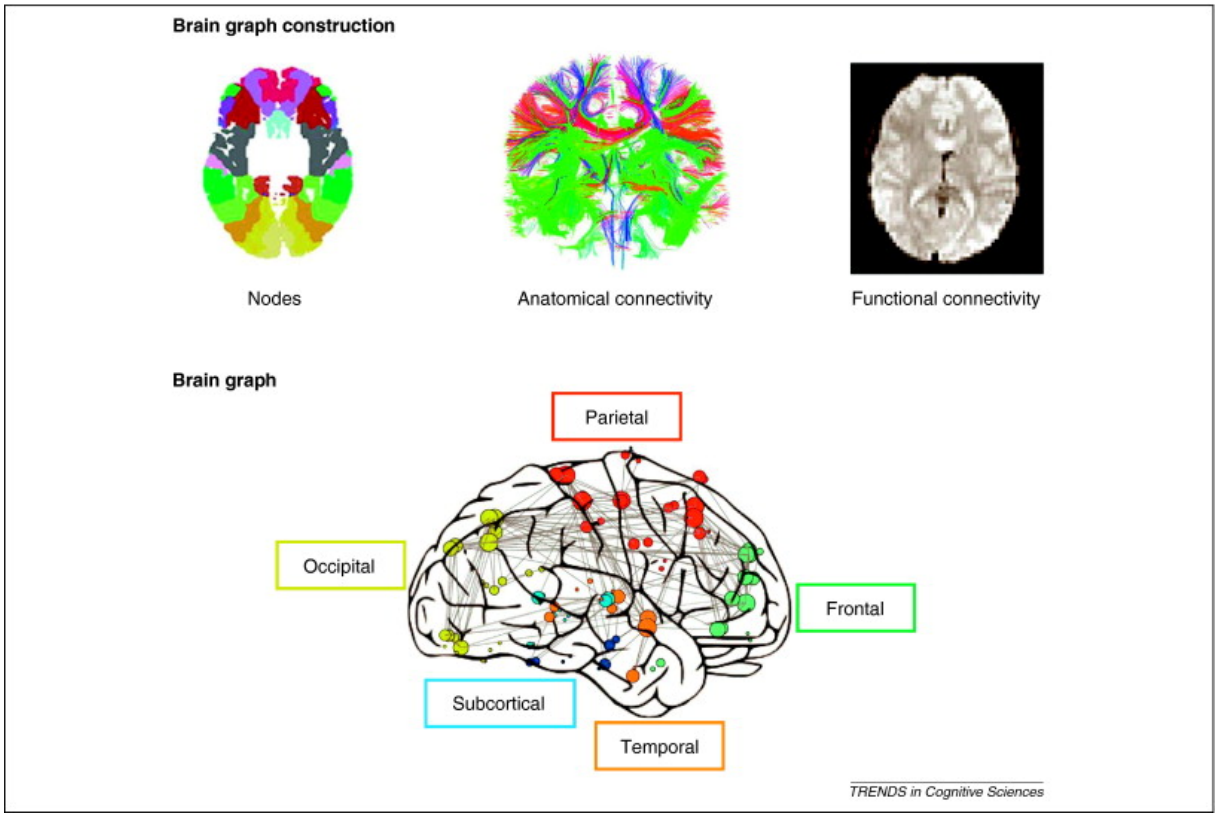

Figure 1.3: **Brain network.** Brain graph as reconstructed from neuroimaging data. Nodes encode brain regions while connections between those regions, whether anatomical (using diffusion imaging) or functional (using fMRI, electroencephalography or magnetoelectroencephalography), are encoded by edges between those nodes. Here, complex network science is applied to neuroscience to build a graph that characterizes the entire brain system according to its components (nodes) and the relations among them (edges). Figure from [38].

guide us in the exploration of the complex interplay between the human brain and mind.

1.3 Thesis overview

This thesis aims to explore, investigate and ultimately enhance our understanding of the complex interplay between the human brain and the mind, with a special focus on such a relation in health and disease. The topic has

been dealt with from a systemic perspective, by leveraging on tools from computational and network neuroscience.

In previous sections, we provided the fundamental ingredients to frame the context and motivation, as well as the perspective and tools of this work. In this section we review, chapter by chapter, the content of this thesis.

The following thesis is comprised of six chapters. Each chapter, except the first (Introduction) and the last (Conclusions and new directions), are presented as a research article, with chapters 2, 3, and 4 already published in peer-reviewed scientific journals.

Each chapter from 2 to 5 begins with an *Introduction* section and ends with a *Concluding remarks* section, including the state of the art, the tackled problem, the proposed approach, methods and experimental results. By only reading the introduction and the conclusive section, the reader should have a concise picture of the whole experimental work. In Fig.1.4 we provide a graphical overview of the thesis.

In chapter 2, we investigate the field of the mind, focusing on semantic memory, i.e. the retrieval of basic knowledge from memory. Understanding how humans cognitively navigate concepts remains elusive, because the underlying topology of concepts cannot be observed directly, and only functional representations are accessible. In this chapter, we overcome those limitations and show that the hypothesis of an underlying, latent geometry characterizing the human mind is plausible. This represents the first innovative aspect of the chapter, where we characterize this latent geometry by means of adequate descriptors for exploring and navigating concepts, demonstrating that they can capture the differences between healthy subjects and patients at different stages of dementia. The second innovative aspect here is the data set itself. In fact, the work of this chapter relies on a joint collaboration between Fondazione Bruno Kessler and the Depart-

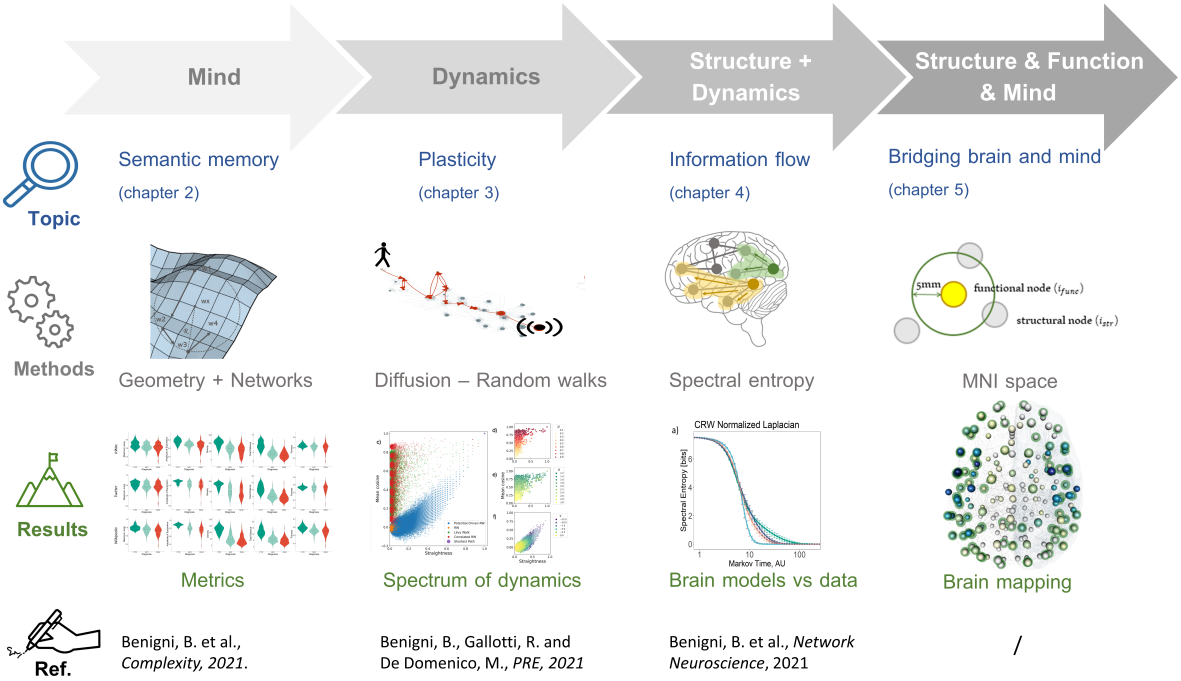

Figure 1.4: **Thesis outlook.** Each column describes a specific investigated area, outlining i) the focus (magnifier) on the specific brain topic addressed within that area, ii) the framework used to address the topic (gear), iii) the achieved results (mountain flag) iv) the reference (writing hand).

ment of Mental Health of APSS (Azienda Provinciale per i Servizi Sanitari della Provincia Autonoma di Trento). This collaboration provides us with a unique and exclusive data set of verbal fluency test records belonging to 185 patients at different stages of dementia plus 30 healthy controls.

In chapter 3, we move on to the dynamics, shifting from the mental navigation to the spatial navigation and in general to the topic of navigation itself. Based on the idea that interconnected systems have to route information to function properly – from the lowest scale of neural cells that exchange electrochemical signals to communicate, to larger scales of animals and humans that move between distinct spatial patches and machines exchanging information via Internet through communication protocols – we observe that non-trivial patterns emerge from the analysis of information

flows, which are not captured either by broadcasting, such as in random walks, or geodesic routing, such as shortest paths. In fact, alternative models between those extreme protocols are still eluding us. In this chapter, we mathematically formalize a new class of stochastic processes, based on biased random walks, where agents are driven by a physical potential pervading the underlying network topology, this constitute the innovative aspect of chapter 3.

In chapter 4, we pay particular attention to the interplay between brain structure and dynamics. In fact, we propose a new information-theoretic approach for the analysis of synthetic and empirical brain networks that naturally accounts for the function of a system in terms of the interplay between the underlying structure and a dynamical process on the top of it at different temporal scales, measured in bits of information required to describe the connectome state. The new information-theoretic approach is based on spectral entropy and is here applied to empirical brain networks reconstructed from both healthy and non-healthy brains, this constitutes the innovative aspect of this chapter.

In chapter 5, we finally (attempt to) address the issue of bridging brain and mind. Here, we propose a new framework for mapping human brain and mind accounting for multiple levels, i.e. structure, function and cognition. To this end, we have considered structural brain networks, cortical plus sub-cortical functional response errors and semantic areas tiling the human brain. This constitutes the innovative aspect of chapter 5.

The sixth and final chapter – Conclusions and new directions – discusses the reached goal of this thesis as well as the relevance and the importance of our research activity. There, we will highlight also the limitations, possible future directions and collaborations of our work.

The thesis ends with two appendices, dedicated respectively to i) the extended results of chapter 2 [49], in appendix A and ii) a parallel work

conducted over the course of COVID-19 pandemic, related to the nexus between environmental conditions and the human activity, during the lock-down in Northern Italy [231], in appendix B.

Chapter 2

The latent geometry of mind's plausible semantic space

In brief

In this chapter we investigate the field of the mind, focusing on semantic memory retrieval, a key cognitive process regarding the recall of basic knowledge from memory. Understanding how human mind navigates concepts remains elusive, because the underlying topology of concepts cannot be observed directly, and only functional representations are accessible. Here, we overcome those limitations and show that the hypothesis of an underlying, latent geometry characterizing the human mind is plausible. We characterize this geometry by means of adequate descriptors for exploring and navigating dynamics, demonstrating that they can capture the differences between healthy subjects and patients at different stages of dementia. The results of this chapter provide the first fundamental step to develop a new unifying conceptual and computational framework that can be used to support the assessment of neurodegenerative diseases from language and semantic memory retrieval tasks, as well as helping develop targeted nonpharmacological therapies to maintain residual cognitive capacity.

2.1 Introduction

One of the main shifts in the new systemic perspective has been the moving from entities *per se* to relations between entities. Linguistic interactions are among the most complex in humans, making mankind uniquely different from the rest of animal species. Language affects human behavior across different scales, from the development of abstract thinking to the creation of sophisticated societies [72]. Also, at the individual scale, speech disorders and language alterations are crucial in neurodegenerative diseases [18, 63, 204, 167, 254, 270, 172, 53], where the inability to recall concepts from memory generates drop-down effects on the ability to express ideas and needs, but also to perform everyday activities. In this chapter, we focus on the individual scale of healthy and non-healthy brains, investigating the navigation of mental pathways – based on exploration of concepts in human mind – and how their alterations can bring evidence of Alzheimer's disease.

This chapter has been published as a research article in the peer-reviewed journal *Complexity*, in 2021 [50] and is available here.

2.2 State of the Art

Exploration of concepts in human mind has long been a topic of debate across different research fields. In the last decades, several attempts have been proposed to explain mechanisms governing the retrieval of basic knowledge from memory – known as semantic memory [230]. However, these attempts can be clustered around two main schools of thought, namely the one of semantic space, and the one of semantic networks.

According to the branch of semantic space, the *search* is a key cognitive feature which operates similarly across different scales and contexts [154],

always requiring to manage a trade-off between exploiting what is known and exploring what is unknown [154]. In this sense, the internal mental search of concepts exhibits similar characteristics to the external physical search in space [152]. According to the theory of optimal foraging [152], the process of retrieving concepts from memory is dynamically similar to the one performed by animals when searching for food between patches of their environment [153]. In fact, the retrieval of concepts from memory is expected to mediate between local exploitation of current information and global exploration of further information, pursuing a sort of semantic foraging [152]. In accordance with the marginal value theorem [75], the semantic memory search is considered optimal if the subject – as the animal does in the optimal foraging – leaves a given cluster of information when the benefit of local exploitation falls to the level of the expected benefit of changing cluster and searching elsewhere [152]. To clarify with a trivial example, if one has to recall the maximum number of animals in a minute, an optimal strategy would be moving from the cluster of farm animals to the one of jungle animals, when no more farm animals can be quickly recalled.

In the clinical field, the intuition that patients cognitively organized the semantic access around semantic clusters, following a *clustering and switching* pattern in search, has been widely used to investigate the semantic retrieval [280] and the semantic impairment [273]. However, in this method, clusters are based on hand-made classification according to taxonomies: limitations can be partially overcome by taking advantage of distributional semantics to define the clustering and chaining of concepts during a semantic memory retrieval task [182].

In summary, according to the semantic space school of thought, the modelling of *searching* in semantic memory requires two main ingredients: i) a structural representation of the search space (hand-coded or statisti-

cally derived) and ii) a model of the search process (e.g. local to global transitions) [153]. However, there is still no clear definition of what a patch is and how to define it in memory [153].

Concurrently, another school of thought, the one of semantic network, demonstrated that the same results obtained with the optimal foraging in semantic space could emerge from a random walk exploring a semantic network [4, 5]. Rather than a clustering and switching processes, this network approach was considering a simpler and single process of exploration on a network of concepts. In this perspective, the navigation of concepts is represented by associative semantic networks [62], fostering the idea that concepts are cognitive units, each represented as a node linked to associated elements [79, 266, 31, 250]. However, a typical issue leveled against the use of semantic networks is that they might end up explaining – or predicting – the memory retrieval by leveraging on models built from similar behaviors, for example when modelling semantic networks from free associations data to explain semantic fluency tasks [165]. Progress in building such networks from fluency data has been made [307] but there is still no consensus about the most appropriate way to construct such networks [306].

Nevertheless, the semantic network approach has been widely used in the clinical field for the assessment of psychosis [201], Alzheimer's disease [74, 178, 53] and in cognitive science, for example, to investigate the levels of creativity [265] and the openness to experience in the human beings [76].

Over the past two decades, vector-space models of words meaning as high-dimensional numerical vectors have become serious contenders of semantic representation [141], for example when studying human psycholinguistic tasks [186] or when exploring the semantic verbal fluency in mild cognitive disorder [182]. Powerful tools involving this kind of spatial representation of words are the so-called word embeddings – bridging distri-

butional semantics and natural language processing – which map words into vectors in a multidimensional space [198]. The underling idea of this approach can be summarized with the words of the English linguist J.R. Firth, "a word is characterized by the company it keeps", meaning that, from a mathematical perspective, the closer the words in the multidimensional space, the closer their meaning in the vocabulary.

2.3 The Problem

As anticipated in Sec.1.1, language and memory retrieval tasks (mostly semantic) are crucial in the identification of neurodegenerative diseases [279, 148, 121] and for this reason they are usually employed in different neuropsychological tests. Among these tests, the categorical semantic verbal fluencies (SVF) play an important role in the assessment of dementia and Alzheimer's disease in particular [280, 238]. Here, patients are asked to pronounce as many words as possible, belonging to a certain category, within a given time interval. Patients' performance is successively evaluated by counting the amount of words pronounced[247] or their response times [63]. To investigate semantic retrieval, further approaches, based on the intuition that patients cognitively organized the semantic access around semantic clusters, has been widely used [280]. Recently, evidence of semantic maps tiling human cerebral cortex has been provided from fMRI data, probing the existence of semantic selectivity in brain areas [162] and further strengthening the idea that language can be organized on a topological space, i.e. on a manifold of concepts. Nevertheless, a clear understanding of the mechanisms governing the navigation of concepts in the human mind still eludes us [226, 189].

The aim of this chapter is to investigate both perspectives of spatial and network representation of concepts, to eventually provide a data-driven in-

sight on why the hypothesis of an underlying, latent geometry characterizing the human mind, is plausible.

2.4 The Proposed Approach

Relying on clinical data of semantic verbal fluency test from 215 subjects and leveraging on word-embeddings tool we aim at defining suitable metrics to indirectly explore this possible, latent geometry. Our work arises within the debate between semantic space and semantic network representations and it examines the exploration process, integrating both perspectives according to an approach which builds upon the geometry at the concept scale and culminates with diagnosis-based semantic networks, passing through the mesoscale organization of concepts (clustering).

Remarkably, our framework allows us to gain new insights about the organization of concepts in the human mind and shed some light on why some existing approaches were successful. In fact, the mechanisms behind the retrieval of basic knowledge, known as semantic memory [230], remains fundamentally still unknown [136]. Here, we fill this gap by i) hypothesizing the existence of an underlying geometry which governs the exploration of concepts in the human mind and ii) demonstrating that such a geometry is able to discriminate between healthy subjects and patients at different stages of dementia. Our hypotheses are based on the assumption that, if a common latent geometry underlying the mental navigation of concepts existed, then subjects with semantic retrieval deficits should show some distortion in such a navigation on top of this geometry. Here, we observe how different population of subjects, in terms of semantic impairment, differently navigate the same geometry by means of suitable metrics characterizing their explorations. If our hypothesis is reasonable, we predict to see significant differences in metrics computed from different diagnoses.

Our study is based on the analysis of semantic verbal fluencies (SVF) data of patients at different stages of dementia, i.e. Alzheimer's and Mild cognitive impairment (MCI), and healthy controls. Specifically, MCI subjects has an increased risk of conversion to Alzheimer's disease (and dementia in general), for this reason MCI is considered a precursor of Alzheimer's disease. During the semantic verbal fluency test, each individual is asked to report all words he/she can remember belonging to category of animals, within a time interval of 60 seconds. Each spoken word is annotated by the neuropsychologist who is testing the patient. No clues nor incentives are given to the subjects during the tests and any repetitions are not marked. The SVF test is a significant test for the assessment of dementia diagnosis [238]. Generally, the semantic impairment is more severe in patient with dementia than MCI patients. The rationale for looking at the semantic fluencies of these two populations aims at testing our guess that, if a latent geometry existed, a different severity in semantic memory retrieval impairment should be reflected in the way such concepts are navigated on a plausible, latent geometry. Thus, instead of focusing only on statistical descriptors of language –e.g. word frequency or vocabulary size – as commonly done in disease, we considered also in which *sequence* the words have been provided: this information is crucial because it allows to map the navigation of concepts in the underlying semantic space.

To characterize the navigability of this space in terms of concepts visited in such unknown, possibly multidimensional, space, we first had to build a plausible geometric proxy (illustrative representation in Fig.2.1). To this aim, we used three distinct word embeddings obtained from the Italian language, namely *Italian Word Embeddings* – trained on the Italian Wikipedia – [2], *itWac* – constructed from the Web limiting the crawl to the .it domain and using medium-frequency words from the Repubblica corpus and basic Italian vocabulary lists as seeds –[77] and *Twitter*

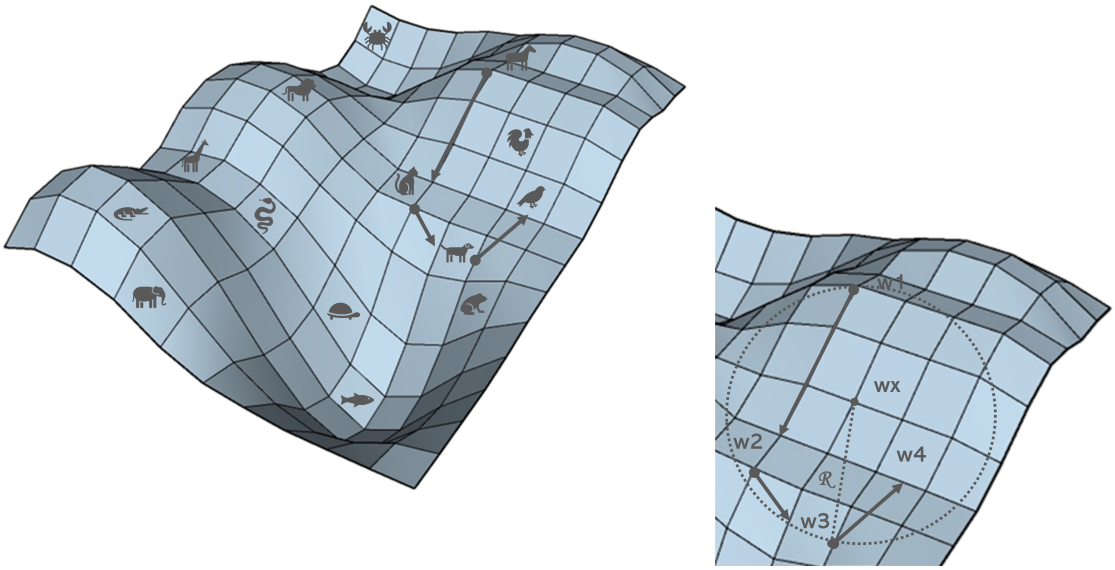

Figure 2.1: **Conceptual representation of semantic space.** On the left, navigation of concepts on the semantic space, arrows define the *sequence* of words. On the right, a zoom outlining the navigation, w_n are the concepts, w_x their centroid and R is the radius of exploration.

–trained on 46.935.207 tweets –[77], all the word embeddings were generated with the popular word representation models, word2vec[198]. By choosing three different word embeddings we are able to evaluate the robustness of our metrics in geometries coming from different sources, i.e. a website (Wikipedia), a social network (Twitter) and a newspaper (La Repubblica). In the following we will refer to word embeddings, semantic spaces or geometries interchangeably. Here, the term *geometry* is justified by the fact that we leveraged on word-embeddings, powerful tools which encodes the semantic relation between the words as a *geometric relationship* between vectors in multi-dimensional space. Word embeddings are built from data corresponding to humans-written documents (in our case Wikipedia, Twitter and La Repubblica, an Italian newspaper) which are then embedded in a multi-dimensional space according to the hypothe-

sis of the distributional semantics. This hypothesis defines the semantic similarity in terms of vector similarity, i.e. the closer the meaning in the vocabulary the closer the points representing the words in the word embeddings (encoded by a vector of coordinates in a multidimensional space). In this sense, by embedding the words pronounced by a sample of subjects into a word embeddings, which is a coordinate space by design, we can study the mental navigation of such subjects on a *geometry of concepts.* For each group of subjects we therefore have three independent semantic spaces, each one used to characterize the local exploration and the overall navigation of the semantic geometry. More specifically, we introduce five different descriptors for this purpose, in order to identify the effects of the underlying geometry, if any. At the smallest scale, i.e. the one of single concepts, geometry is probed in terms of:

1. maximum jump $MaxJ$, i.e. the maximum distance, in the word embeddings, between two consequent words pronounced during the test, it defines the maximum instantaneous capacity to change context;

2. diameter of exploration DOE, i.e. the maximum distance, in the word embeddings, between the words pronounced during the test, whatever the order, it defines the maximum capacity to change context in the whole test duration. To be consistent, we call this metric DOE, when it is computed with the euclidean distance and AOE, amplitude of exploration, when it is computed with the cosine distance;

3. density of exploration ρ_w, it corresponds to the total amount of animal words potentially available in the hypersphere built from the exploration radius R, half the DOE, and which has as its center the centroid C of spoken words in the word embeddings. It returns a measure of density in the volume of words explored by the subject. Specifically, it defines the density of pertaining words (i.e. belonging

to the category of animal) in the area explored by the subject in the geometry;

4. distance d, it is the total distance covered during the test, it quantifies the magnitude of the overall exploration;

5. and farness far – i.e. the average distance of the words pronounced, it defines the ability *to go far* with a certain number of jumps.

Mathematical details about each descriptor are provided in the next section *Methods* (2.5), while their significance in discriminating the three groups of subjects is evaluated by means of Kolmogorov–Smirnov statistical tests and t-tests.

Afterwards, in line with the idea that the semantic access is cognitively organized around semantic clusters [280, 152] we probed the mesoscale organization of concepts by performing a semi-supervised clustering algorithm in the three geometries. Accordingly, we define the explorative potential of the navigation for each category as the total number of visited clusters and as the total number of words included in the visited clusters. This descriptor is a proxy for the cognitive effort spendable during the navigation and it defines the total amount of clusters/words, potentially visitable/retrievable during the test. Clusters are then given as input to a hierarchical clustering algorithm which provides the spatial hierarchy of such clusters based on their relative distance. By comparing the distances between the visited clusters, we are able to evaluate the existence of a hierarchy in the way subjects explore concepts (technical details about clustering and explorative potential can be found in the next section 2.5).

Taking inspiration from the process of clustering and switching when retrieving concepts from memory, network scientists provided a new kind of random walk over a graph as a Markov process – i.e. *the switcher random walk* [131] – to generalize the exploration task on a network. In this vein

and by following the idea of the semantic network navigated by a random walk [5], we finally tested the navigation of concepts by means of their Markov representation, to probe the possible alterations of mental pathways emerging from the exploration of concepts in patients with dementia. Mathematically, this corresponds to define the transition probability from one state (i.e. cluster) to another, regardless of previously visited states. Operationally, we build three Markov chains, one for each group – i.e. the two diagnoses and the healthy controls –, considering all the clusters visited by each group as the states of the Markov chain of that group, and setting the transition probabilities equal to the relative transition frequencies from one state to another in each group. Each Markov chain is characterized by the steady state distribution and the mean first passage time matrix. In the following, we provide the intuitions on how to interpret these two descriptors for each network of concepts. Our intention is to compare metrics that uniquely identify the pattern of exploration – as given by steady state and MFPT – for each category of subject in this way we can detect any possible differences between such patterns.

The intuitions behind the steady state distribution and the mean first passage time (MFPT) matrix are given by the purpose to investigate and to characterize the search process pursued by each diagnosis on its network of concepts. Being the mathematical model of the network of concepts assumed as a Markov chain, the steady state distribution and the MFPT are the key descriptors to investigate such a navigation dynamic. We assume that, if it is true that different diagnoses explore the network of concepts in different way, the steady state distributions and the MFPT should highlight these differences. In fact, the steady state distribution defines the unique distribution to which the exploration converges as the number of transitions increases, regardless of a Markov chain's initial state. Here, the steady state is a vector, computed for each category, representing the

probabilities to be in each of the cluster of words visited by that category, after a sufficient amount of time. It is to be noticed that each subject has one minute to complete the SVF test but practically no patient uses it all because he finishes the words before the one minute ends. In this sense, one minute is enough to reach a regime situation, which is mathematically represented through the steady state distribution. However, it would be experimentally impossible to test a subject for an infinite amount of time.

For what concern the intuition behind the MFPT matrix, it encodes the mean amount of time required to go from one state i to another state j of a Markov chain. In our case, the MFPT matrices encode the mean number of transitions to go from one cluster of words to another. Specifically, we define a MFPT matrix for each diagnosis. The entries of such a MFPT matrix answer the question: starting form one cluster of words i, how long does it take, on average, for this specific category to reach a specific cluster of words j for the first time? In this sense the MFPT matrix characterizes the exploration dynamic of each diagnosis since it returns an average measure of the time spent to navigate the underlying network of concepts. In summary, MFPT matrix defines the average number of steps needed to reach a certain state from another for the first time. This idea, redefined on the network of concepts, corresponds to the average time required for each diagnosis to pass from one cluster to another for the first time. In this way, we are able to measure the time needed to travel for the first time a certain mental link connecting two groups of concepts.

Taken in isolation, the steady state distribution (ss) and the MFPT give us an insight on how the exploration of each diagnosis evolves on the network over time. Essentially, these indicators provide us information on how heterogeneously the clusters will be explored after a sufficient number of transitions (ss) and on how much time it takes before a cluster is visited for the first time (MFPT). To investigate possible differences in the dy-

namic of exploration between the diagnoses and the healthy control group these descriptors are then compared by means of similarity measures between the three groups, i.e. Pearson correlation, Spearman's correlation, euclidean norm, Frobenious norm and covariance (for mathematical details about Markov chains we refer to the next Sec.2.5).

2.5 Materials and Methods

2.5.1 Dataset

The dataset we relied on consists of semantic verbal fluencies (SVF) test – belonging to animal category – recorded from 185 patients and 30 of healthy controls (CTR). Among them:

- 92 suffer of dementia (DEM, M=40%, F=60%, age=75 ± 7, yrs of education=9 ± 4), which includes vascular dementia, frontotemporal dementia, degenerative dementia and Alzheimer's disease;
- 93 suffer of Mild Cognitive Impairment (MCI, M=48%, F=52%, age=77 ± 6, yrs of education=9 ± 4), a precursor of Alzheimer's disease;
- 30 are healthy controls (CTR, M=60%, F=40%, age=32 ± 7, yrs of education=17 ± 0.40).

The SVF records report the *sequence* of Italian words, belonging to the category of animals, spoken by each of 215 subjects during the test. Our work is a retrospective study of data previously collected by the Department of Mental Health, Division of Psychology, Azienda Provinciale per i Servizi Sanitari, in Trento, Italy. All the data was collected in accordance with relevant guidelines and regulations with participants' written informed consent. DEM and MCI diagnoses were made, as well, at Azienda Provinciale per i Servizi Sanitari of Trento, Italy, by consensus

of medical specialists as geriatricians, neurologists and psychiatrists on the basis of physiological medical data and neuropsychological tests (i.e. blood tests, resonances, CT scans, liquor samples, PET, Mini MentalState Examination, ENPA subtests, Naming, Verbal fluency on phonemic cue, Verbal fluency on semantic cue, Digit span forward/backward, Corsi span, Babcock story recall test, Rey–Osterrieth complex figure, Modified Taylor Complex Figure, Attentional matrices, Frontal assessment Battery, Clock Drawing Test, Copy of Rey–Osterrieth complex figure, Copy of Modified Taylor Complex Figure, Cornell scale for depression in dementia, Activities of daily living, Instrumental activities of daily living). For the curious reader, we provide a detailed analysis of neuropsychological tests in Subsec.A.1.1 of Appendix A. It is to be precised that the fact of grouping together different type of dementia conditions is motivated by the small number of samples related to each dementia category we can rely on. By grouping together all dementias we obtain a sample which is comparable with that of MCI. Anyway, for our assessment, we rely on official and specialist sources which report: "the boundaries between different forms of dementia are indistinct and mixed forms often co-exist" (WHO, https://www.who.int/news-room/fact-sheets/detail/dementia).

The Semantic Verbal Fluency (SVF) tests were conducted at the Department of Mental Health, Division of Psychology, Azienda Provinciale per i Servizi Sanitari, in Trento, Italy, following a specific clinical protocol. In particular, the neuropsychologist asked each individual to report all words he/she can remember belonging to category of animals, within a time interval of 60 seconds. No clues nor incentives are given to the subjects during the tests. As soon as the patient pronounces a word the neuropsychologist takes note by hand of the spoken word, the neuropsychologist also notes the order in which the words are pronounced as well and any repetitions are not marked.

2.5.2 Semantic Space

As plausible geometric proxy of semantic space, we leveraged on word embeddings. Particularly, we have used three distinct word embeddings, obtained from the Italian language and generated with the popular word representation models, word2vec[198]:

- *Italian Word Embeddings*, trained on the Italian Wikipedia, embedded in 300 dimensions [2];
- *itWac*, constructed from the Web limiting the crawl to the .it domain, using medium-frequency words from the Repubblica corpus and basic Italian vocabulary lists as seeds. Words are embedded in a 128 dimensional space[77];
- *Twitter* trained on 46.935.207 tweets, embedded in a 128 dimensional space[77].

Geometry At the scale of single concepts, we provided five different indicators useful to characterize the local exploration of concepts and eventually to discriminate between healthy and non-healthy subjects. Each subject p speaks an amount of words N during the SVF test, we call this set of words $W^p = \{w_i \; with \; 0 \leq i \leq N\}$. For each patient and for the healthy controls we define the following metrics:

1. Maximum jump $MaxJ$, it is the maximum distance, in the semantic space, between two consequent words pronounced during the test. It defines the maximum instantaneous capacity to change context. In formulas:

$$MaxJ^p = max\left(dist\left(w_t, w_{t+1}\right)\right) \; where \; w_t, \; w_{t+1} \in W^p \tag{2.1}$$

Where *dist* can be both euclidean distance and cosine distance. Results are presented considering the cosine distance for all the metrics (in Sec.2.6).

2. Diameter of exploration DOE, it is the maximum distance, in the word embeddings, between the words pronounced during the test, whatever the order, it defines the maximum capacity to change context in the whole test duration. In formulas:

$$DOE^p = \max\left(dist\left(w_i, w_j\right)\right) \; where \; w_i, w_j \; \in W^p \tag{2.2}$$

According to the measure of distance, i.e. euclidean or cosine distance, this metric is defined respectively as Diameter of exploration DOE or Amplitude of exploration AOE.

3. Density of exploration ρ_w, it corresponds to the total amount of animal words potentially available in the hypersphere built from the exploration radius R, half the DOE, and which has as its center the centroid C of spoken words in the semantic space. In formulas:

$$\rho_w^p = \sum_{a=1}^{A} \left(dist\left(C^p, \; w_a\right) < R^p\right), where \; w_a \in A \tag{2.3}$$

where C^p is the centroid of spoken words by patient p and for each coordinate x of the semantic space, it is defined as follow:

$$C_x^p = \frac{1}{N} \sum_{w=1}^{N} x_{w_i} \tag{2.4}$$

according to the dimension of the word embedding, the centroid will have 300 or 128 dimensions, while A is the complete set of animals in the word embeddings and R is the radius of exploration, i.e.half the DOE. To map the complete set of animals A in the word embeddings, we translated into Italian the list of animals made by Greg Borenstein, available on github.

4. distance d, it is the total distance covered during the test. In formulas:

$$d = \sum_{i=1}^{N-1} dist\left(w_i, w_{i+1}\right), where\ w_i \in W^p \tag{2.5}$$

5. farness far, it is the average distance of the words pronounced, it defines the ability to go far with a certain number of jumps. In formulas:

$$far = \frac{\sum_{i=1}^{N-1} dist\left(w_i, w_{i+1}\right)}{N-1} \tag{2.6}$$

The significance of the above defined indicators in discriminating the three groups of subjects is evaluated by means of Kolmogorov-Smirnov statistical test and t-test, with a 95 % confidence interval (detailed results available in Tables A.4, A.5 of Appendix A). Since we are testing if each metric is able to separate between the three categories –DEM, MCI, healthy controls – (in each word embedding), we are in a case of multiple testing and for this reason we have adjusted the p-values of each performed test (Kolmogorv-Smirnov and t-test) according to the Holm–Bonferroni method.

Hierarchy For each geometry, we provided its mesoscale organization of concepts by performing a semi-supervised clustering, using the linear algorithm of k-means, and setting the number of clusters accordingly to the elbow method (see Fig.2.2). Relying on these clustering configurations, we defined the explorative potential of the navigation as the total number of visited clusters and as the total number of words included in visited clusters, for each subject. These descriptors report the total amount of clusters potentially visitable during the test and the total number of words potentially retrievable during the test. As well as for geometric indicators of previous paragraph, even in this case the significance of the two explorative potential metrics in discriminating the three groups of subjects

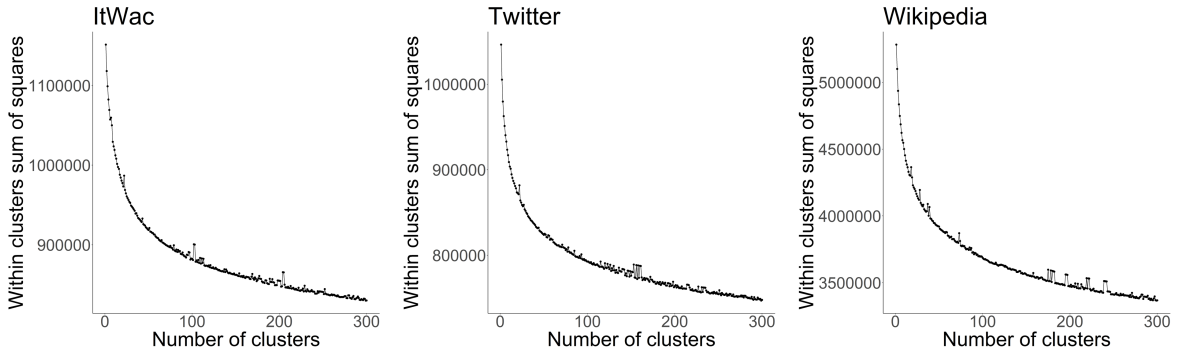

Figure 2.2: **Elbow plots** of each geometry.

has been evaluated by means of Kolmogorov-Smirnov statistical test and t-test, with a 95% confidence interval and adjusted p-values (resulting values available in tables A.6, A.7 of Appendix A) .

By performing a clustering analysis between the embedded visited clusters, we are able to evaluate the existence of a hierarchy in the way subjects explore concepts. Once the clustering configuration for each geometry has been obtained, it is possible to extract the hierarchical configuration of these clusters thanks to the coordinates of the centroids of each cluster in the geometries. In other words, the clusters are the same of k-means output and, given the position of each cluster in the geometry (identified by the centroid), it is possible to define a spatial hierarchical relationship between such clusters, in terms of distances between centroids.

Particularly, we computed the clusters' distance matrices for each group, setting the distance between not visited clusters equal to the double of the maximum distance between visited clusters (i.e. a proxy to infinite) in this way we assure that the not visited clusters will not be relevant in the hierarchical analysis of that group. With the distance matrices so computed, we performed a hierarchical clustering algorithm to discover the relationship between clusters. Hierarchical relationship among clusters visited by

a group is shown through dendrograms, while differences between hierarchies, i.e. in the way different groups explore concepts, are displayed through tanglegrams Fig.2.4. Finally, we investigated the correlation between the three groups by computing the Baker's Gamma correlation coefficient in pairs for the three groups' trees (dendrograms) and by testing it against a null model.

For a better understanding of clustering analysis, we summarized below what we have done in two main steps:

1. **Clustering configuration**: we defined the mesoscale organization of concepts, i.e. we identified the clusters of concepts for each category (DEM, MCI, healthy control), and for each geometry, by means of linear semi-supervised clustering algorithm (k-means). These clusters represent how the expressed concepts grouped together on a semantic space (and they will constitute the states of the Markov chains). Through k-means clustering we also provided the explorative potential which define the total amount of clusters explored by each category (see Fig.A.2 of Appendix A).

2. **Hierarchical configuration of clusters:** the clusters identified by the k-means algorithm are then given as input to a hierarchical clustering algorithm which provides the spatial hierarchy of such clusters based on their relative distance. Intuitively, since the three categories explore different clusters, the study of the hierarchy give us an insight about the way such clusters are explored. In order to detect any possible difference in the hierarchy, we compute the values of Baker's gamma correlation, a measure of similarity between two trees (dendrogram) of hierarchical clustering (see Fig.2.4).

Networks At the macroscale, i.e. the scale of clusters, the navigation of concepts is tested by means of its Markov representation, to probe the possible alterations of mental pathways emerging from the exploration of concepts in patients with dementia. Mathematically, this corresponds to define the transition probability from one state (i.e. cluster of concepts) to another, regardless of previously visited states. Operatively, we build three Markov chains, one for each group g – i.e. the two diagnosis and the healthy control –, considering all the clusters visited by each group as the states of the Markov chain of that group, and setting the transition probabilities m equal to the relative transition frequencies from one state (r) to another (s) in each group g. In formulas:

$$m^g_{r,s} = \frac{\sum_{p}^{P^g} E_{(r \longrightarrow s)^p}}{\sum_{p}^{P^g} \sum_{s}^{S} E_{(r \longrightarrow s)^p}} \tag{2.7}$$

where P^g is the total number of subject of group g, S is the total number of visited clusters by group g and $E_{(r \longrightarrow s)^p}$ is the outgoing edge from cluster r to cluster s for patient p^{th}. After calculating the entries $m^g_{r,s}$ we obtain, as result, the transition probability matrix $\hat{M}$ for each category of subjects. Here, we assume that each subject of each category behaves as the "typical subject of that category", whose navigation corresponds to a possible realization of the typical exploration of that category. For practical reasons (e.g to guarantee the ergodicity of Markov chains), we modify the transition matrix by adding a damping effect given by the Page Rank algorithm. Specifically, we are assuming that the process of exploration behaves 85% of time according to the probabilities of the above determined Markov chain and 15% of the time according to a discrete uniform distribution [135, 214, 197, 252] (for more detail about the choice of teleportation parameter in the PageRank algorithm we refer to the dedicated section A.2

in Appendix A). In formulas:

$$\hat{T} = \alpha\hat{M} + (1-\alpha)\frac{1}{S} \tag{2.8}$$

where $\hat{T}$ represents the new transition matrix, α is equal to 0.85 according to the PageRank algorithm and S is the number of states of the Markov chain.

Each Markov chain is then characterized by the steady state distribution $\vec{\pi}$ and by the mean first passage time matrix $MFPT$. Through the former we gain information about the process at the equilibrium, while through the latter we can have an insight into the dynamic of the process during the exploration of concepts. Bearing in mind the memoryless property of Markov chains and that the probability of being in state r after n steps is the r^{th} entry of:

$$\vec{\pi_n} = \vec{\pi_0}T^n \tag{2.9}$$

where $\vec{\pi_0}$ is the probability distribution of the initial state, the steady state corresponds to the long-run equilibrium whatever the starting state. In formulas:

$$\vec{\pi_s} = \lim_{n\to+\infty} T^n_{r,s} \tag{2.10}$$

The steady-state distribution is found by solving the system of equations obtained by imposing

$$\vec{\pi}T = \vec{\pi} \tag{2.11}$$

with the constraint that all the components of $\vec{\pi}$ must sum up to 1. The steady state distribution can be obtained also by means of eigenvectors. In this case $\vec{\pi}T = \vec{\pi}$ can be seen as

$$\vec{v}A = \lambda\vec{v} \tag{2.12}$$

therefore $\vec{\pi}$ can be obtained from to the left-eigenvector of the square matrix T corresponding to the eigenvalue λ=1.

The $MFPT$ is finally obtained from the *fundamental matrix* Z:

$$Z = (I - T + W)^{-1} \tag{2.13}$$

where I is the identity matrix and W is a matrix of rows identical to $\vec{\pi}$. The $MFPT$ it is determined by:

$$mfpt_{i,j} = \frac{z_{j,j} - z_{i,j}}{\pi_j} \tag{2.14}$$

We compare each descriptor (i.e. $\vec{\pi}$ and $MFPT$) according to four different metrics: Pearson correlation, Spearman's correlation, covariance and euclidean norm of the difference. For $MFPT$, we compare also its Frobenius norm. When computing the metrics for the $MFPT$, we consider the common visited states by the groups and we take the matrix as a vector (resulting values available in tables A.8-A.14 of Appendix A).

2.6 Experimental Results

In this section we provided the summary of salient results, highlighting whether and when our framework can be used to discriminate between healthy and non-healthy subjects.

2.6.1 Geometry

Overall, the metrics defined to characterize the local exploration prove to be suitable for discriminating between healthy and non-healthy subjects in all the three spaces. The results for the three semantic space are shown in Fig.2.3. Specifically, according to the results of t-tests all the metrics in all geometries, except for far in twitter geometry, are able to discriminate between healthy and non-healthy subjects, all having p-values ≤ 0.0104 (see table A.5 of Appendix A for detailed results of t-tests). As well, according

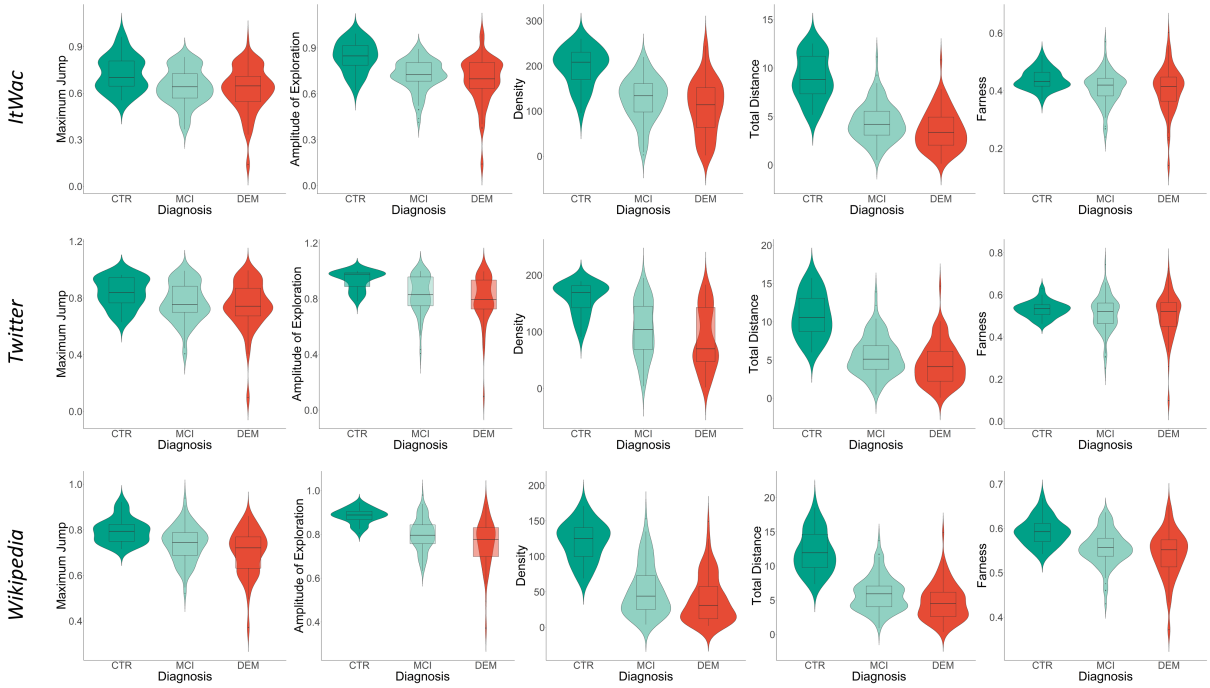

Figure 2.3: **Geometry.** Descriptors of local exploration of concepts for CTR, MCI and DEM. The distribution of the five local descriptors are represented by boxplots within violin plots for each geometry and for each group of subjects. All the metrics are computed using the cosine distance.

to the results of Kolmogorov–Smirnov statistical test, all the metrics, except for Max_j in itwac geometry and far in twitter geometry, reveals to be able in discerning between healthy and non-healthy subjects all having p-values ≤ 0.0304 (see table A.4 of of Appendix A for detailed results of Kolmogorov–Smirnov statistical test). Remarkably, the distance d is always significant not only in discerning between healthy and non-healthy subjects but also between different stages of dementia according to both Kolmogorv-Smirnov and t-test (p-values of KS test in all the geometry are ≤ 0.0209, p-values of t-test in all the geometry are ≤ 0.0076). Interestingly, in the *wikipedia* geometry, all the metrics turn out to be significant in distinguishing between all the three categories, i.e healthy controls and the two stages of dementia MCI and DEM (all KS tests having p-values

≤ 0.0233), except for far and Max_j. As well, also for the t-tests the metrics are significant, (all having p-values ≤ 0.017867), except for far.

Results on local exploration can be summarize as follow:

- all the metrics can be used in all the geometries to separate between healthy and non-healthy, except for Max_j in itwac geometry and far in twitter geometry;
- all the metrics should be used only in the Wikipedia geometry, excluding the far and Max_j, to discriminate between the three categories (DEM, MCI and healthy);
- the distance d metric is robust across the three word embeddings in separating all the three categories. It should be used when considering the itWac and the Twitter geometry to discriminate between different stages of dementia.

It is worth noting that the Wikipedia word embedding is a multidimensional space of 300 dimensions, that is, more than double compared to the other word embeddings used in this study (itWac and Twitter), which have 128 dimensions. This means that, to some extent, the Wikipedia geometry contains more information encoded in the relationship between words. Thus, it could be possible that metrics computed in the Wikipedia geometry are able to discriminate between all the three categories precisely because of this higher information stored in such a word embedding.

2.6.2 Hierarchy

The explorative potential is able to discriminate between healthy and non-healthy subjects according to both KS tests and t-tests strengthening what we found at the local scale (p-values ≤ 0.0026, see tables A.6,A.7 of Appendix A for detailed results).

Figure 2.4 shows the tanglegrams of the pair MCI-DEM for the three semantic spaces. It reports as well the values of Baker's Gamma correlation [29] compared with the null models for all the pairs. What is clear in this analysis is the strong correlation between MCI and DEM in the hierarchy through which the concepts are explored. This is evidenced by the values of Baker's correlation – equal to 0.88 in *itWac*, 0.97 in *Twitter* and 0.73 in *Wikipedia* – and is validated by the null model, in contrast with the correlation for all other pairs. In fact, the values of correlation between the stages of dementia and healthy controls, are always close to zero in the three geometries (two-dash lines in Fig.2.4).

2.6.3 Networks

Network of concepts, generated through Markov chains, are displayed in Fig.2.5. Because of clustering mapping, the number of nodes in the networks varies within the same group according to the geometry (Itwac: CTR 19, MCI 13, DEM 11; Twitter: CTR 16, MCI 12, DEM 9; Wikipedia: CTR 32, MCI 25, DEM 28). Overall, non-healthy patients explore a smaller portion of the semantic nodes with respect to healthy control. Interestingly, for the geometries of *itWac* and *Twitter*, there is a progressive decrease in the number of visited nodes going from CTR to MCI and from MCI to DEM, fostering the idea of a progressive loss in semantic memory due to dementia. Not all the considered correlation measures between the steady states and the mean first passage time matrices agree in ranking the similarity between the analysed groups, and only some specific combinations of geometry-correlation measure highlight higher correlation for the couple MCI-DEM. In particular, this is true for the values of Spearman correlation in *Itwac* and *Twitter* geometries and for the ones of Pearson correlation in *Wikipedia*, when considering the steady states (specific results are reported in tables A.8-A.10 of Appendix A). Finally, the higher correlation

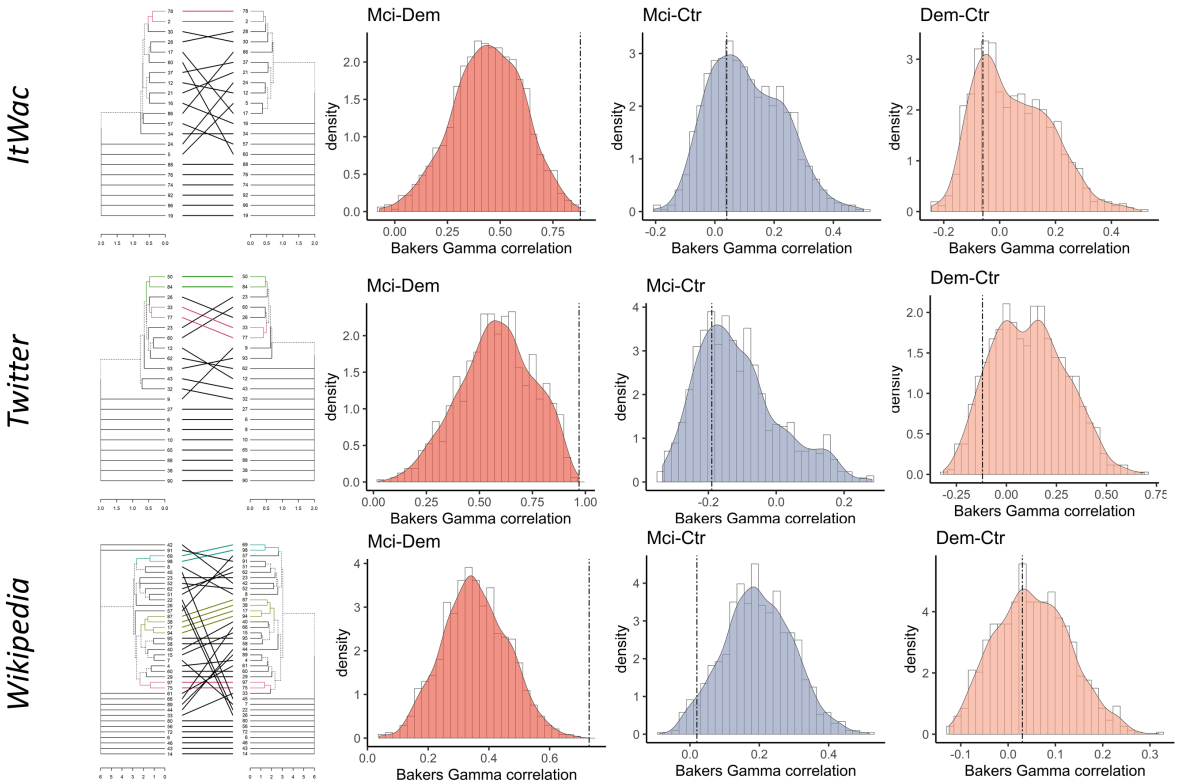

Figure 2.4: **Hierarchy in exploration of concepts.** Tanglegrams of the pairs MCI-DEM with null models of Baker's Gamma correlation for all the pairs, for each semantic space. Colored density functions represent Baker's Gamma correlation of the null models while two-dash vertical intercept is the real value of correlation.

between MCI and DEM is confirmed in mean first passage time matrices, where the values of Pearson correlation are the highest for the couple MCI-DEM while the euclidean norm of their difference is the smallest, evidence of similarity between the two groups in all the geometries (specific values reported in tables A.11-A.13 of Appendix A).

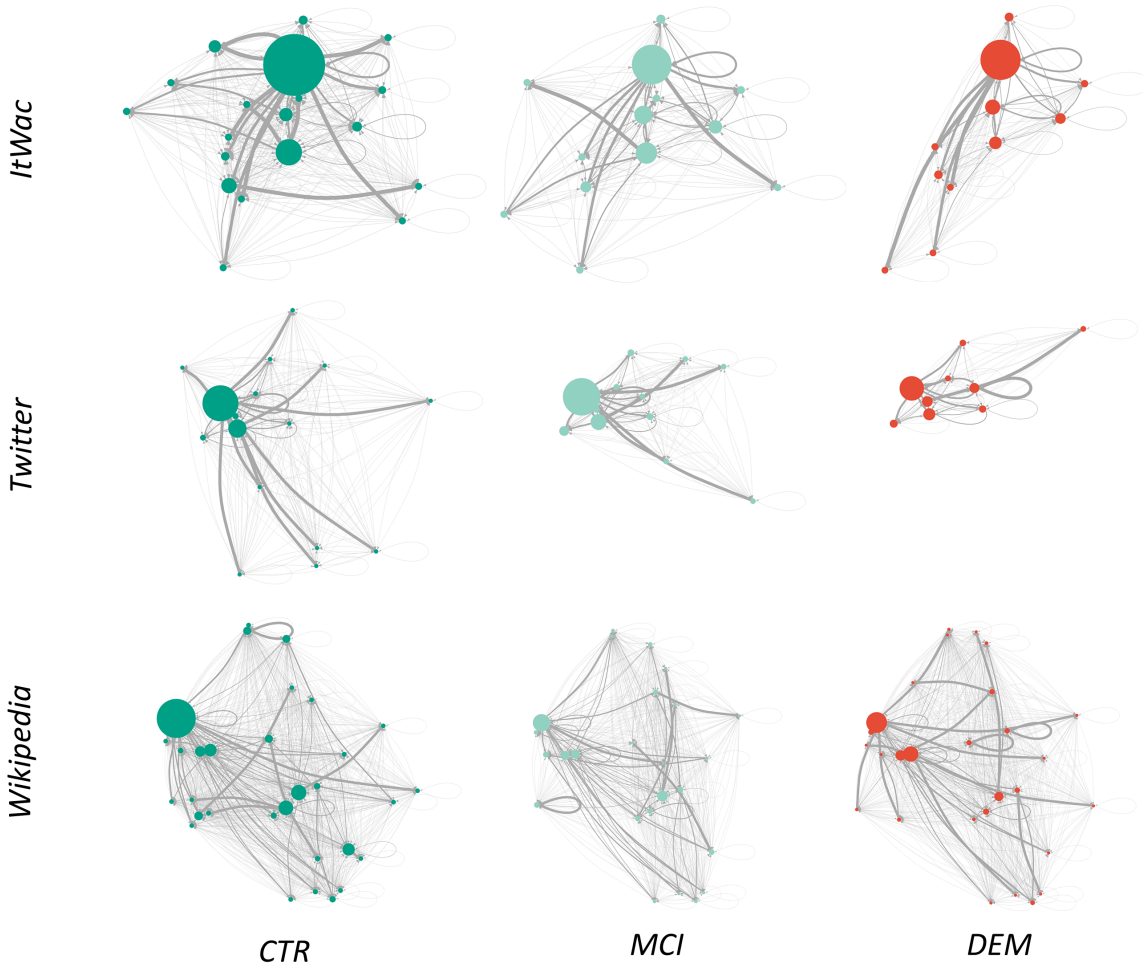

Figure 2.5: **Networks.** Mapping mental pathways emerging from the navigation of concepts in healthy controls (CTR), mild cognitive impairment subjects (MCI) and patients with dementia (DEM). Networks of concepts as reconstructed from semantic verbal fluency tests, for the three semantic spaces. Colored nodes encode clusters of concepts reported by patients while performing the test where they are asked to report words belonging to animal category. The size of nodes is proportional to the nodes' strength, while the thickness of the edges is proportional to their weight.

2.7 Concluding Remarks

In this chapter, we focused on mental pathways, considering the exploration process in the human mind, in both health and disease. Aware of the historical dichotomy between semantic space and semantic network when modeling the exploration process, here we probed the hypothesis of semantic space by testing *how plausible is* the existence of a *latent geometry* underlying exploration of concepts in human mind. As well, we probed whether this geometry is suitable to discriminate between healthy and non-healthy subjects.

This work relies on a unique (and exclusive) clinical data set, including semantic verbal fluency records of 215 subjects, among which there are patients at different stages of dementia (DEM, MCI) and healthy controls (CTR). By leveraging on three different word embeddings and by formalizing suitable metrics, we measured and characterized the spatial navigation of concepts. Remarkably, we demonstrated why is plausible that the mental navigation process occurs on a latent geometry, understood as an organized manifold of lexical information, explored during the process of memory retrieval.

We examined the exploration process, integrating both perspectives – space and networks – according to an approach which builds upon the geometry, at the concept scale, and culminates with diagnosis-based semantic networks, passing through the mesoscale organization of concepts. From the one hand, semantic networks give not satisfactory strength of evidence in discerning between the considered categories (CTR, MCI, DEM). Despite our approach succeeds in reproducing a degradation in the semantic network structure [63] passing from healthy to non-healthy subjects, results vary according to word embeddings and correlation measures, consequently proving the semantic network approach to be indicative but not

definitive. On the other hand, the geometric approach gives significant results in revealing differences between healthy and non-healthy subjects, not only through local descriptors but also at the mesoscale. Our results suggest how the proposed metrics, coupled with word embedding, should be chosen according to the purpose (i.e. discriminate between healthy and non-healthy and/or discriminate between all the three considered categories, Alzheimer's disease, Mild Cognitive Impairment, healthy).

We conclude that the geometric framework is an effective and robust approach to investigate the semantic memory retrieval and to assess its abnormal navigation in patients at different stages of dementia. For this reason, our metrics could be used in support of the clinical assessment as a data-driven tool for confirming – and not *yet* predicting – the diagnosis. This would help planning the longitudinal referral, for example by establishing a six-month visit interval for DEM patients and a one-year interval for MCI patients, avoiding stressing the latter ones with close in time visits.

Our investigation represents the very first step to provide a new data-driven framework to eventually predict the diagnoses from fluency data, when more of such clinical data will be available. Further development of this work should include also a cohort of elderly healthy controls.

Possibly, knowing if a patient is more performing in the density of explored concepts – many words of similar meaning – or in changing context – $MaxJ$, DOE – could help developing future targeted cognitive stimulation based on the value of such metrics. In fact, cognitive stimulation [213, 28] can tremendously prevent patients from abusing of pharmacological therapy in favor of personalized and more targeted exercises for the maintenance of residual capacities. In other words, improving our understanding of memory retrieval task and impaired cognitive search could considerably improve the life quality of people with dementia, often prone to develop secondary diseases, such as depression [234], related to the inability to

express or recall concepts. Finally, given the robustness of our results in separating healthy and non-healthy subjects, the geometric approach could be wisely used to develop digital pre-triage tools, categorizing *healthy/non-healthy* before the clinical examination. This would be of tremendous help in avoiding unnecessary visits to healthcare facilities. Our goal might seem ambitious and definitely challenging but maybe not so unrealistic considering the historical moment we are living in due to COVID-19. In fact, preventing most susceptible subjects – such as those elderly people suspected of dementia – from unnecessarily going to healthcare facilities, could considerably safeguard their lives.

In the next chapter, we will dive more theoretically into the dynamical process of navigation, intended as the result of a routing strategy. Based on the fact that exploration in real-world scenarios is somehow driven by hybrid choices, balancing efficiency and randomness due to external factors, we observe that such choices are far from being adequately explained by existing routing protocols, e.g. random walk or shortest path. To bridge this gap, we provide, and mathematical formalize, a new class of stochastic processes, based on biased random walks, able to span from randomness to efficiency.

Chapter 3

A new model for exploration: the Potential-Driven Random Walk

In brief

In this chapter we investigate the process of *navigation*, from a theoretical point of view. In real-world scenarios, interconnected systems have to route information to function properly: at the lowest scale neural cells exchange electrochemical signals to communicate, while at larger scales animals and humans move between distinct spatial patches and machines exchange information via Internet through communication protocols. Non-trivial patterns emerge from the analysis of information flows, which are not captured either by broadcasting, such as in random walks, or geodesic routing, such as shortest paths. In fact, alternative models between those extreme protocols still elude us. Here, we propose a new class of stochastic processes, based on biased random walks, where agents are driven by a physical potential pervading the underlying network topology. Methodologically, our potential-driven random walks open the doors to a broad spectrum of new analytical tools, ranging from new random-walk centralities to geometry induced by potential-driven network processes.

3.1 Introduction

The *search* is a key cognitive feature which operates similarly across different scales and contexts [154]. Indeed, as discussed in the previous chapter (Sec.2.2), the search for concepts in memory is remarkably similar to the search for resources in space (e.g. optimal foraging) [152, 154]. Most importantly, the search at various levels is permeated by the ineluctable trade-off between exploiting what is known and exploring what is unknown [154]. In this chapter, we made a step further in the modeling of such a trade-off, by formalizing a new stochastic process that balances efficiency (exploitation) and randomness (exploration). Our work arises from the need for a continuous spectrum of dynamics spanning from shortest-path to random-walk routing, able to incorporate simultaneously local and global information when modeling real-world scenarios. For example, human movements and information flows (e.g. across the brain [26]) are known to lie in the grey area between random and geodesic paths.

This chapter has been published as a research article in the peer-reviewed journal *Physical Review E*, in 2021 [51] and is available here.

3.2 State of the Art

Communication, transport, mobility are just few examples of real domains involving the movement of particular entities – information, commodities, animals or human beings – from one place A to another place B. *How* point B is reached from A varies according to the routing strategy adopted by the agents. Notably, routing strategies on networks are mostly based on shortest path or random walk protocols. On the one hand, shortest path protocols assume global knowledge of the network, driving agents to follow the routes minimizing a cost function among the available ones.

However, this approach is not always feasible because either we lack global knowledge about the system or the computational resources to exploit it, as for the search in the World Wide Web. On the other hand, random walk protocols rely only on local knowledge and, consequently, take a longer time to reach a destination, therefore providing a misrepresentation of real-world navigation processes where, for example, it is rare for an agent to randomly proceed on her journey.

The limits of this dichotomy is manifest if we consider the human navigation, where route choice strategies are, in first approximation, driven by the objective of minimizing time and travel costs [293]. However, route choice can be at same time also influenced by other external factors, such as traffic restrictions, unexpected queuing times due to special events [42], the application of congestion pricing schemes [256], the relative pleasantness of routes [229], or other preferences such as the desire of minimizing the number of turns [187] which may strongly variate the cost function between individuals. On the other hand, while being the most efficient way of proceeding, even when considering possible detours due to traffic congestion or other user initiatives, following the shortest path requires a complete knowledge of network topology [192]. Often, such knowledge is not available and only partial information on network structure can be considered (i.e. the degree of neighbors). The problem of routing information within a network without global knowledge about the system is related to a variety of applications from neuroanatomy and social sciences to communication and infrastructure engineering. For instance, it has been shown that the small-world topology of some systems, which are characterized by the presence of long-range links, favor the finding of paths which allow for the efficient delivery of information towards the destination [171] (see also [170] for a review), as well as for the efficient navigation of an interconnected system, the latter being favored by the presence of a la-

tent metric space [60]. Recently, the trade-off between information routing through the shortest path, network entropy and stability has been pointed out [107]. Even when complete information is available, human navigation is anyways limited by the cognitive resource that can be assigned to the task [119] which has as consequences the need for heuristics to simplifying mental representation of the space [188] and the over-reliance on habitual routes [175]. The combination of all these uncontrollable and individual factors yields to the ensembles of trajectories empirically observed a high level of randomness. Regardless of the urban layout, a significant portion of trajectories within a city does not follow the shortest path between two specific origin and destination points [309], but rather prefers some other eligible paths contained in the ellipse generated from these origin and destination points, coinciding with the two foci of such an ellipse [180]. As a consequence, even if it is known that the human routing is based on cost minimization, for some scenarios of analysis also random walks have also been proposed as suitable alternative to develop routing strategies on networks [192, 7, 126]. It is thus clear that real human trajectories over transportation networks fall between these two opposite paradigms, shortest path routing and random walks. The same can be said in other notable cases such as the flow of information across the brain [26] or animal movements, where the "base" model is that of random walks and diffusion, but observed paths often display high level of correlation at microscopical level [78] and are ultimately driven by optimized strategies reached through evolution [290].

3.3 The Problem

As observed in the previous section, a myriad or real-world routing strategies are somehow sub-optimal, lying in the grey area between random and

geodesic paths. Nevertheless, alternative models between those extreme protocols are still eluding us. There is therefore a need for a continuous spectrum of dynamics between shortest-path and random-walk routing that can describe paths balancing efficiency and randomness integrating at the same time local and global information [26]. Moreover, the need for overcoming deterministic routing strategy and embracing a degree of randomness is motivated by a realm of ordinary and extra-ordinary situations where uncertainty eventually proves to be useful. Avoid congestion and/or avoid predictability of a routing strategy for security purposes are a few common examples of such an eventuality. This problem is known in the literature as randomized shortest-path problem (RSP) [237]. As illustrated in the previous lines, in the field of human mobility, the ensembles of trajectories empirically observed exhibits emergent behaviors that overcame the shortest paths demonstrating that humans do not make optimal decisions, but suboptimal. As anticipated in the Introduction (Subsec.1.1.1), neuroplasticity enables brain neural networks to change, reorganize and grow leading to significant implications for healthy development, learning, memory, adaptation to changing environment and recovery from brain damage [219]. This means, for example, that brain routing strategies are flexible and not fixed to one optimal path [218]. Thanks to this flexibility, pattern of cortical activation can change over time allowing for new skills and abilities to be learnt [218]. The behavior of people moving in a city and the one of neural connections evolving in the brain thanks to neuroplasticity could be lively examples of an effect due to a particular field influencing such a behavior. In the animal kingdom, a phenomenon known as stigmergy drives animals to follow some preferential paths according to the trace left in the environment by other individuals of the same species. Stigmergy is an example of indirect communication where individuals communicate with each other by modifying the surrounding

habitat. In this case we could say that a field emerges from the interaction between animals and their environment. An extraordinary example of routing strategies evolving in space based on the availability of resources is given by the brainless slime mold, whose efficiency to forms networks is comparable to those of real-world infrastructure networks [276]. This is brilliantly proved in a study where, arranging food in a scattered pattern as the one of Japanese cities around Tokyo, makes the slime mold building networks of nutrient which strikingly resemble the layout of the Japanese rail system [276]. Here we could compare the food resources to physical particles giving rise to a field and driving the slime mold towards specific targets. Finally, a system can benefit from continuous exploration, mostly when considering nonstationary conditions: for instance, one can think about the animal foraging in a changing environment, where agents routing towards the optimal path would miss the opportunity to encounter new patches to feed on. Exploitation of what is known and exploration of what is unknown is an ineluctable trade-off in space, society and even in the human mind [154].

3.4 The Proposed Approach

Here, we take a step further in modelling the trade-off between exploitation and exploration, by overcoming pure deterministic routing strategies and allowing for a continuous exploration of the system, embedding our model with information about pre-existing fields or emerging fields.

To work in this direction, we build upon the most recent literature about random walks on networks. Two main approaches of *biased* random walk have been proposed that encapsulate any available information on particular network features. The first approach is the *degree-biased random walk* [105, 176, 117, 61], here the transition probability from one node to

its neighbors is biased according to the degree of its neighbors. Depending on the sign of the bias parameter, the walker will explore the network by visiting the hubs or by passing through poorly connected nodes. The second approach is the *maximal-entropy random walk* [130, 251] where the step transitions probabilities are defined in such a way that the walker disperses maximally in the network. Also in this second case, the transition probabilities from one node to another one are biased according to some topological features (e.g. degree), or to any relevant property for the diffusion dynamics (e.g. level of congestion), of its nearest nodes. Recently, a *memory-based random walk* has been proposed to extend the local information up to the next nearest neighbors [33]. Despite the efforts made to include more and more information about nodes' features up to the second order nearest neighbors, little is known about routing strategies when the known information is scattered over the network or when it affects only some particular nodes. In the last decade, in parallel to the family of *biased* random walks, a new framework aimed to interpolate between shortest path and random walk rised up, i.e. the Randomized Shortest Paths (RSPs) [237, 47, 169]. The RSPs exploits a thermodynamic formalism by considering the temperature distribution over paths. By adjusting such temperature parameter the walker mediates between a minimal travel cost and the maximal exploration of the network. A close proposal, similar in intents – i.e. interpolating between shortest path and random walk – yet different in the implementation, has been provided to investigate the routing of neural signals [26]. This last proposal suggests a possible model for network communication merging local and global information about topology and generating a new kind of biased random walk. For each node, the bias is encoded by a degree of knowledge of the underlying network topology [26]. Specifically, the transition probabilities from one node to its neighbors depend on two factors, i.e. the length of the edge

connecting the node with its neighbors (local information) and the degree of knowledge regarding the distance of such neighbors from the target node (global information). Nevertheless, the shortest path between all pairs of nodes is always required to build the transition matrix of such a random walk [26]. In fact, in all cases except for the trivial unbiased random walk, the shortest path between all pairs of node contributes in defining the degree of (global) knowledge of the network, properly modulated by a bias parameter.

In this chapter, we define a new walk, grounded on physics, which tends to minimize distances (like a shortest path; a global feature) while keeping some flexibility in random exploration (like a random walk; a local feature). In particular, we propose a new process, the potential-driven walk, that effectively interpolates between shortest path and random walk routing protocols thanks to the presence of a potential field defined on the top of the network and acting at each node. By combining knowledge of local features and (partial) global information about network topology, we propose a new type of biased random walk where the bias is generated by the potential, which in turn can take different functional forms and can be expressed in different ways depending on background assumptions. The potential-driven random walk does not require to control the randomness of exploration by fixing the entropy spread – or other global variables – on top of the network nor to define a temperature parameter regulating the free wandering in the system (as in the case of RSPs), which is a computational advantage besides being a conceptual shift. In our framework, we do not fix nor constrain any variables a priori (e.g. entropy constraint), instead we establish where to put the potential node. The dynamical process we proposed minimizes the distances while allowing for some flexibility in the exploration of the system, by relying on simple and well-known network measures, properly biased to continuously

interpolate between random walk and shortest path. Thereby, our walker acts as a physical particle which moves according to stochastic rules but potential-driven. Notably, our methodology allows for embedding the transition matrix with information about pre-existing fields or emerging fields. Remarkably, our framework is able to reproduce some salient feature regarding animal and human movements.

3.5 Methods

3.5.1 Potential-Driven Random Walk

Let us consider a finite connected graph of nodes $i = 1, ..., N$ whose connectivity is defined by the adjacency matrix $\mathbf{A}$. The element $a_{i,j}$ of $\mathbf{A}$ is equal to 1 if a link exists between node i and node j and 0 otherwise. Now let us arbitrarily choose a drifting node ℓ and imagine the following dynamical process: a free wandering walker moving from node i to node j is subjected to a potential responsible for drifting the walk towards (or away from) the drifting node ℓ of the system. The master equation of the potential-driven random walk reads:

$$p_j(t+1 \mid \ell) = \sum_{i=1}^{N} T_{ij}(\ell) p_i(t \mid \ell) \tag{3.1}$$

where $p_j(t+1 \mid \ell)$ is the probability of being in j at time $t+1$ given the presence of ℓ and $T_{ij}(\ell)$ is the transition probability of the potential-driven random walk from node i to j. Specifically, we proposed a biased transition matrix whose elements are defined by:

$$T_{ij}(\ell) = \frac{c_j(\ell) a_{ij}}{\sum_{n=1}^{N} c_n(\ell) a_{in}} \tag{3.2}$$

It is to be noticed that the denominator serves as a normalization factor and n is an other index indicating the network nodes. At this point we have to define what is the bias factor $c_j(\ell)$. As stated before, the bias generated by the potential can take different functional form. To define the bias of the potential-driven random walk, we consider the combination of two fundamental variables: i) the topological distance from the potential $d(\ell)$ and ii) the node's degree k. Here, we assume that the potential has a gravitational-like form and it is centered in a node ℓ so that a walker in node i will randomly select a neighbor j while i) being attracted (repulsed) by ℓ inversely (directly) proportional to their relative topological distance; and ii) being biased by the presence of network hubs in its neighborhood. Under these assumptions the bias factor $c_j(\ell)$ reads:

$$c_j(\ell) = d_{j\ell}^{\gamma} k_j^{\beta} \tag{3.3}$$

where $d_{j\ell}$ is the topological distance between j and the potential ℓ and k_j is the degree of node j, γ and β are the bias parameters. It is to be noticed that, when there is no dependence on any other node in the network but only of the neighbor at most, i.e. when $c_j(\ell) = c_j$ we would have the classical biased random walk. When, instead $c_j = const$ it is easy to show that the classical non-biased random walk is restored. In Fig.3.1 we report an illustrative example of the so defined potential-driven random walk. For ease of reading, only the topological distance from potential is considered in the bias factor (i.e. $c_j(\ell) = d_{j\ell}^{\gamma}$), which actually represents the innovative aspect of this work.

By tuning the bias parameters γ and β we define the dependence of the process on the potential and on nodes degree. When $\gamma < 0$ the walker is drifted towards the node ℓ, while $\gamma > 0$ implies a repulsive potential from ℓ, $\gamma = 0$ is the classical biased random walk. Hence, in case of attractive

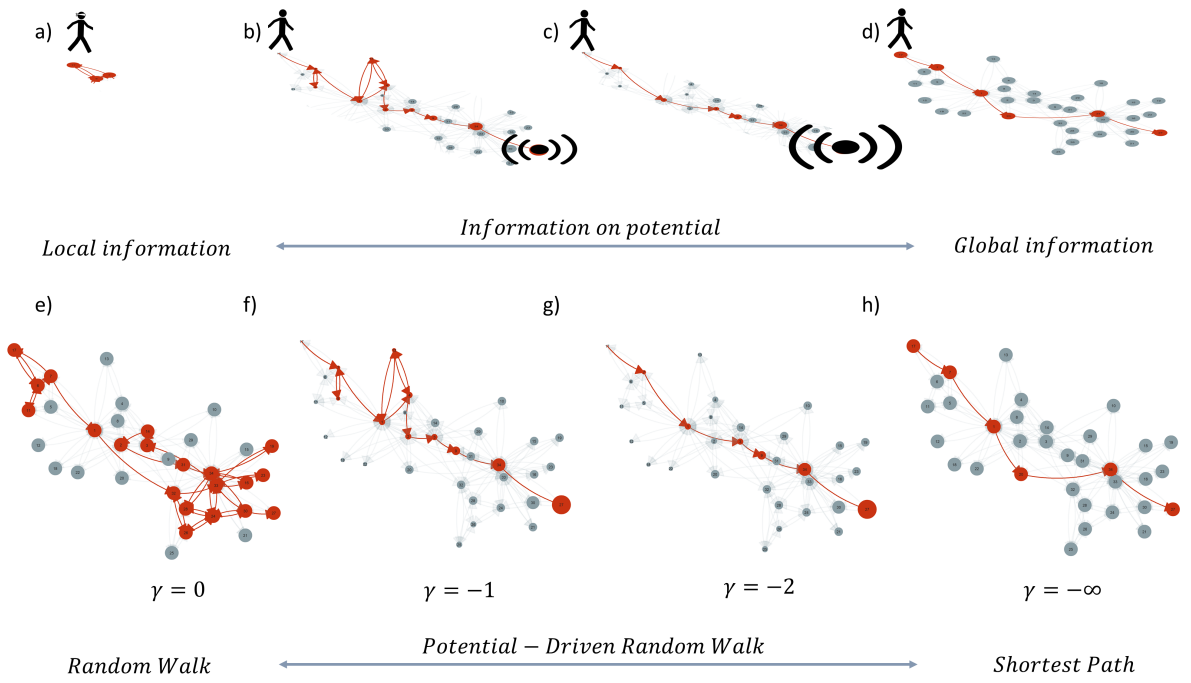

Figure 3.1: **Interpolating between random walk and shortest path: the potential-driven random walk.** Illustrative example of potential-driven random walk with different values of bias parameter γ on the Zachary's karate club network [304].The group of networks on the top half of the figure (panels a),b),c),d)) encode the same concept of the group on the bottom (panels e),f),g),h)) but in terms of available amount of information. Specifically, the random walker in a) knows ("sees") nothing about the network topology, while the walkers in b),c) are driven by the potential in ℓ (stylized by a black dot with waves) and they thus know ("feel") something about network topology. Finally, the walker in d) knows ("measures") everything about network topology and can therefore take the shortest path. Red nodes and red links encode the path followed by the potential-driven random walker varying γ. When $\gamma = 0$ in a),e) the classic random walk is restored. When $\gamma = -1$ in b), f) and $\gamma = -2$ in c), g) we are in the case of *attractive* potential-driven random walk. When $\gamma = -\infty$ in d), h) we are in the case of shortest path. Note that the size of the nodes in case of potential-driven random walk, i.e. in b),c),f),g), is inversely proportional to the distance from ℓ, which corresponds the target node (node id=27).

potential, the target node of a potential-driven random walk coincides with ℓ. When $\beta < 0$ the motion is biased towards poorly connected nodes, while if $\beta > 0$ the walker will favor hub nodes. In case $\beta = 0$ (and $\gamma = 0$)

the classical random walk is restored. To sum up: γ defines where the walker is potential-driven, towards or away from ℓ, and β establish how the walker is driven, i.e. towards hubs or poorly connected nodes. By considering the stochastic process of the potential-driven random walk in terms of its Markov chain representation we can characterize the walk through the steady-state distribution $\mathbf{p}^*$ and the mean first passage time matrix **MFPT**. In fact, if the Markov chain is ergodic, i.e. every state of the chain can be reached by any other state (the graph is connected), then the steady-state distribution $\mathbf{p}^*$ exists, is unique and

$$\lim_{t\to\infty} T^t(\ell)\mathbf{p}(0) = \mathbf{p}^*(\ell) \quad \forall \mathbf{p}(0) \tag{3.4}$$

Where $\mathbf{p}(0)$ is the distribution of the initial state. Following a procedure similar to the one presented in [130], in the next lines we derive the analytical expression for the steady-state distribution $\mathbf{p}^*(\ell)$ of the potential-driven random walk. Let us consider the probability to go from node i to node j in t time steps $P_{i\to j}(t)$. If the network is undirected then $a_{ij} = a_{ji} \forall i, j$ and so the relation between the probability of going from i to j in t time steps and the probability of going from j to i in the same time can be defined as [130]:

$$b_i c_i P_{i\to j}(t) = b_j c_j P_{j\to i}(t), \tag{3.5}$$

where $b_i = \sum_j a_{i,j} c_j(\ell)$. For the steady-state distribution $\mathbf{p}^*$, the the same relationship applies so that $b_i c_i p_j^* = b_j c_j p_i^*$ and, through the detailed balance condition, it can be shown that:

$$p_i^*(\ell) = \frac{b_i(\ell)c_i(\ell)}{\sum_v b_v(\ell)c_v(\ell)} = \frac{\sum_j a_{i,j} d_{j,\ell}^{\gamma} k_j^{\beta} * d_{i,\ell}^{\gamma} k_i^{\beta}}{\sum_v \sum_j a_{v,j} d_{j,\ell}^{\gamma} k_j^{\beta} * d_{v,\ell}^{\gamma} k_v^{\beta}} \tag{3.6}$$

Note that, in case γ and β are equal to 0, the classic random walk is restored:

$$p_i^* = \frac{\sum_j a_{i,j}}{\sum_v \sum_j a_{v,j}} = \frac{k_i}{2m} \tag{3.7}$$

with m corresponding to the number of edges in the network. At this point, we probe the mean first passage time matrix **MFPT** of the potential-driven random walk. The **MFPT** matrix defines the average number of steps required to a walker starting in node i to reach a specific node j. To obtain the **MFPT** matrix we followed the matrix solution proposed by [137]. Particularly, we make use of the fundamental matrix $\mathbf{Z}$:

$$\mathbf{Z}(\ell) = (\mathbf{I} - \mathbf{T}(\ell) + \mathbf{W}(\ell))^{-1}, \tag{3.8}$$

Where, in our case, $\mathbf{I}$ is the identity matrix, $\mathbf{T}$ is the transition probability matrix of the potential-driven random walk and $\mathbf{W}$ is a matrix having all rows equal to $\mathbf{p}^*(\ell)$. For an ergodic Markov chain, the entries $m_{ij}(\ell)$ of the mean first passage time matrix **MFPT** can be obtained from the fundamental matrix $\mathbf{Z}(\ell)$ as [137]:

$$m_{ij}(\ell) = \frac{z_{jj}(\ell) - z_{ij}(\ell)}{p_j^*(\ell)} \tag{3.9}$$

Finally, we can compute the estimated variance numerically, while its analytical formulation lies outside the purpose of this current work. For the reader interested in proceeding with this formulation we refer to [161]

3.6 Synthetic and Experimental Results

We now have defined the key descriptors for the dynamical process of the potential-driven random walk, i.e the steady-state distribution and the

mean first passage time matrix. In this section, we put these indicators into play on different network topologies. In particular, we show how the stationary distribution varies according to the presence of attractive or repulsive potential(s) in case of one single potential (monopole), two potentials (bipole) and more than two potentials (multipole) on top of ordered topology networks, i.e. on lattices. Specifically, in the case of monopole, a single node is considered as a source of potential – which can be either attractive or repulsive –, while in the case of multipole a scenario with multiple sources of potential (nodes) – attractive, repulsive or both – is considered. We prove as well that our approach is effective for computing the mean first passage time matrix by comparing analytical results with simulated results on disordered network topologies, i.e. on random networks, scale-free and small-world networks, random geometric graphs, (hierarchical) stochastic block models and Lancichinetti-Fortunato-Radicchi (LFR) networks. Finally, we provide a measure, that defines to what extent the potential-driven random walk deviates from the shortest path in different topologies according to the value of bias parameter γ and β. We call this measure straightness index on networks, reminiscent of the homonymous index defined by Batschelet in 1981 [45] to define the tortuosity of animal's paths in the physical space.

3.6.1 Lattices

Let us suppose the following scenarios. Imagine one is in a city and she has to go, for instance, to the mall. Which route would she (most likely) follow? What if there is a more convenient mall around or multiple ones? One can also imagine the scenario where, in addition to a potential destination (e.g., a mall), there are also restricted traffic zones that one should avoid [90]. How the knowledge of all this information shapes one's routing strategy? In this section, we illustrate how the potential-driven random walk provides a

suitable way to model such scenarios in a physically grounded and elegant way, giving plausible answers to these questions. Before illustrating the modeling of the aforementioned scenarios, we generalize the bias factor and the steady-state distribution to the case of multipole, as in following Eq.(3.10) and Eq.(3.11) respectively:

$$c_j(\ell_1, ..., \ell_L) = k_j^{\beta} \prod_{\ell=\ell_1}^{\ell_L} d_{j\ell}^{\gamma} \tag{3.10}$$

where ℓ is the variables indicating the potential nodes within the system,

$$p_i^*(\ell_1, ..., \ell_L) = \frac{\sum_j a_{i,j} k_j^{\beta} \prod_{\ell=\ell_1}^{\ell_L} d_{j\ell}^{\gamma} * k_i^{\beta} \prod_{\ell=\ell_1}^{\ell_L} d_{i\ell}^{\gamma}}{\sum_v \sum_j a_{v,j} k_j^{\beta} \prod_{\ell=\ell_1}^{\ell_L} d_{j\ell}^{\gamma} * k_v^{\beta} \prod_{\ell=\ell_1}^{\ell_L} d_{v\ell}^{\gamma}} \tag{3.11}$$

It is to be noticed that the generalization to the multipole requires the product of the distance from the nearest neighbors (j) to all potential nodes $(\ell_1, ..., \ell_L)$.

Let us consider a 9×9 regular lattice (81 nodes) and first pick a drift node ℓ on top of this lattices (as in the first lattice of Fig.3.2a).

Now imagine a walker, subjected to the presence of such a drift node ℓ, i.e. a potential-driven random walker. According to the nature of this potential – repulsive or attractive – the dynamical process described by the master Eq.(3.1) will drive the walker respectively far from the node ℓ or towards node ℓ. This is well described by the value of the steady state distribution (SS), represented by the node's size, in the first lattice of Fig.3.2b – repulsive potential – and in the first lattice of Fig.3.2c – attractive potential. The steady state distribution has been computed by means of Eq.(3.6)considering a linear dependence from the distance from

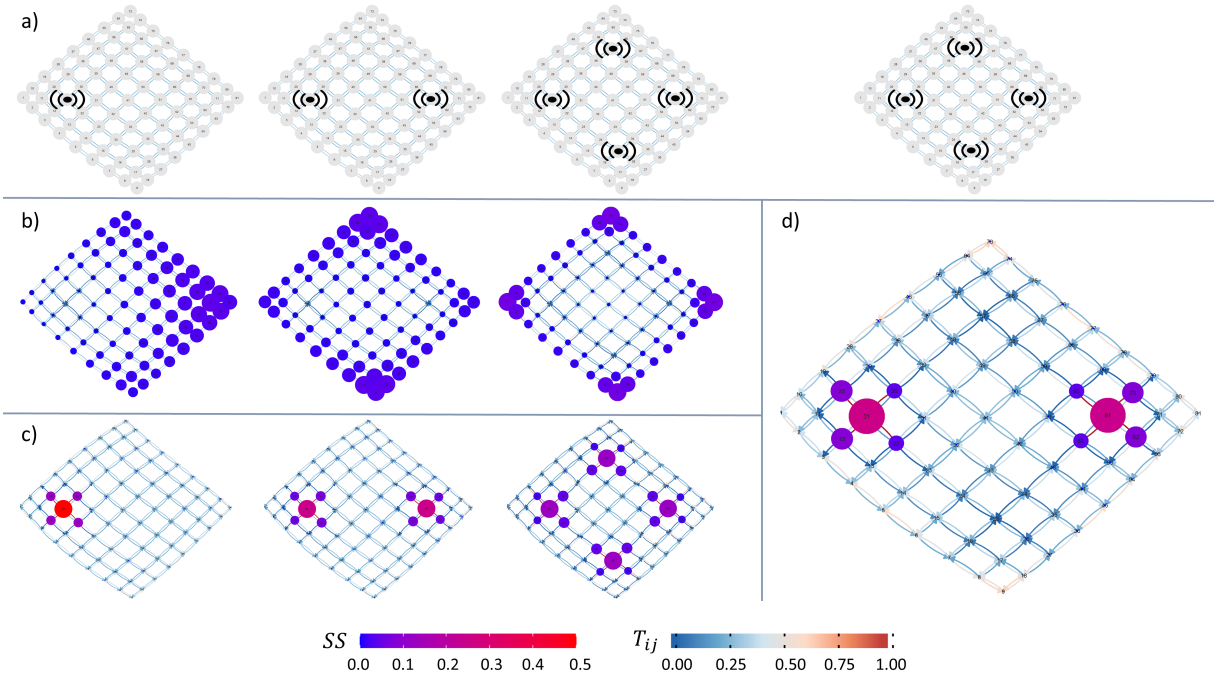

Figure 3.2: **Probing the potential-driven random walk on lattices.** In a) we indicate the position(s) of the potential(s) (i.e. where are the potentials) on top of the lattices, represented as a black dot with waves. From left to right we have the case of monopole, bipole and multipole (shown twice), to test distinct scenarios of interest. In b) we show the values of the steady-state (SS) distribution for each node in the case of repulsive potential(s), specifically for $\gamma = 1$, i.e. what happens if the potentials were repulsive. In c) we show the values of the steady state distribution for each node in the case of attractive potential(s), specifically for $\gamma = -1$, i.e. what happens if the potentials were attractive. In d) we report a mixed case where potentials are both attractive – extreme left and extreme right – and repulsive – up and down – i.e. what happens if the potentials were mixed. In d) attractive potentials have $\gamma = -1$, and repulsive potentials $\gamma = 2$. The color of nodes encodes the value of its steady state and the color bar applies to all lattices. As well, the size of the node is proportional to the value of the steady state but it is rescaled for each lattice, in this way one can better appreciate the direction towards which the walker is driven. The bigger the node, the bigger the probability to find the walker there at the steady state. Edges color encode the probability to drive along that link (T_{ij}).

ℓ (i.e. $\gamma = \pm 1$). Dealing with lattices, we neglected the bias on the degree (i.e. we put $\beta = 0$) in computing the steady state. Curiously, in the case of repulsive potential (first lattice of Fig.3.2b) the highest probability of

the steady state is not in the farthest node from ℓ (id node=81), which is a node on the border. Instead, the highest value of the steady state distribution corresponds to the farthest node from ℓ of maximum degree (id node=71). In fact, the steady state distribution of a node i depends on its distance from ℓ but also on the distance of all its neighbors from ℓ (see Eq.(3.6)). Therefore, being in a node i having neighbour nodes far from ℓ contributes to increase the probability of being in that node i. The same is true in the case of repulsive bipole and multipole (second and third lattice of Fig.3.2b). Specifically, in the case of bipole the highest probability of the steady state divides between the 4 nodes of highest degree which are simultaneously the farthest nodes from the two repulsive potentials (id nodes=8,18,64,74). Similarly, in the case of multipole, the nodes where the walker is most likely to be when time goes to infinity are the most distant from the 4 poles and the ones of maximum degree simultaneously. The situation is completely reversed in case of attractive potential. As it can be seen in the first lattice of Fig.3.2c, the drift node ℓ generates a basin of attraction that drives the walker toward the neighbors of ℓ and ℓ itself. In particular, the probability of being in ℓ when time goes to infinity is 0.5 (we are in the case of linear dependence from the distance from ℓ, i.e. $\gamma = -1$). The rest of the steady state distribution equally divides between the 4 nodes nearest to ℓ. A similar situation appears in case of attractive bipole and multipole (second and third lattice of Fig.3.2c). Specifically, in the case of bipole two basins of attraction arise around the two potentials, but the steady state probability divides unequally around them. In fact, the nearest neighbors of one pole which are also the nearest to the other pole (the "internal nodes") have a greater occupation probability than the external ones. The same unbalanced configuration arises in the case of multipole, where the "internal" nodes have a greater occupation probability than the "external" ones. It is to be noticed that the pattern around each

pole is the same (see the second and the third lattice of Fig.3.2c). We now reveal what happens in the case of mixed multipole. Let us pick, for example, two attractive potentials and two repulsive potentials on our lattice (Fig.3.2d). Let us assume also that the two flavors of the potential – repulsive and attractive – act with different intensity on the lattice, for example establishing a linear dependence on the distance from attractive potentials and a quadratic dependence on the one from repulsive potentials. The arising pattern of the steady state is equal – in terms of distribution – and, at the same time, opposite – in terms of direction – to the one resulting from the case of attractive multipole (second lattice in Fig.3.2c). In fact, also in this case the two attractive potentials share half of the occupation probability (i.e. 0.25 each). The second half of the stationary probability is divided among the nearest neighbors of these two attractive potentials, but this time the "external" nodes (id nodes=12,20,62,70) have a greater probability than the "internal" nodes (id nodes =22,30,52,60). The reason why this happen is due to the presence of repulsive potentials concomitantly with the attractive ones, which drives the walker towards (one of) the two basins of attraction generated by the attractive poles while keeping the walk as far as possible from the repulsive poles within the basin of attraction, or, more precisely, while preferring nodes far from repulsive potentials among the nearest neighbors of the attractive potentials.

3.6.2 Disordered topologies

Usually, real systems are far from being adequately modeled by lattices. Brain networks, for example, exhibits small-world properties [41] as the Internet [9] or social interactions [295]. Other examples are protein-protein interactions which besides being small-world reveal to be scale-free [298] as the world airline network [140]. Furthermore, some key features of real systems, such as modular structure or spatial embedding, are properly re-

produced when considering more complex topologies, such as stochastic block models and random geometric graphs, respectively. For this reason, in the current section we overcome regular lattices to consider more disordered topologies. Specifically, we now investigate the dynamical process of potential-driven random walks considering 8 different models, each one encoding one specific feature, covering a broad spectrum of the topological characteristics emerging from real-world networks. These models are Barabási-Albert (BA) [8], Erdös-Rényi (ER) [106], Hierarchical Stochastic Block Model [221] with four dense groups per level (HSBM4), Lancichinetti–Fortunato–Radicchi (LFR) [174], Stochastic Block Model [156] with 4 dense groups (SBM4), Random Geometric Graphs (RGG) [84], Scale-Free[8] with scaling exponent -2 (SF2) and Watts-Strogatz (WS) [295]. All networks consists of 256 nodes and their parameters are chosen to obtain an average degree $\langle k \rangle = 12$ or, equivalently, to have about 3,000 links, on average.

To prove that our approach is effective for computing the mean first passage time (**MFPT**) matrix we run 200 simulations of the potential driven random walk for each topology and we compute as well the theoretical values of the **MFPT** by means of Eq.(3.9). It is to be noticed that we can only compute the **MFPT** matrices for the values of $\gamma \leq 0$ (and for all values of β). In fact, for values of $\gamma > 0$ the Markov chain would have a transient state coincident with ℓ (the node where we put the potential). This means that when starting in ℓ there is a non-zero probability to never return in ℓ. For this reason, the Markov chain would not be ergodic consequently making Eq.(3.9) non-applicable. This is the reason why we compute the MFPT only for $\gamma \leq 0$ (and $\forall \beta$), or in other words, in case of attractive potential, i.e. when ℓ coincides with the arrival node. In Fig.3.3 we report, as an example, the values of the simulated mean first passage time versus the theoretical ones, for all $\gamma \leq 0$ and for $\beta = -2$.

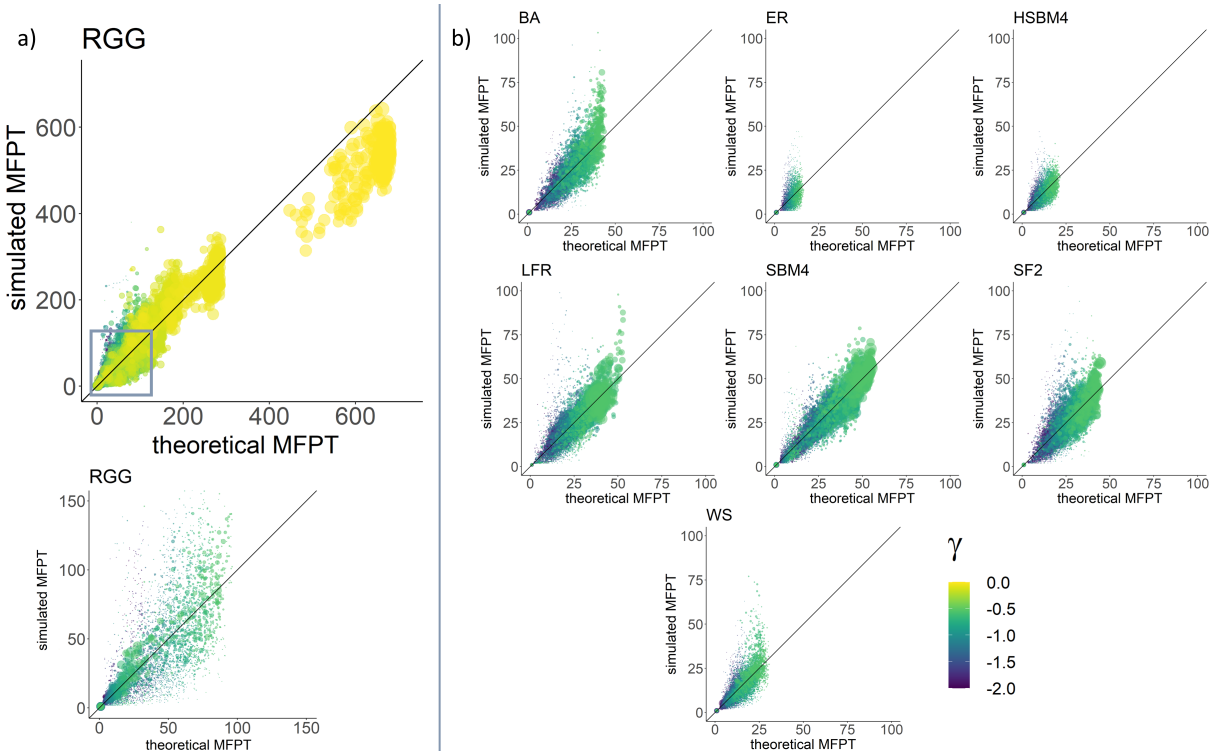

Figure 3.3: **Theoretical versus simulated Mean First Passage Time from all possible source nodes to the target node on different network topologies.** In the top of a) we report the values of simulated mean first passage time versus the theoretical ones for all values of $\gamma \leq 0$ and for $\beta = -2$ considering a Random Geometric Graph (RGG) of 256 nodes. Underneath, we display a zoom of the same graph (in cobalt square) to better appreciate the values of mean first passage time for potential-driven random walk (i.e. when $\gamma < 0$). In b) we directly report the zooms for all the considered network topologies of 256 nodes: Barabási-Albert (BA), Erdös-Rényi (ER), Hierarchical Stochastic Block Model (HSBM4), Lancichinetti–Fortunato–Radicchi (LFR), Stochastic Block Model (SBM4), Scale-Free (SF2) and Watts-Strogatz (WS). The color of the points encodes the values of γ while the size of the node is proportional to the frequency of that sampled values in the simulations.

In particular we plot the value of mean first passage time from all the possible source nodes to the target node on the 8 different network topologies. By design, the target node is the one where we put the (attractive) potential. In each plot of Fig.3.3 the size of the points is proportional to the frequency of that sampled values in the simulations. As it can be noticed,

the most of the values lie on the bisector: these values are also the most frequent in the simulations (bigger points), showing that the theoretical results are in agreement with the simulations. At this point, we investigate how the theoretical values of the MFPT change for different values of bias parameters, results are shown in Fig.3.4. As it can be seen in Fig.3.4, the trend of the theoretical MFPT is qualitatively similar for all the analyzed topologies, with the values of the MFPT increasing as γ increases, until the peak in $\gamma = 0$, i.e. when the random walk is restored. Interestingly, for some topologies there are critical points in γ, i.e. points where increasing β does not lead to decreased values of the MFPT. This regime shift is visible in the following topologies: LFR, RGG, SBM4; and partially visible also in BA and SF2. Let us now randomly pick a simulated values of the **MFPT**

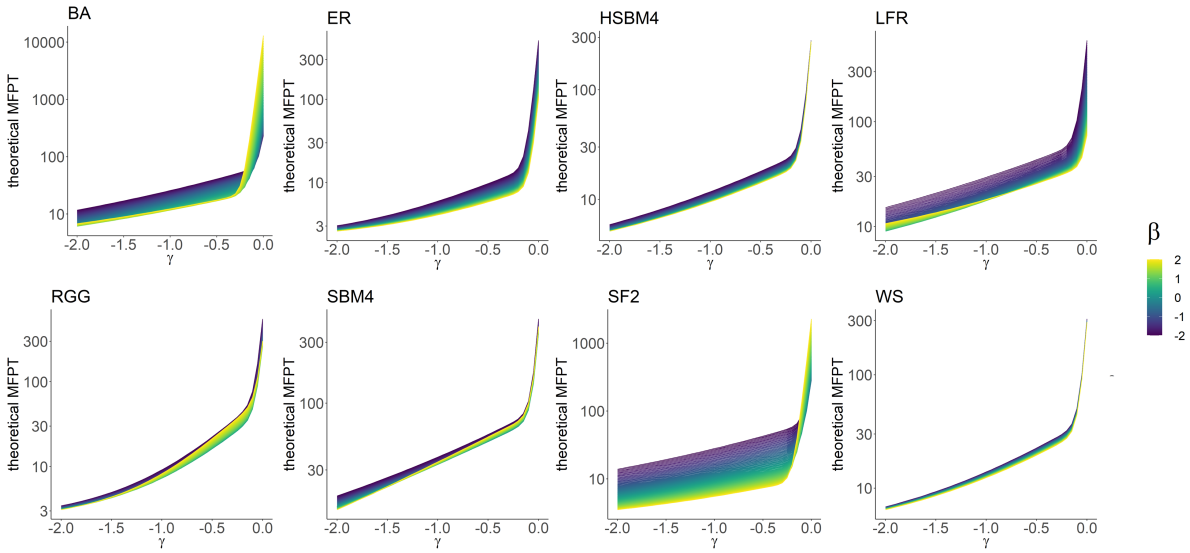

Figure 3.4: **Theoretical Mean First Passage Time for all values of γ and β**, for all the considered network topologies: Barabási-Albert (BA), Erdös-Rényi (ER), Hierarchical Stochastic Block Model (HSBM4), Lancichinetti–Fortunato–Radicchi (LFR), Random Geometric Graph (RGG), Stochastic Block Model (SBM4), Scale-Free (SF2) and Watts-Strogatz (WS). The color of the line encodes the value of β.

from a source node s to a target t. We investigate how good we are in

returning the corresponding values of γ and β, i.e. in guessing to what extent the process is potential-driven. The rationale behind the proposed speculation on matching the right value of γ and β is motivated by the intention to recast a stochastic routing strategy to a potential-driven random walk. More specifically, we investigate if and when we are able to infer the values of γ and β given only the information on i) estimated mean first passage time and ii) the topology of the network. Tracing back the value of γ and β would allow for a more informed definition of a dynamical diffusion process, providing information about the direction towards which and the way a walker reaches a specific destination simply by measuring the time spent on a given topology. This proposal has potential broad applications, e.g. in the contest human and animal mobility to determine if a walker was forced to avoid a given restricted area and/or to establish if the path strategy was preferring hubs or poorly connected nodes, given the values of mean first passage time (MFPT) from source node to target node and the network topology. To this end, we compare a given estimated value of the MFPT to the whole spectrum of the theoretical MFPT values resulting from all values of γ, in the range $[-2, 0]$, and β in the range $[-2, 2]$. We compute the absolute value of the difference between the estimated value of the MFPT and each theoretical value. The theoretical MFPT giving the minimum of such an absolute value determines the inferred values of γ and β. On average, for all the topologies we match the right value of γ 70% of the time, which is 47% more than what we match for β. This makes us speculate that the process is more sensitive to the bias on the distance from the potential (γ) than to the bias on the degree (β). Specifically, we are more likely to guess the values of γ in case of stochastic block models and hierarchical stochastic block models, followed by Erdös-Rényi and random geometric graph. Instead, for what concern scale-free networks, we only match the values of γ 55% of the time. However, the theoretical value

of the MFPT closest to the simulated one – in terms of absolute value – always results to be within one standard deviation.

3.6.3 Straightness index on networks

In 1981, E. Batschelet, a mathematician devoted to the study of animal paths orientation, defined a novel indicator to measure the tortuosity of such animal paths: the *straightness index*. In this vein, we provide a similar indicator for the purpose of measuring to what extent the potential-driven random walk deviates from the shortest path (or how close it gets to the random walk) in different topologies, according to the value of bias parameters γ and β. We called this measure *straightness index* on networks and, given a source node s and a target node t, we define it as follow:

$$sI = \frac{SPL}{L(\ell, \gamma, \beta)} \tag{3.12}$$

Where SPL is the shortest path length between s and t, while $L(\ell, \gamma, \beta)$ is the length of the potential-driven random walk from s to t, i.e. the path length of a potential-driven random walk in terms of traversed links to reach target node t from source node s, given a potential node ℓ and the bias parameters γ and β. It is to be noticed that a similar formulation was used to develop the straightness centrality for spatial networks [83]. The straightness index on networks is bounded between 0 and 1. Specifically, when $sI = 0$ we are in the case of random walk, while $sI = 1$ corresponds to the shortest path. For $0 < sI < 1$ we are in the case of a potential-driven random walk. Figure 3.5 shows how the value of sI changes on different network topologies, varying γ and β. In particular, in panel a) of Fig.3.5 we report the values of sI in the 8 different topologies considering γ and β as the axes of the heatmaps. The color of the tile encodes the values of sI, the closer the value is to dark blue the closer the walker behavior is

to that of a random walker. Instead, a color tile close to yellow indicates a behavior that tends to the shortest path. By design, when $\gamma < 0$ the

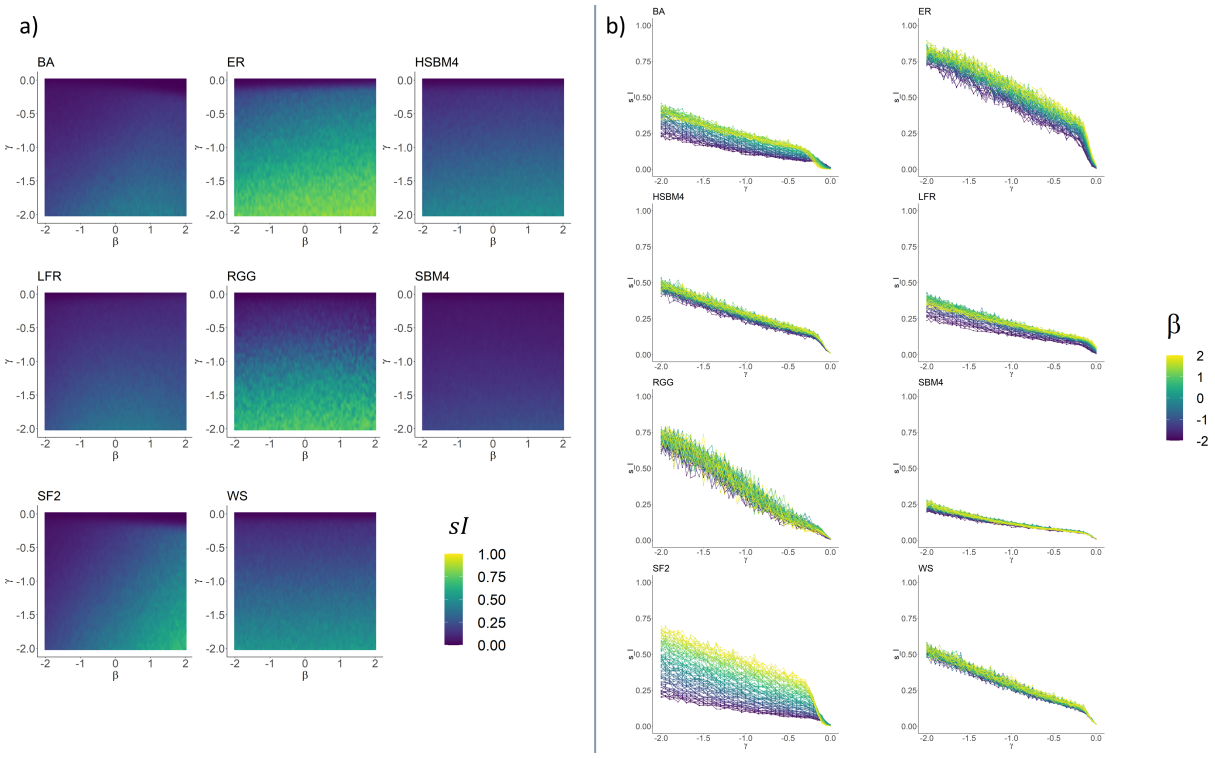

Figure 3.5: **Straightness index on networks.** In a) we report the values of sI for all the considered network topologies of 256 nodes: Barabási-Albert (BA), Erdös-Rényi (ER), Hierarchical Stochastic Block Model (HSBM4) Lancichinetti–Fortunato–Radicchi (LFR), Random Geometric Graph (RGG), Stochastic Block Model (SBM4), Scale-Free (SF2) and Watts-Strogatz (WS). The values of bias parameter γ and β are the axes of the heatmap, while tile color encodes the values of sI. In b) we express the values of sI as a function of γ, color line encodes the value of β.

potential node ℓ coincides with the target node, while when $\gamma = 0$, the position of ℓ does not affect the process since we are in the case of random walker. As it can be seen from these heatmap, the values of sI closest to the shortest path are reached in the Erdös-Rényi network topology, in random geometric graph and in the scale-free topology. To better appreciate how the pattern of sI evolves by varying γ we refer to panel b) of Fig.3.5. For

each topology is evident that the lower the value of γ the higher the value of sI, i.e. the closer the walk to the shortest path. This is because the walker is potential driven towards the target node, coincident with the attractive pole ℓ. As γ approaches zero, the value of sI tends to zero as well, denoting a random walk behaviour. At $\gamma = 0$, the walker is no longer affected by the potential and the value of sI dramatically goes to zero with an apparently jump discontinuity in all network topologies. The process at this point is a random walk. Compared to γ, the value of β is less critical to determine how the process approaches a shortest path behavior rather than a random walk, albeit in different ways for each topology. Quantitatively, the BA, SF2 and LFR topologies seem to be more sensitive to the variation of this bias parameter β, while qualitatively all topology exhibit similar behaviour. For example, β is crucial in the scale-free networks, and, to some extent also for BA topologies, to achieve high values of sI, i.e. to be close to the shortest path. This means that, unsurprisingly, in these topologies a walker favoring hubs would reach the target node faster. A slighter dependence from β in determining the values of sI, concurrently with γ, is also shown in HSBM4, LFR and ER topologies. Conversely, in these cases there is not the transition at $\gamma = 0$ as in scale-free networks. Finally, RGG, SBM4 and WS seem to be not affected by the bias on the degree, β, in reaching the target node, as much as they are by γ.

To sum up, a potential-driven random walk with negative low values of γ can resemble a shortest path when considering ER, RGG and SF2 network topologies. Also for the other topologies (HSBM4, SBM4, LFR, BA and WS) the most efficient path – in terms of path length – can be reached with lower values of γ, but in this case the path length is, at most, twice the shortest path. Weather lower values of γ than those considered in this study would ensure more efficient route should be investigated in further development of this work. For what concern the degree-bias β,

it mostly affects the SF2 topologies and, in smaller portion, also the BA topologies, while the potential-driven random walk on the other networks seems not to be influenced by this bias in reaching the target node. In other words, for all the analyzed networks it is evident that γ is the leading bias parameter in determining the values of sI. In fact, considering the analyzed range of γ, the potential-driven random walk spans from very short paths, sometimes even very close to the shortest path (as in ER, RGG and SF2), up to completely different and longer paths, regardless of the bias on the degree (β) in all network topologies. This demonstrates that the potential-driven random walk is able to effectively interpolate between shortest path and random walk.

3.6.4 Empirical 2D trajectories

As discussed in the State of the Art, the movements of both humans and animals do not strictly follow neither the shortest path or the random walk paradigm, but their routing falls somewhere in between. In this sub-section, we show that applying our potential-driven random walks over a very stylized network allows us to successfully reproduce the very broad range of characteristics that are observed in empirical human trajectories.

In most cases, the empirical data collected about human and animal trajectories are embedded into a bi-dimensional space. Note that the analysis presented in this sub-section comes without any biological or ecological context. In fact, the empirical trajectories here are taken into account for the sole purpose of verifying the model reliability in reproducing the diffusion component of both animal and human mobility, whatever the causes or the contexts. To create walks over a network reproducing a similar condition, we place our synthetic walkers over networks defined as square lattices having side L of varying sizes (so that the total number of nodes is $N = L \times L$). For humans, a lattice can be seen as a null model for a

street network over which the movements are constrained. On these lattices, similarly to what we have for other networks in the attractive case $\gamma < 0$, we also define a potential node which coincides with the target node. The initial position of the walker and the target node are indicated as green circles and red squares respectively in the examples on the top-left of Fig. 3.6. Being all networks considered for this analysis square lattices, all nodes with the exception of the borders have the same same degree $k = 4$, therefore the effect of a varying β would be here only an effect of attraction or repulsion at the boundaries. We instead focus on the effect of varying γ in the attractive range $-2 \leq \gamma \leq 0$ and the lattice size $L \in [9, 13, 17, 21, 25, 29, 33]$.

This approach clearly interprets animal and human trajectories as goal-oriented trajectories, at the end of which a attractive site is located. Our model allows a description where the movements of a living organisms is informed and directed toward a goal, but this information is incomplete or noisy. The stronger the potential, the more information leading towards the goal is readily available. For humans we would expect this goal-oriented behavior to be strong in recurrent mobility, as it is known that the tendency of returning to previously visited locations [257, 118] is a clear driver of this behavior. For animals, it will surely depend upon the species, but several examples of attraction driven movement are known [281], and the cause of attraction can be either because the path is towards one's nest, lair is known, or information about the attractiveness of particular areas is available through the organisms' senses.

To characterize both the synthetic trajectories generated over the lattices and the empirical trajectories we use the Straightness index sI discussed above as indicator of tortuosity and the mean cosine mC between the trajectory steps as indicator of autocorrelation defined as the average along the trajectory of the cosine of the turning angle θ between two

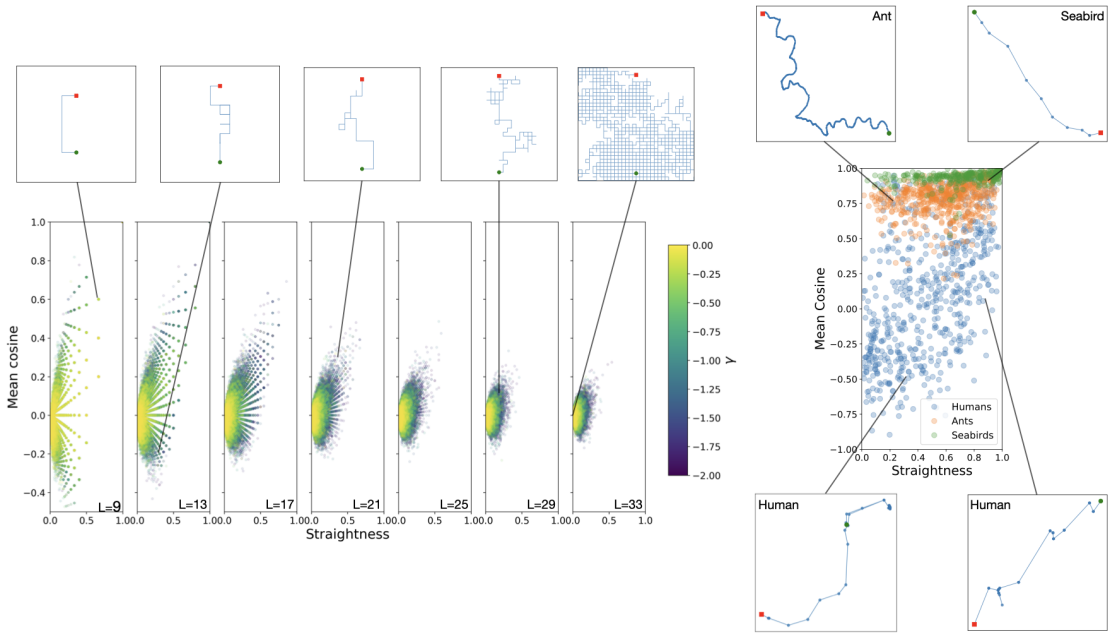

Figure 3.6: **Straightness vs Autocorrelation diagrams for walks in a 2D space.** Left) Potential-driven walks over a square lattice. We display the values of sI and mC for a range of values of lattice sizes L (different subplots) and γ (different colors). The trajectories above the plot illustrate examples of the trajectories generated, the black line identifying the associated values of sI and mC. Right) Empirical trajectories of humans, ants and seabirds. We display the values of sI and mC for three types of empirical trajectories: 600 humans trajectories (blue), captured by anonymized GPS data generated by mobile phone applications; 600 ants trajectories (orange), captured optically in lab conditions around an artificial nest; 300 seabirds trajectories (green), captured by GPS trackers. In these cases, trajectories are again on a plane, but not limited to follow the lattice topology. Above and below the plot we illustrate two examples of Human trajectories and one example each for ants and seabirds (a Wandering Albatross in particular), again with the black line identifying the associated values of sI and mC. The ant trajectory is highly auto-correlated although not straight, while the albatross example is at the same time straight and auto-correlated. The two human examples allow us to show instead a trajectory with negative mC (probably accumulated in the small scale movements on the top-right of the diagram) and a straight but not strongly correlated trajectories.

subsequent steps [78].

As we can see on the left side of Fig. 3.6, where we represent the distribution of sI and mC in our synthetic trajectories over lattices, for $\gamma = 0$,

the paths generated are pure random walks. These random walks are characterized by vanishing values of both sI and mC as the trajectories wrap around themselves. For decreasing values of γ, the trajectories become progressively straighter, as they align more and more to the shortest path which, given the origin and destination set on our lattices, is simply a straight line. The values of mC characterize the tendency for a trajectory over the lattice to locally deviate from the shortest path or backtracking with steps inverting the direction with respect to the previously taken one. Differing from what often happens for most animal or human trajectories [281, 32, 180], the potential-driven random walks we used here allow for backtracking, which is possible, although progressively more unlikely, for stronger attractive potentials and decreasing values of γ. Another factor influencing the likelihood of backtracking is here the size L of the lattice, as the larger is the number of steps made, the more likely the event of a deviation from the shortest path even for stronger potentials. For this reason, the synthetic trajectories with the larger values of sI and mC are found for small lattices and strong attractive potentials. This can be seen in our coarser lattices $L = (9, 13, 17)$, where we observe very broad distribution of values of sI and mC spacing (please note that in our plots both are limited to values of about 0.8 due to the discrete nature of the trajectories).

On the right side of Fig. 3.6 we represent the distribution of sI and mC of three types of empirical trajectories: i) privacy enhanced GPS trajectories describing the movements of anonymized users of mobile applications who opted-in to location based services through a GDPR compliant framework, randomly extracted from a database provided us by Cuebiq (a location intelligence and measurement platform that collects GPS trajectories from mobile apps users who have opted-in to provide access to their aggregated location data anonymously) covering the Trentino province, an

area approximately 6.000 km^2 wide in northern Italy (blue); ii) optically tracked trajectories describing the movements of *Temnothorax albipennis* ants while exploring a large arena outside of an artificial nest [160] (orange); iii) GPS trajectories describing the movements of three types of seabirds (Wandering Albatross, Laysan Albatross, Streaked Shearwater) [302] over the ocean surface (green). Note that in all three cases considered, the trajectories have been segmented with the Infostop library [21] and only the movements between two stopping points have been analyzed. The distribution of points in the sI-mC diagram for humans is very broad and most trajectories are way far from both a pure random walk and a straight line. Animals trajectories present instead a high level of autocorrelation, probably due to the fact that the movements of these animals over the ocean for seabird and in the arena created for the ants is relatively unconstrained. This is different for humans whose movements are constrained over the topology of the street network.

Comparing the diagrams of the synthetic trajectories on the left panel and empirical ones on the right one, we can appreciate how our very stylized model, which include a single potential source over a square lattice, allows us to already partially reproduce the very broad range of trajectories characteristic of human mobility. A clear improvement in this sense is observed when we used a coarser description of the movement space (small L) which on one hand possibly better describes the limited options dictated by the street network, and on the other hand limits the incurring of backtracking which is not expected for humans. The trajectories of ants and birds appear instead to be largely more auto-correlated to what we were able to describe with the few ingredients we introduced here.

The exploration in Fig. 3.6 is however limited by the parametric span of $\gamma \in [-2, 0]$. For this reason, in Fig. 3.7 we expand the simulations, again over a 33×33 square lattice, to $\gamma \in [-12.5, 0]$ with the goal of covering

a broader range in the straightness-cosine plane by extending towards the shortest-path area (1,1) our observations. Furthermore, to show the utility of our model as compared to competing models of animal movements describing directed paths, we also simulated 1000 times Correlated Random Walks [78] and Lévy Walks [303].

As can be appreciated in Fig. 3.7 a), Similarly to the $L = 33$ example in 3.6 left, we use a relatively large square lattice to generate trajectories embedded into a 2D metric. The origin and destination nodes lie at distance 2 from the sides of the square. The shortest path is in this case a

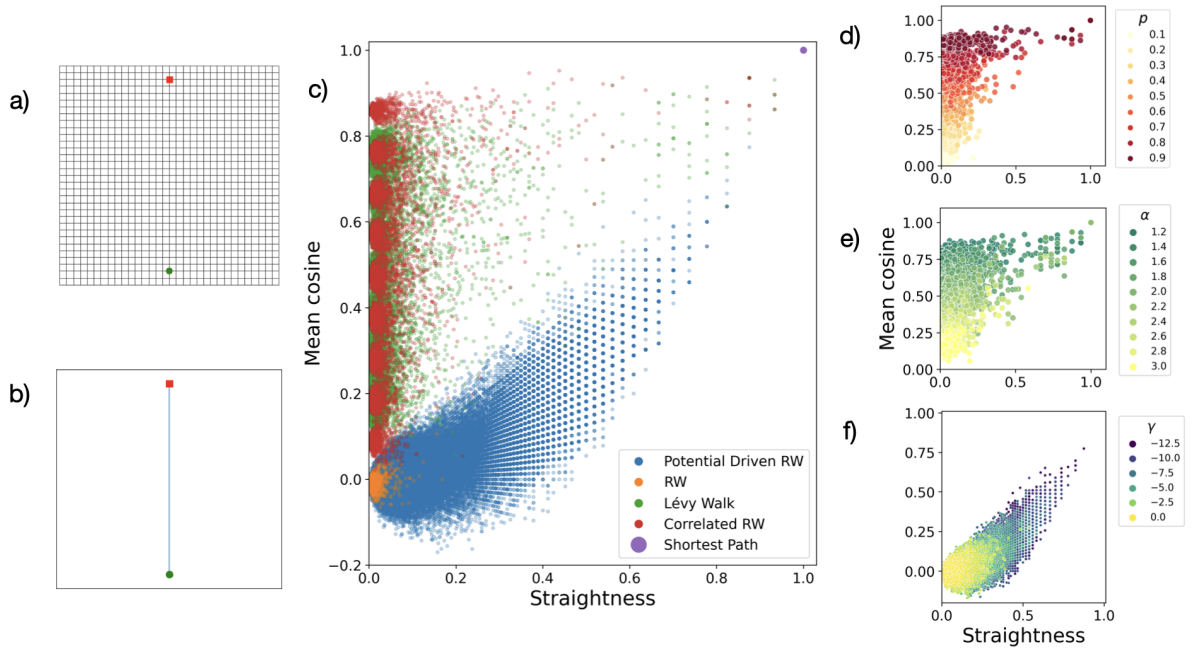

Figure 3.7: **Comparison of different walk models on a 33×33 lattice.** a) The square lattice over which the trajectories are run from the origin point (green circle) to the destination (red square). b) The shortest path, in this case a straight line. c) The sI–mC diagram describing the range of characteristic values for trajectories generated with the different models. d) Same values as c) for Correlated Random Walks, where it is highlighted the dependency over p. e) Same values as c) for Lévy Walks, where it is highlighted the dependency over α. f) Same values as c) for Potential Driven Random Walk, where it is highlighted the dependency over γ.

straight path across 29 edges, dividing the e square in two (Fig. 3.7 b). In panel c), we first can appreciate how the shortest path (purple circle), is characterized by $sI = 1$ and $mC = 1$. Random walks (RW, orange dots) are instead distributed around $sI = 0$ and $mC = 0$. We further compare with i) Correlated Random Walks (red dots) generated via Poisson process a probability $p > 0$ of having a step of the walk on the same direction of the preceding (otherwise, the step is random as in RW), thus generating movements constituted by sequences of steps aligned towards the same direction, forming straight displacements of length ℓ, where ℓ follows an exponential probability distribution. ii) Lévy Walks (green dots), where the path is again formed by sequences of steps towards the same direction, but where the lengths of the sequences of aligned steps is instead distributed as a power law $p(\ell) \propto \ell^{-\alpha}$. Comparing the different model, we see how the Potential Driven Random Walk successfully bridges between random walk (0,0) and shortest paths (1,1) as the potential becomes stronger when the value of $-\gamma$ increases from 0 to 12.5. iii) our Potential Driven Random Walks (blue dots), with $k = 0$ and γ ranging here between 0 and -12.5. The same data is presented in parameter d),e),f) to illustrate the dependence over the model's free parameter. The Correlated Random Walk is close to a normal random walk for small p, and then has increasing values of mC as p grows. Since we have origin and destination nodes aligned over the network, for large values of p we observe walk coinciding with the Shortest path. The Lévy Walks behave similarly to the Correlated Random Walk, with α mostly driving the value of mC and with even more likelihood of having some paths close to the shortest path for large α given the opportunity of making a long jump towards the destination. In the Potential Driven Random Walk, as the potential becomes stronger (larger values of $-\gamma$) we have increasing values of both sI (as the path becomes more similar to the shortest path) and $mC = 1$ (as the path become more straightly

directed towards the destination).

These stylized examples can be of course largely improved in order to better describe specific types of behaviors. We offer here three possible directions. First, the network topology can be surely refined from a simple lattice in order to describe the real physical constraint faced by the moving individual. Second, introducing a penalty to backtracking would allow to create artificial trajectories closer to the trajectories observed pushing towards shapes normally describes as composite correlated random walks. Third, introducing multiple potentials activated at specific times, such for instance after the arrival at an intermediary destination, would permit to account for more complex behaviors like round trips or the chaining of multiple way-points in navigating a complex environment.

3.7 Concluding Remarks

In this chapter, we focused on the dynamics regarding the navigation process. Realizing that several interconnected systems in real world have to balance efficiency and costs in their routing strategies, we observe that a continuous spectrum of dynamics interpolating between these extremes, still lacks.

Here, we have introduced a novel stochastic process, the potential-driven random walk, which effectively interpolates between shortest path and random walk protocols on a network by taking into account at the same time a preference for nodes of high or low degree and the effect of attraction towards the destination node. This new dynamical process aims at minimizing the distance (as the shortest path) by only considering partial information about the network, i.e. the position of a drifting node ℓ, and by maintaining a certain flexibility in the exploration of the network (as random walk). We characterized the process described by the potential-

driven random walk by means of its steady state distribution and mean first passage time matrix. We investigated the patterns of these indicators on synthetic networks considering both ordered topologies (i.e lattices) and disordered topologies (8 different network models), providing evidence of agreement between simulations and theoretical expectations. As well, we investigated how the theoretical values of the MFPT change varying the values of bias parameters, pointing out a regime shift in the MFPT corresponding with some critical points in the bias parameter γ. By generating a large number of paths over networks characterized by a disordered topology, we also showed how the process can be inverted as we were able to successfully infer most of the times (70% overall) the values of the parameter γ only on the basis of the observed the Mean First Passage Time. Inspired by ecologic studies related to the movement of animals in physical space, we proposed a new metric, the *straightness index* on networks, quantifying to what extent the potential-driven random walk is close to shortest path (or to the random walk). Specifically, by tuning the bias parameter related to the distance from the potential, γ, we can define efficient paths which in some specific topologies reveal to be very close to the shortest path when $\gamma = -2$, while stronger potentials are necessary in large lattices. In general, it is evident that γ is the leading bias parameter in determining the values of the *straightness index* on networks, i.e. in drifting the process towards a shortest path or a random walk, in all the analyzed topologies.

The straightness index, together with a measure of trajectory autocorrelation on a 2D space, allowed us to also compare empirical trajectories of human and animals with walks generated on a square lattice with a single attractive potential at the destination node. Even within the strong limitations inherent with the very stylized model presented here, we were able to show how our model is able to replicate the broad range of behaviors

typical of real human trajectories better than alternative models such as correlated random walks or Lévy walks.

Our results provide a fundamental starting point to build a novel understanding of the movements of agents and information over a network in terms grounded on physics potentials. On the one hand, a more accurate description of real trajectories will be possible by building over our model, which can be possibly extended to include memory effects and already can account for more complex time-varying potentials that can combine positive and negative charges to describe at the same time attractiveness of certain areas and the avoidance of others. On the other hand, our framework has a broad spectrum of methodological applications: for instance, one can use potential-driven random walks to analytically define new network indicator able to identify the centrality of nodes in a continuous between the family of random walk [207] and geodesic [64] centralities, such as betweenness and closeness centrality, in both classical and multilayer systems [255]. Such indicators would allow for a whole new set of applications in scenarios such as urban mobility [7] or network neuroscience [26], where human and information flows are known to lie in the gray area between random and geodesic paths. We expect, in particular, that a new perspective over these networks will be driven by the fundamental question of what topological conditions makes possible to radically change the distribution of the random walk centrality when even small potentials are introduced. Finally, the framework is expected to open new doors for the analysis of functional clusters emerging from collective phenomena, where diffusion geometry induced by random walk dynamics [86] can be extended to span from diffusion to geodesic distance, allowing the analysis of the complex interplay between structure and dynamics from a new perspective.

In the next chapter, we will pay particular attention precisely to the interplay between brain structure and dynamics. By leveraging on spectral

entropy, we propose a new information-theoretic approach for the analysis of synthetic and empirical brain networks, in health and disease. Our approach naturally accounts for the interplay between the underlying structure of the system and a dynamical process on the top of it at different temporal scales, measured in bits of information required to describe the connectome state.

Chapter 4

Persistence of information flow: a multiscale characterization of the human brain

In brief

In this chapter we investigate the interplay between structure and dynamics, focusing on information exchange within the human brain, being it crucial for vital tasks and to drive diseases. Neuroimaging techniques allow for indirect measurements of information flows among brain areas and, consequently, for reconstructing connectomes analyzed through the lens of network science. However, standard analyses usually focus on a small set of network indicators and their joint probability distribution. Here, capitalizing on network information theory, we propose a new framework for the analysis and comparison of empirical and synthetic human connectomes, in health and disease. We find that the spectral entropy of empirical data lies between two generative models, indicating an interpolation between modular and geometry-driven structural features. Remarkably, we demonstrate that significant differences between healthy individuals and the ones affected by Alzheimer's disease arise at the microscale.

4.1 Introduction

The human brain has a complex multiscale organization in both spatial and temporal domain. Such a multiscale organization grants the human brain network to be robust, adaptive and evolvable, besides being crucial for the global communication efficiency within the cortex (see Subsec.1.1.1). In this chapter, we provide a new way to characterize the multiscale nature of human brain, from an information-theoretic perspective. Specifically, we define a novel framework that leverages on spectral entropy to define the connectome state in health and disease. Especially, we elaborate a function of the system in terms of the interplay between the underlying structure and a dynamical process on the top of it, at different temporal scales, measured in bits of information required to describe the connectome state.

This chapter has been published as a research article in the peer-reviewed journal *Network Neuroscience*, in 2021 [52] and is available here.

4.2 State of the Art

The human brain is usually referred to as an emblematic example of efficient complex systems, where neurons (i.e., the units) process a huge amount of information by signaling through synaptic transmission (i.e., the links). To better understand how information flows within the brain, imaging techniques are widely used to infer structural and functional relationships between distinct areas of the brain obtained according to some parcellation in regions of interests [22, 283]. The resulting maps coarse-grain the brain into complex networks of much smaller size, typically of the order of a few hundreds or thousands areas, that are analyzed through the lens of network science [113, 67, 196, 97, 305, 68, 216, 100, 39, 299, 242].

On the one hand, network descriptors are used for a variety of applications, from quantifying the characteristic geodesic distance among units to unravel their mesoscale organization into functional modules [55, 260], from identifying nodes central with respect to information exchange to more sophisticated roles such flow attraction and connector hubs [183, 68, 163, 284, 54], from both nodal and link perspectives [109]. Recently, more sophisticated models such as multilayer networks [92] have been used to this aim: in that case, the layers encode distinct types of relationships among units, either accounting for multimodal measurements [46, 139] or for correlations in the temporal [40] or frequency [91, 65, 296] domains (see [87] for a review).

Network science has proven to be a powerful analytical tool for unraveling the properties of the human brain, and several models have been proposed to reproduce the most widely observed salient features, from small-worldness [203, 37, 179], usually related to an amount of triadic closure higher than chance together with a characteristic geodesic length lower than random expectation [294], to modularity [260, 55], i.e., the organization of units into groups [112] with a biological function, enhancing our understanding of brain structure and function in both health and disease [228, 10, 73, 11, 235, 236, 95, 110, 150, 111, 91, 138, 16, 134, 177]. For instance, it has been recently shown that interareal Euclidean distance plays an important role in shaping the structural organization of brain networks [58], opening the door to the exploration of models driven by geometry (see [289, 56] and references therein) and latent geometry [13, 308].

4.3 The Problem

Usually, methods to characterize human brain network are limited to consider a small set of network indicators (e.g., centrality, clustering, modu-

larity, so forth and so on) and their joint probability distribution. Most of the time these indicators, and in particular the idea of centrality, are referred to structural features. Traditionally, the degree of importance of a node depends on its topological traits. For example, when dealing with network integrity – the existence of a path between two nodes enabling information exchange – or network robustness – the ability of a network to survive after a failure or attack – the role of the network structure and the nodes centrality have been considered dominant for decades [124]. This concept stresses the position that, for example, to disintegrate a system a large fraction of it must be damaged. In this regard, a recent study has brilliantly shown that removing nodes that are central for structural connectivity might be insignificant for the information flow within the system [124]. In other words, the network integrity from a structural point of view is fundamental but, at the same time, it is not sufficient to guarantee or quantify the effect of potential damages on system's functionality [124]. This means that topological metrics can fail – and have failed [124] – to identify nodes that are central from a functional point of view, e.g. for the flow dynamics, eventually challenging the widely accepted assumption that the sole topological indicators are enough to inform and comprehend how complex systems operate [126]. In this vein, we apply a similar reasoning to the brain connectome, with the intent to overcome its characterization from the sole topological point of view, by integrating such a characterization with the interplay between structure and function.

Here we provide a more comprehensive analysis for the comparison of brain networks than standard techniques, as it accounts for the contribution of the whole network state encoded into a density matrix [88, 127], a mathematical representation of the system which shares important physical and information-theoretic similarities with its counterpart widely used in quantum statistical physics (more details in Sec.4.5).

4.4 The Proposed Approach

In this chapter, we propose an information-theoretic approach for the analysis of synthetic and empirical brain networks with a two-fold aim. The outcome of our procedure naturally accounts for the function of a system in terms of the interplay between the underlying structure and a dynamical process on the top of it, at different temporal scales, measured in bits of information required to describe the connectome state. To this aim, we use two distinct diffusive processes for exchanging information among units: i) a classical random walk (CRW), where the walker has no global knowledge of the connectome and performs decisions based only on local knowledge of the connectivity, while keeping a uniform probability of choosing a connection for jumping [208]; ii) a max-entropy random walk (MERW), where the walker has global knowledge of the connectome and jumps through a connection while keeping a uniform probability of choosing any trajectory on the network [69]. Thanks to these distinct dynamics, we are able to describe the network state from two distinct perspectives: one where only local knowledge is used to explore the connectome (CRW) and one where global knowledge is used instead (MERW).

On the one hand, we use our framework to compare a large set of real connectomes from healthy subjects against a selected pool of network models, characterized by distinct structural features and increasing amount of complexity. Specifically, we built 400 synthetic brain networks based on four generative models, i.e the Erdős-Rényi model [106], the configuration model [206], the stochastic block model [156] and the hyperbolic model [215]. These generative models [57] allow for obtaining samples of synthetic data (networks) while maintaining some specific features of empirical connectome (see sec.4.5 for a more detailed illustration of the generative models considered for this work). On the other hand, we compare the

function in healthy subjects against the one in patients at different stages of dementia, namely mild cognitive impairment (MCI) and Alzheimer's disease (AD) from a network information theory perspective.

Here we use spectral entropy, based in statistical physics and information theory – field devoted to the study of transmission, processing, extraction, and utilization of information –, to investigate the structure of human brain networks. In general, the spectral entropy captures the complexity of a system in terms of the mixedness of information flow through the network. Our method provides a comprehensive analysis for the comparison of brain networks as it accounts for the contribution of the whole network state encoded into a density matrix [88, 127], a mathematical representation of the system which shares important physical and information-theoretic similarities with its counterpart widely used in quantum statistical physics. Moreover, it has been systematically shown that the spectral entropy framework performs better than the traditional methods, previously introduced to investigate information dynamics within complex structures, in characterizing the global aspects of complex networks [268].

We find that simple models, like the Erdős-Rényi and configuration models, have smaller spectral entropy at the mesoscale, where mid- or long-range communications between the nodes are considered, and, consequently, require a significantly smaller amount of bits (up to 1.5 bits) for their description than empirical human brains from healthy individuals. Conversely, degree-corrected stochastic block models and hyperbolic models (see Methods), accounting for the inferred modular structure of the connectome and its latent hyperbolic geometry, respectively, provide similar descriptions of the network state, with differences smaller than 1 bit. It is worth remarking that the geometry-driven model exhibits higher **information entropy** for increasing temporal scale – i.e. moving from the mesoscale to the macroscale– denoting a larger persistence of **informa-**

tion flow – i.e., entropy tends to decay slower with Markov time – in this type of networks, at variance with stochastic block models and empirical connectomes. Results are compatible when the two types of dynamics, CRW and MERW, are considered. In general, p-values from statistical tests indicate the mesoscale as the suitable scale to highlight differences (and similarities) between empirical data and synthetic models. Moreover, we find out that, considering the MERW dynamics, the stochastic block model can significantly reproduce the empirical brain across all scales.

When applied to connectomes obtained from healthy and unhealthy subjects, we identify significant differences between healthy individuals and the ones affected by Alzheimer's disease at the microscale (adjusted p-value smaller than 0.1%; maximum posterior probability smaller than 1%) and at the mesoscale (adjusted p-value smaller than 1%; maximum posterior probability smaller than 10%), in the case of CRW. The results are confirmed, at one order of magnitude larger, for MERW and only at the microscale. Remarkably, our approach is able to capture this difference despite the topologies of the two groups exhibit a certain amount of similarity with respect to more traditional network indicators.

In the final section (4.7), we describe the interpretation of our results from a neuroscience perspective, highlighting that our approach is well suited to capture the multiscale nature of neural dynamics that is embedded in the hierarchical modular organization of brain structure. Furthermore, our method allows to identify precisely the scale at which abnormalities can alter information flows when studying brain network in patients with AD disease.

4.5 Materials and Methods

4.5.1 Data

In this work we rely on two structural connectivity data sets. For structural connectivity is intended the topological interconnection of brain regions as identified through diffusion tensor imaging (DTI) techniques and summarized in adjacency matrices according to some specific indicator (e.g., fractional anisotropy). The two data sets are:

1. A structural connectivity data set provided by the Nathan S. Kline Institute - Rockland Sample (NKI-RS), consisting of 196 healthy subjects [3];

2. A structural connectivity data set of 71 subjects from [181], among which 22 with Alzeimer's disease, 23 affected by mild cognitive impairment and 26 healthy controls.

The first data set [209] consists of resting-state structural data, that represent physical structure of brain networks, of 196 healthy subjects at rest without any mental or physical disorder. The sample is made up of 114 males and 82 females and the age range is rather large: the youngest person is 4 and the eldest is 85. By looking at the age variable distribution, the first quartile is equal to 20, and the third quartile is equal to 47; for this reason, the sample can be considered representative of age variability. The NKI-RS has been designed as a community-ascertained sample and the representativeness is maximized according to demographic characteristics of the United States. Brain structural networks are mapped with DTI (Diffusion Tensor Imaging) measures (137-direction, 2 mm isotropic), provided by the Center for Magnetic Resonance Research at the University of Minnesota for the Human Connectomes Project. All data were

publicly shared through the Collaborative Informatics and Neuroimaging Suite (COINS) developed by the Mind Research Network.

The second data set consists of structural networks reconstructed from DTI data. In particular, to reconstruct the networks, Lin et al. applied a streamline-based fiber tracking algorithm on voxelwise diffusion tensors with these set parameters: random whole-brain seeding, 200,000 reconstructed streamlines, anisotropy threshold of 0.15, angular threshold of 45°, and streamline length between 30 and 300 mm (for more details about this data set please refer to [181]). Here, the nodes of the brain networks corresponds to the 90 cerebral regions from the automatic anatomical labeling (AAL) template [282], while the edges are quantified by computing the fractional anisotropy (FA) along the interconnected streamlines between two different AAL regions. According to Lin et al. [181], measurements obtained from tract-specific metrics (e.g., fractional anisotropy and diffusivity) reveal to be more sensitive and interpretable than those obtained from metrics based on streamline count. These findings motivate our choice to rely on data obtained from fractional anisotropy tract-specific metric for building the empirical brain networks.

Fractional Anisotropy is the degree of anisotropy in a diffusion process and is bounded between 0 and 1, where 0 means that diffusion is isotropic and 1 that diffusion occurs along one axis. To establish the presence of links in a binary way, and to avoid, at the same time, using arbitrary thresholds, the links of the networks used in this work are the result of a sampling assuming that the probability of existence of each link is uniformly distributed. Specifically, we defined the link between i and j in the FA data set as w_{ij} and, interpreting w_{ij} as a probability, we extract a random number r from a uniform distribution $U(0,1)$ and we assign the binary link according to the Heaviside Θ as $a_{ij} = \Theta(w_{ij} - r)$. In other words, when the value of FA is greater then the corresponding random

value the link exists, otherwise it is discarded. In this case, the sampling is well suited given the FA values bounded between 0 and 1 and can be safely interpreted as the probability of a link to exist. In fact, since FA values measure the degree of anisotropy of diffusion occurring on a given tract and being such values bounded between 0 and 1 – where 0 means isotropic diffusion and 1 anisotropic diffusion – they can be safely interpreted as the probability to have a structural connection among brain regions. The choice of avoiding to adopt a specific threshold is motivated by recent studies showing that, in the case of probabilistic or correlation networks, it is desirable to account for the intrinsic uncertainty in the existence of each link [232].

4.5.2 Generative Models

Generative models are statistical processes allowing one to obtain a sample of synthetic data. The synthetic networks obtained through such processes can share some properties with the observed data and this procedure is guaranteed by the use of parameters that are usually obtained by fitting the observed data. In this study, we consider four different types of generative models: for each type, we fit the underlying parameters of each model for each empirical connectome separately, and generate 100 independent realizations, to obtain an ensemble of synthetic networks for each connectome. Therefore, we have a total of 400 synthetic networks for each empirical network.

The Erdős-Rényi model (ERM) generates random graphs with the same number of vertices and the same number of edges of the real network. These topological features are preserved each time the model is produced, whereas the network structure randomly changes.

The configuration model (CM) reproduces the degree distribution of the real network, preserving the degree of the nodes while avoiding multiple

edges, in the literature, this model is also known as degree-preserving random rewiring model [191]. Parameters used to fit this data-driven model are as many as the number of nodes N, and each represents the corresponding node degree k_i ($i = 1, 2, ..., N$). From each node, k_i *stubs* (edge halves) start and, by changing the connectivity pattern, link to different nodes, obtaining a network with no topological correlations which preserve the observed connectivity.

The stochastic block model (SBM) allows one to define an ensemble of random models which reproduce the mesoscale organization present in the real network. A block consists of a group of nodes which have a higher likelihood of being connected among them than making external connections with nodes from other groups. Here, we use *graph-tool* [222], an efficient Python module for statistical analysis of graphs and network manipulation, to fit the degree-corrected SBM.

The hyperbolic model (HM) is based on two important parameters, the popularity and the similarity [215], whose trade-off is responsible for the network structure: the two parameters are physically formalized and geometrically interpreted, and their product is optimized in order to obtain connections in the network. To fit this model, we use the *Mercator* method [120], which maps real complex networks into a hyperbolic geometric space, which is able to provide a more accurate interpretation of the connectome structure than Euclidean geometry. We use Mercator [1] to generate this class of synthetic networks [13].

4.5.3 Random walks on connectomes

Information flow in complex networks, such as human connectomes, has been modeled by diffusive processes like random walks [193]. As Markovian processes, different types of random walks are defined in terms of transition matrices encoding the probability of jumps from nodes to neighbors. In

this work, we use two important types, including the classical random walk (CRW) [208] and maximal entropy random walk (MERW) [69].

For both types of dynamics, the Laplacian matrix is defined by $\mathcal{L} = \mathbf{I} - \mathbf{T}$, where $\mathbf{T}$ is the transition matrix governing random walk dynamics and $\mathbf{I}$ is the identity matrix. Let us assume that the i–th components of the vector $\mathbf{p}(\tau)$ indicates the probability to find the random walker in node i at time τ. The evolution of the probability vector is governed by the master equation

$$\mathbf{p}(\tau + 1) = \mathbf{p}(\tau)\mathbf{T}. \tag{4.1}$$

In the continuous-time approximation, Eq. 4.1 reduces to :

$$\frac{\partial \mathbf{p}(\tau)}{\partial \tau} + \mathbf{p}(\tau)\boldsymbol{\mathcal{L}} \;=\; 0, \tag{4.2}$$

with solution given by $\mathbf{p}(\tau) = \mathbf{p}(0)e^{-\tau \boldsymbol{\mathcal{L}}}$.

In a classical random walk on a binary network, the transition matrix is defined as $T_{ij}^{(CRW)} = A_{ij}/k_i$, where k_i is the degree of i-th node and $\boldsymbol{A}$ is the adjacency matrix. In MERW the transition matrix is defined in terms of the largest eigenvector of the adjacency matrix. Assume the eigenvalues of the adjacency matrix are ordered as $a_\ell, \ell = 1, 2, ...N$, where a_N has the maximum value, and their corresponding eigenvectors are given by $\mathbf{q}^{(\ell)}$. The transition matrix, in this case, is given by $T_{ij}^{(MERW)} = \frac{A_{ij}}{a_N}\frac{\mathbf{q}_j^{(N)}}{\mathbf{q}_i^{(N)}}$. One of the interesting features of MERW is that the probability of a transition from one node to another within τ steps of time is independent of the intermediate transitions and all trajectories from i-th to j-th node with the length of τ are equiprobable.

The Laplacian matrix for CRW is $\boldsymbol{\mathcal{L}}^{(CRW)} = \mathbf{I} - \mathbf{T}^{(CRW)}$, while for MERV it is defined by $\boldsymbol{\mathcal{L}}^{(MERV)} = \mathbf{I} - \mathbf{T}^{(MERV)}$. Therefore, each dynamical process can be obtained from Eq. 4.2 by choosing the relevant Laplacian matrix.

4.5.4 Statistical physics of information dynamics

Characterizing the flow of information between nodes in a complex network is challenging, requiring a deep understanding of the network topology, relevant dynamical processes and the interplay between them. Recently, a statistical field theory has been introduced to describe the information flow between the components of complex systems in terms of the dynamics of a field on top of the network, moving among nodes. In this framework, for a network denoted as G, the dynamical process governing the flow can be described in terms of a general differential equation which, after linearization, reduces to a Schrodinger-like equation with a quasi-Hamiltonian $\hat{\mathbf{H}}(G)$ and the propagator $e^{-\tau\hat{\mathbf{H}}(G)}$ which determines the flow trajectories at time τ. Furthermore, the propagator can be eigen-decomposed to obtain an ensemble of operators acting like information streams, directing the flow of the field from unit to unit [127]. The topological factors, the type of the quasi-Hamiltonian and τ affect the size of the streams and consequently, each stream can be active or non-active (i.e., having negligible size) under a specific system configuration.

To study the macroscopic properties of these microscopic interactions between the nodes, it has been shown that a superposition of the information streams, weighted by their activation probabilities, provides a Gibbsian-like density matrix describing the state of the system:

$$\hat{\boldsymbol{\rho}}_\tau(G) = \frac{e^{-\tau\hat{\mathbf{H}}(G)}}{Z_\tau(G)}, \tag{4.3}$$

where $Z_\tau(G) = Tr[e^{-\tau\hat{\mathbf{H}}(G)}]$ plays the role of the **partition function** and is related to the transport properties of the network [126]. Using the above density matrix, one can quantify the mixed-ness of the information streams in terms of the von Neumann entropy as

$$\mathcal{S}_\tau(G) = -Tr[\hat{\boldsymbol{\rho}}_\tau(G)\log_2\hat{\boldsymbol{\rho}}_\tau(G)], \tag{4.4}$$

which is also a measure of diversity of the flow dynamics. The maximum value for the von Neumann entropy of the system is $\log_2 N$ corresponding to the state where all information streams are active with the same size and to capture the dynamics, one needs to consider all the streams. At large temporal scales τ, the entropy of a connected network is expected to decay, as the distribution of the field becomes less dependent on the initial conditions. Interestingly, it has been shown that the von Neumann entropy can be used to measure the functional diversity of nodes as senders of information [127]. In fact, in a system where the overlap between the flow distribution originated from different nodes is high, we get lower values for the entropy.

It is worth noting that if the dynamical process is continuous diffusion governed by the combinatorial Laplacian, the von Neumann entropy obtained from the above statistical field theory is equal to the spectral entropy [88], introduced to analyse complex networks from an information-theoretic perspective.

Here, we consider random walk dynamics as a proxy for information transport in human connectomes. Therefore, the quasi-Hamiltonian equals $\boldsymbol{\mathcal{L}}^{(CRW)}$ for classical random walk and $\boldsymbol{\mathcal{L}}^{(MERW)}$ for maximal entropy random walk.

4.5.5 Information-theoretic analysis of human brain networks

Before discussing our results, it is important to introduce a few basic concepts that will be used in the following. Let us frame our problem in terms of a communication process, where one encodes the description of a complex network to transmit it through some noiseless communication channel to a receiver, who has to decode the corresponding information, in bits, in order to reconstruct the original network. Since the channel is assumed to be noiseless, it has maximum information capacity (amount of information

allowed to pass through a communication channel in a given time period), i.e., the mutual information between the sent and received information is maximum. Note that the communication we are referring to should not be confused with signalling or communication among distinct areas of the brain.

One way to quantify the average number of bits required to describe a network state G is to build the corresponding density matrix $\hat{\boldsymbol{\rho}}_\tau(G)$ and calculate the spectral entropy $\mathcal{S}_\tau(G)$, mathematically equivalent to the von Neumann entropy of an entangled quantum system [88]. Here, the parameter τ indicates the Markov time of the dynamical process used to propagate information among nodes: the idea is that an ensemble of signals, whose dynamics is governed by a propagator, is sent from each node to the others for a time τ and contributes to collect information about the underlying topology, therefore reducing uncertainty about the structure. In fact, at time $\tau = 0$, no signal propagates and, consequently, the entropy is maximum because no information at all is available about network structure. Recently, it has been shown [127] that the density matrix describes the trajectories of information flow through the network and the entropy provides a measure of diversity of information dynamics in the system (see Fig. 4.1 for an illustration).

Interestingly, one can show that a network's topological complexity, like the presence of modularity or hierarchy, can boost the diversity of information dynamics within the system and the functional diversity of nodes as senders of information [127]—i.e., the modularity separates the groups of nodes from each other and the hierarchy differentiates between the groups, both making asymmetries between the nodes as senders and receivers of information and diversifying the trajectories of information flow within the system. Here, we go beyond the analysis of synthetic networks and investigate real connectomes, in comparison to null and generative models. To

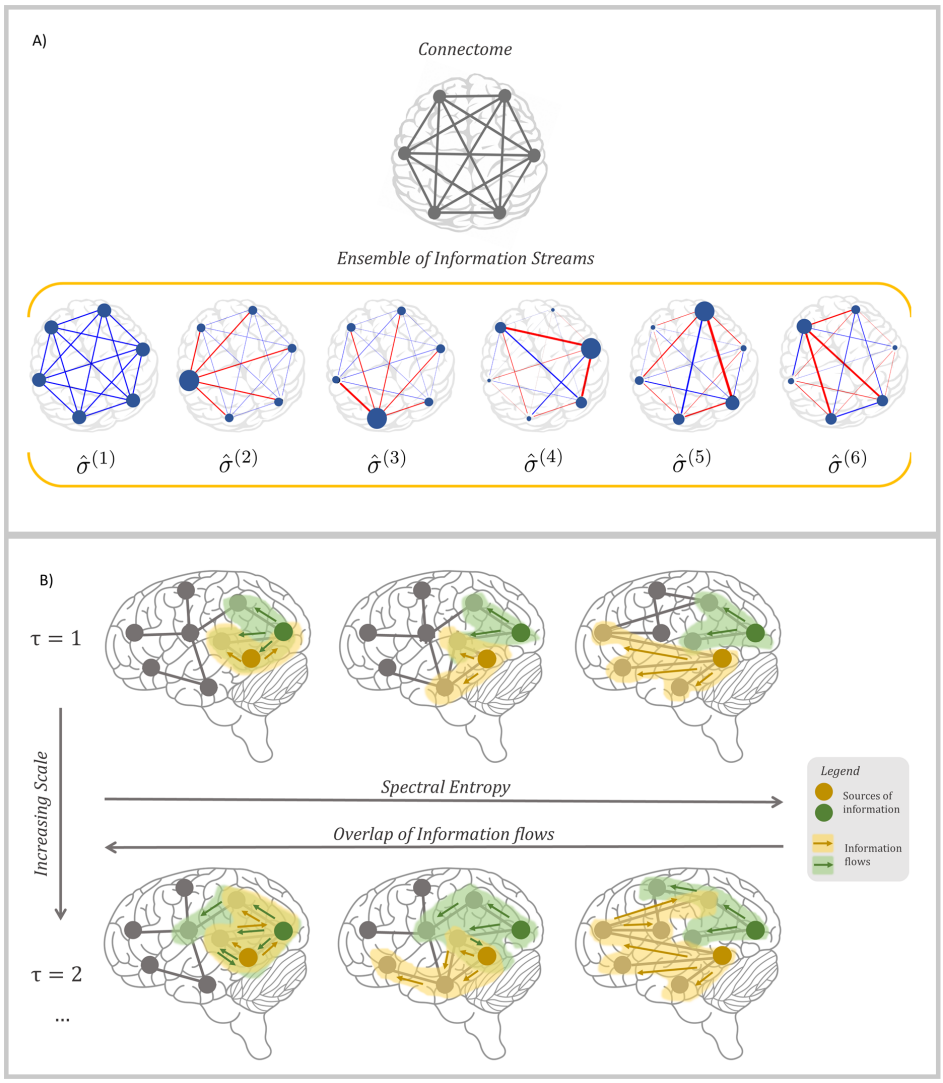

Figure 4.1: **Illustrating network information entropy in the case of a human connectome.** A) A schematic view of the human connectome as a fully connected network with 6 nodes. Information dynamics within the connectome is regulated by an ensemble of information streams, mathematically shown as $\hat{\sigma}^{(\ell)}, \ell = 1, 2, ...6$. The way each stream contributes to the flow of information is represented as a diagram, where blue and red arrows, respectively, represent positive and negative fluxes and the size of each node represents the amount of field trapped on top of the node. B) Snapshots of possible functional diversity in a schematic connectome at two different Markov time (i.e. $\tau = 1$ above and $\tau = 2$ below). From left to right spectral entropy increases as the overlap of information flows decreases. Colored nodes encode the sources of information, shaded areas encode the flows of information, colored arrows the directions of such flows.

avoid confusion, it is worth remarking that the entropy is a macroscopic descriptor of the system as a whole, i.e., it does not quantify pairwise information transfer between nodes.

Another desirable feature of this framework is that one can vary τ to characterize the network state at different scales, from microscopic ($\tau \sim 1$) to mesoscopic ($\tau \sim \sqrt{N}$) and macroscopic ($\tau \sim N$) one. Note that the scales we are referring to are topological, but the tunable parameter used to span from the microscopic to the macroscopic one is of temporal nature, since it is the time required by a dynamical process defined on the top of the network, such as a random walk, to propagate information. More specifically, we use the temporal evolution of a statistical field to explore the topological scales of the connectome, a procedure successfully adopted for the analysis of other complex systems, from the human proteome [125], to the human microbiome [88] and to social and transportation systems [127].

For instance, a network of size N with no connectivity at all would have an entropy equal to $log_2 N$ bits, the maximum attainable value, whereas a fully connected network (i.e., a clique), would have the lowest possible entropy, tending to 0 bits in the limit of large τ.

We consider two distinct dynamical processes, namely a classical random walk (CRW) and a maximal entropy random walk (MERW), and use the variation of spectral entropy with Markov time τ to characterize synthetic and empirical human brain networks across multiple scales. The persistence of information flow is characterized by the decay of the spectral entropy: the slower the decay, the more persistent the flow through the network.

4.5.6 Maximum posterior probability

To quantify the statistical significance of the differences (or similarities) within the connectomes coming from two distinct groups (e.g., empirical

data vs. model, control vs. disease, etc.) considered for this work, we performed pairwise t-tests, adequately corrected for multiple test comparison. In particular, we tested two distinct null hypotheses (H_0): i) the generative models reproduce the real data (data set 1); ii) the spectral entropies in healthy and non-healthy brains are equal (data set 2). Since we are performing multiple tests, i.e. we tested real data against the four generative models and the healthy controls against different stages of dementia, we adjusted the resulting p-values by means of the Bonferroni-Holm method. All pairwise t-tests are performed by considering a 95% confidence interval.

To avoid confusion in the interpretation of the p-values, here we use a Bayesian approach for p-value calibration proposed by Sellke et al. in 2001 [246], so that p-values can be interpreted from both a frequentist and a Bayesian perspective. Specifically, we compute the Bayes factor as:

$$B(p) = -ep\log(p) \tag{4.5}$$

for $p < 1/e$, which corresponds to the lower bound on the odds provided by the data for H_0 and H_1, the latter being the alternative hypothesis. If we consider the frequentist error probability of rejecting H_0 when it is true (type I error), the calibration is given by

$$\alpha(p) = \left(1 + B^{-1}(p)\right)^{-1} \tag{4.6}$$

where, in this case, p is the adjusted p-value. Therefore, we have two possible interpretation for the outcome of this calibration. From a frequentist perspective, it precisely coincides with the error probability of rejecting a true null hypothesis. From a Bayesian perspective, it is the (maximum) posterior probability of H_0 provided that the Bayes factor corresponds to the one expressed in Eq. 4.5 and assuming that H_0 and H_1 have equal prior probabilities of 1/2. The results of t-test thus can be either interpreted as the probability of rejecting the null hypothesis when it is true and as the

probability of the null hypothesis itself. In other words, lower recalibrated p-values are indicative of lower accordance between the samples that we are testing – lower maximum posterior probability –, while higher recalibrated p-values can be interpreted as higher probability of accordance between the samples under consideration.

4.6 Experimental results

4.6.1 Probing synthetic models of the human brain

Our first analysis concerns with quantifying the differences between empirical connectomes from healthy subjects, as measured from 196 individuals within the Nathan S. Kline Institute - Rockland Sample, and synthetic networks obtained from a pool of generative models.

Persistence of information flow is used to this aim: we calculate the average spectral entropy $\langle S_\tau(G_{data})\rangle$ over the whole set of subjects, as well as the average spectral entropy $\langle S_\tau(G_{model})\rangle$ over the ensemble of different independent realizations of a generative model, for each generative model separately, and for the two distinct dynamical processes separately. Results are shown in Fig. 4.2. Specifically, results shown in Fig. 4.2 have been generated by considering a sample of 196 subjects. For each subject we generate 100 different realizations of each generative model, resulting in 19600 samples which are later used to estimate each synthetic curve shown in the figure.

As expected, when considering the values of spectral entropy varying with Markov time, τ, the generative models exhibit distinct behavior across scales, and their ordering with respect to the value of entropy allows one rank them from the simplest to the most complex one. In fact, as it can be seen in a) and c) of Fig. 4.2 the Erdös-Rényi model (ERM) and the configuration model (CM) require a smaller amount of bits for their description

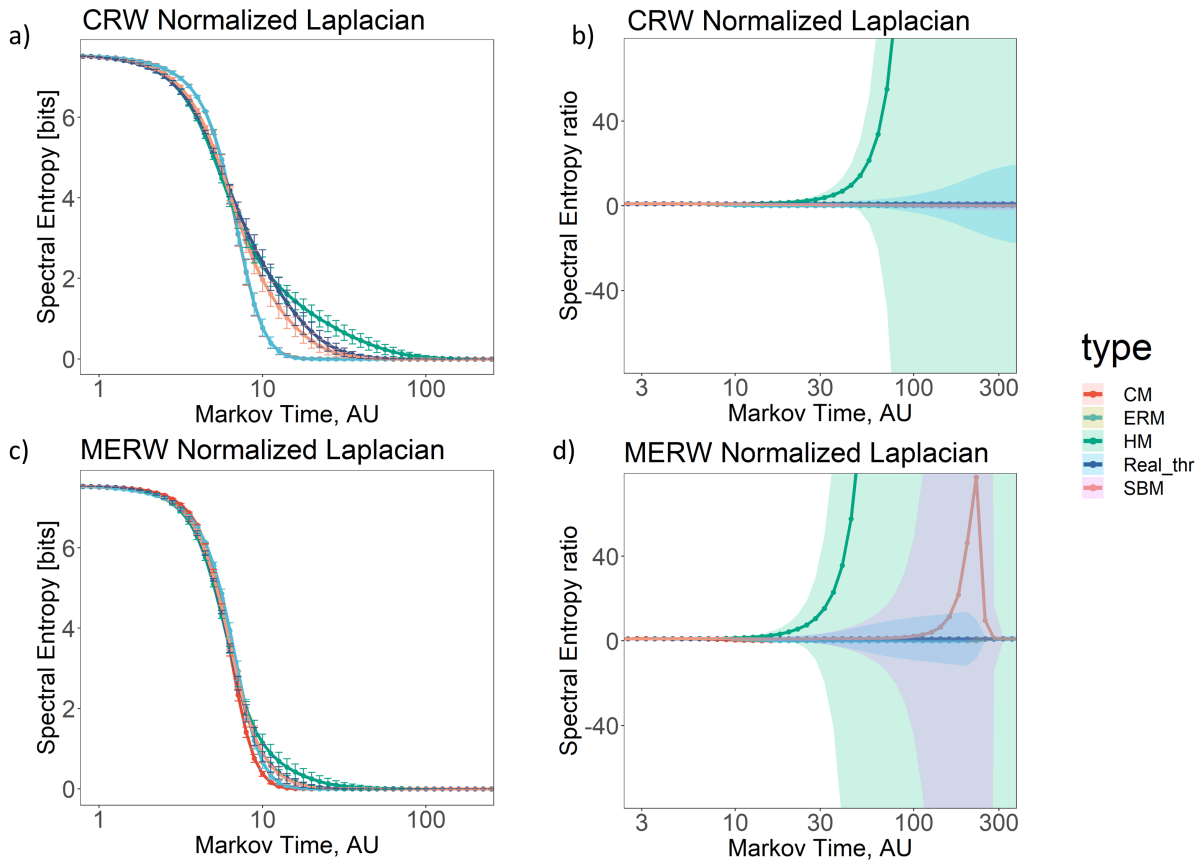

Figure 4.2: **Persistence of information flow in human brain and generative models.** In a) and c) we report the average value of spectral entropy varying the Markov time, τ, for the real data (blue line) and for all the considered generative models (encoded with colored lines), i.e. Erdös-Rényi model (ERM), configuration model (CM), hyperbolic model (HM) and the stochastic block model (SBM), obtained from the classic random walk (CRW) and the maximal entropy random walk (MERW) dynamics, respectively. In b) and d) we report the ratio between the average value of spectral entropy – varying the Markov time – of each generative model and the value of spectral entropy of real data, by considering the classic random walk (CRW) and the maximal entropy random walk (MERW) dynamics, respectively. All the curves have been generated considering networks of 188 nodes and each synthetic curve results from a sample of 19600 realizations of the network. For all the plots, the x axis is expressed in logarithmic scale. Shaded areas in b) and d) represent the error as one standard deviation.

than empirical connectomes, followed by the more complex stochastic block model (SBM) and finally by the hyperbolic model (HM), for both CRW and MERW dynamics. Interestingly, the spectral entropy of the empirical brain

lies between these last two more complex generative models, providing an indication of its possible mixed nature, interpolating between the modular feature encoded by SBM and the latent geometry encoded by HM. This result is robust across the two type of considered dynamics – CRW and MERW. It is worth noticing that differences between the spectral entropy of the connectomes and their synthetic counterpart obtained from generative models are visible while spanning from the micro to meso-scale ($\tau \approx \sqrt{N}$) and that these differences are amplified at the mesoscale ($\sqrt{N} \leq \tau \leq N$), where N is the number of nodes of each network and is equal to 188 (thus, $microscale < \sqrt{188}$, $\sqrt{188} \leq mesoscale < 188$ and $macroscale \geq 188$). The fact that spectral entropy values remain higher for increasing Markov time denotes a larger persistence of information flow, i.e., a slower entropy decay, as in the case of the hyperbolic model. To further appreciate the differences between the entropy of synthetic and empirical networks we compute the entropic ratio $r_\tau(G_{model}, G_{data}|\mathrm{RW}) = \langle S_\tau(G_{model})\rangle / \langle S_\tau(G_{data})\rangle$ for each value of τ, generative model and random walk (RW) process (see panels b) and d) of Fig. 4.2).

In this case, differences are visible at the mesoscale and are amplified at the macroscale ($\tau > N$). CRW dynamics shows an important difference between the empirical brain and the hyperbolic model, highlighted by a high entropic ratio. This difference also appears when considering MERW dynamics which, in addition, reveals the deviation of the SBM from the empirical brain at the macroscale, highlighted by a high entropic ratio.

Leveraging on the multi-resolution nature of our information-theoretic approach, we tested if there are significant differences between the empirical connectomes and their pool of generative models, by considering the values of spectral entropy at (and across) different scales defined by τ. Results of t-tests between spectral entropy values coming from real data and synthetic models are provided in terms of adjusted p-values and maximum

posterior probability, and are reported in Fig. 4.3. At the microscale, all

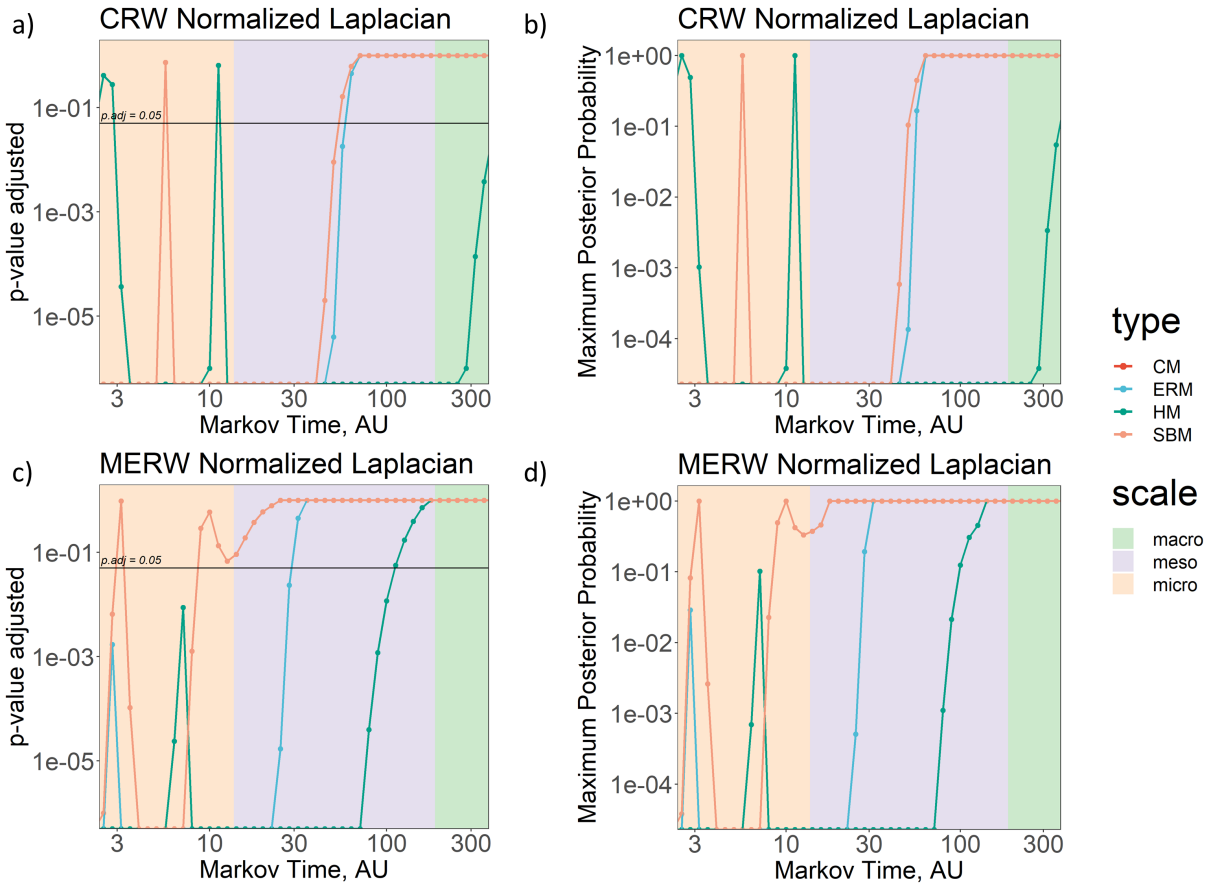

Figure 4.3: **Identifying significant differences between human brain networks and generative models.** In a) and c) we display the adjusted p-value resulting from the t-test between real data and all the considered generative models (encoded with colored lines), i.e. Erdös-Rényi model (ERM), configuration model (CM), hyperbolic model (HM) and the stochastic block model (SBM), by considering the classic random walk (CRW) and the maximal entropy random walk (MERW) dynamics, respectively. In b) and d) we display the values of maximum posterior probability recalibrated from the adjusted p-values. All plots are expressed in log-log scale. Shaded areas represent in the order the micro, meso and macro-scale coincident with $\sqrt{N}$ (from micro to meso) and N from meso to macro-scale, with $N = 188$. It is to be noticed that there is an overlap between the ERM and the CM.

generative models are significantly different from the human brain networks they attempt to reproduce when considering the CRW dynamics, except for a few values of spectral entropy in HM and SBM. Instead, MERW

dynamics shows significant similarity between real data and the stochastic block model not only at the microscale but also across the mesoscale and macroscale. For $\tau \geq 30$, above the mesoscale the synthetic networks, except for the ones generated by HM, are significantly similar to the empirical ones, when considering CRW. In the case of HM, the similarity is well established in the macroscale. In the case of MERW dynamics, the similarity with HM emerges slightly before the transition from the mesoscale to the macroscale, and across the macroscale. To further strengthen our results, we report, as well, the values of maximum posterior probability, obtained by recalibrating the p-values adjusted, in b) and d) of Fig. 4.3. Under some specific assumptions, this corresponds to the error probability in rejecting the null hypothesis H_0 – the generative models reproduce the real data –, from a Bayesian perspective.

To sum up, the mesoscale seems to be the suitable scale for distinguishing the differences (and the similarities) between the empirical brain and its possible generative models, since at the microscale the real data are significantly different from all the synthetic models, while at the macroscale there are not significant differences between data and models. Curiously, when considering the MERW dynamics, the empirical brain can resemble a stochastic block model across all scales, thus supporting the broad application of community detection algorithms and stressing their importance for the analysis and the understanding of the human brain.

4.6.2 Information capacity at different stages of dementia

Here, we wonder if we can use the same framework to identify differences between healthy subjects and patients at different stages of dementia, namely mild cognitive impairment (MCI) and Alzheimer's disease (AD). For details about the data set used for this analysis, we refer to Materials and Methods.

To spatially characterize different diffusion processes (i.e CRW and MERW) on top of the network in healthy brain (H) and at different stages of dementia (MCI and AD), we provide brain maps encoding the steady state of the two considered dynamics, corresponding to the leading eigenvector of the transition matrix defining the process (see Fig.4.4).

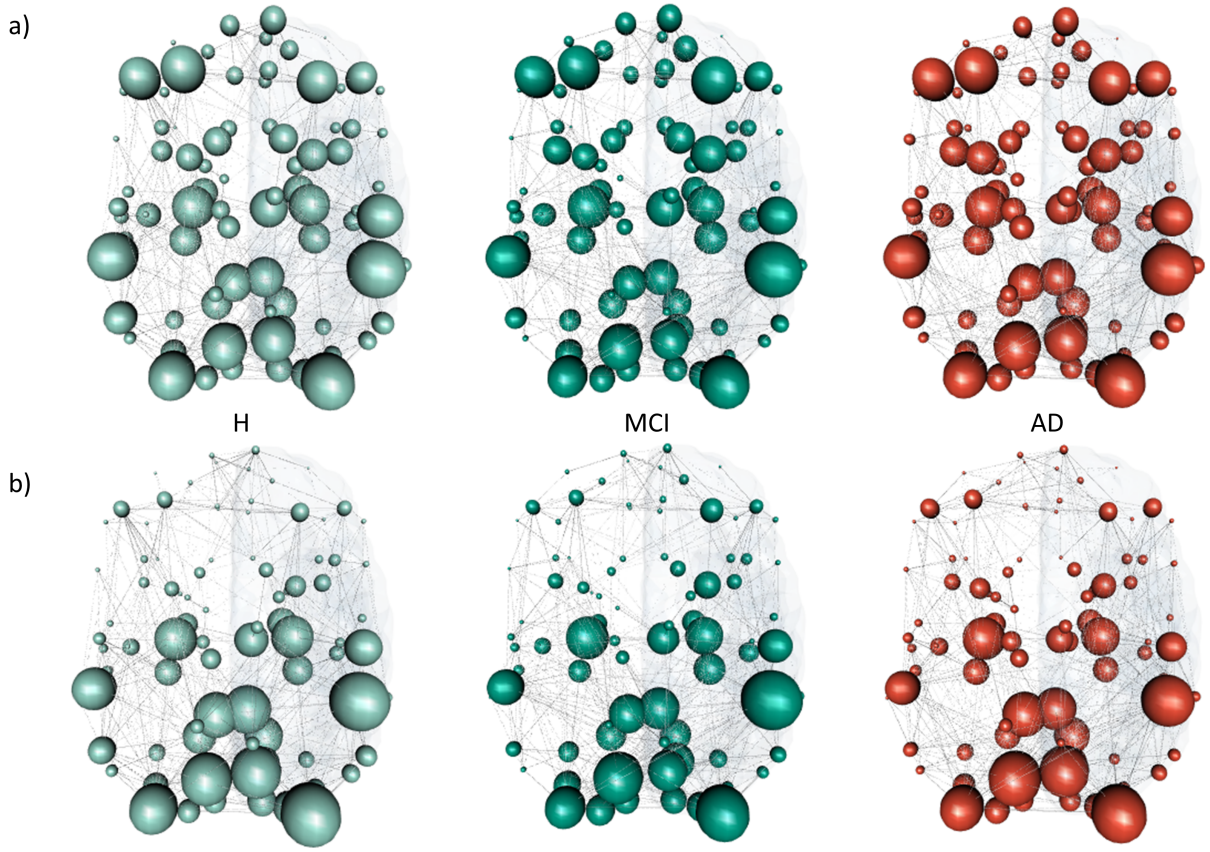

Figure 4.4: **Brain maps of the steady state distribution for the CRW and MERW dynamics in healthy brain (H) and at different stages of dementia (MCI and AD).** In a) we report the steady state for the CRW dynamics, while in b) the steady state for the MERW dynamics. The size of the node encodes the value of the steady-state corresponding to the leading eigenvector of the process.

Using the same approach as before, we show the results in Fig4.5. At the turn of micro and mesoscale, when considering CRW dynamics, the values of spectral entropy in the connectome of Alzheimer's disease pa-

tients show some differences from both healthy subjects and MCI patients. Intriguingly, the connectomes of AD patients exhibit a (slightly) higher spectral entropy than the ones of healthy and MCI subjects, denoting a larger persistence of information flow. As in the previous case, to further highlight differences between healthy and different stages of dementia we compute the ratio between the corresponding values of spectral entropy (see plots b and d of Fig.4.5). Differences between AD patients and the other two considered groups of subjects (healthy and MCI) are visible at the mesoscale and are amplified at the macroscale, while no differences appear between MCI and healthy. These results are in agreement for the two dynamics, CRW and MERW. Also in this case, we tested the significance of the differences between the spectral entropy of the two stages of dementia and healthy controls by means of t-tests, results are displayed in Fig.4.6. According to the p-values adjusted obtained when considering the CRW dynamics (see plot a of Fig.4.6), the spectral entropy in AD patients is significantly different from the one of healthy controls for most of the Markov time values at the micro, meso and macroscale. For what concerns the MERW dynamics (see plot c of Fig.4.6), the same is true only at the microscale. Interestingly, the only significant differences between values of spectral entropy in MCI and in healthy controls arises at the microscale and only for the CRW dynamics. Finally, resulting values of maximum posterior probability strengthen the results at the microscale for the AD patients (probability of the error $< 1\%$), when considering CRW dynamics.

4.7 Concluding Remarks

In this chapter, we presented a multiresolution analysis of the human brain building on statistical physics and information theory of complex networks.

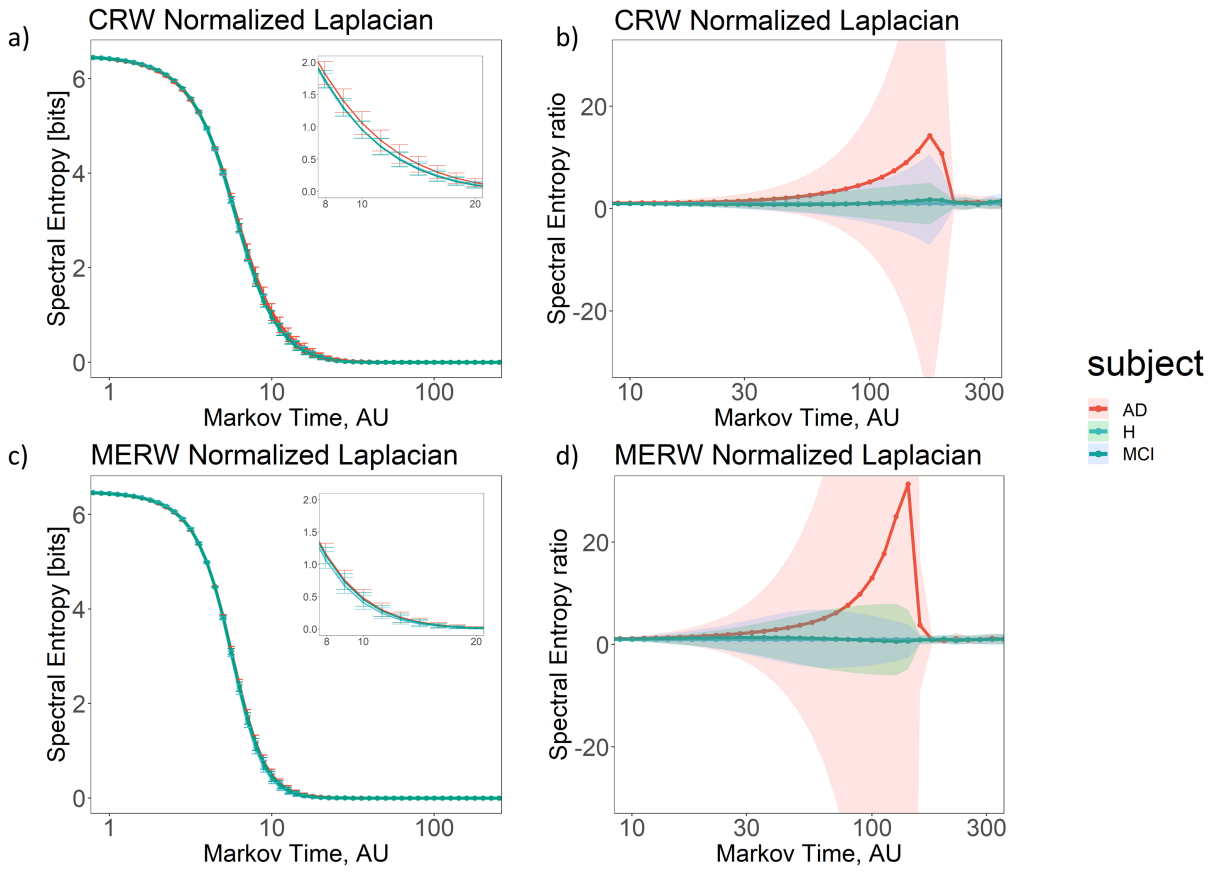

Figure 4.5: **Persistence of information flow in healthy brain (H) and different stages of dementia (MCI and AD).** In a) and c) we report the average value of spectral entropy varying the Markov time, τ, for healthy subjects (H,light-blue line) and different stages of dementia (MCI in teal and Alzheimer's disease in red), by considering the classic random walk (CRW) and the maximal entropy random walk (MERW) dynamics, respectively. The inset on the top right represents a zoom on the region at $\tau = [8 - 20]$. In b) and d) we report the ratio between the average value of spectral entropy – varying the Markov time – of each stage of dementia and the value of spectral entropy of healthy subjects, by considering the classic random walk (CRW) and the maximal entropy random walk (MERW) dynamics, respectively. For all the plots, the x axis is expressed in logarithmic scale. Shaded areas in b) and d) represent the error as one standard deviation.

Patterns of distributed activity, or modes, of the brain are neural dynamics unfolding on anatomical connectivity structures [158]. Topological structure of brain has been investigated using many functional and struc-

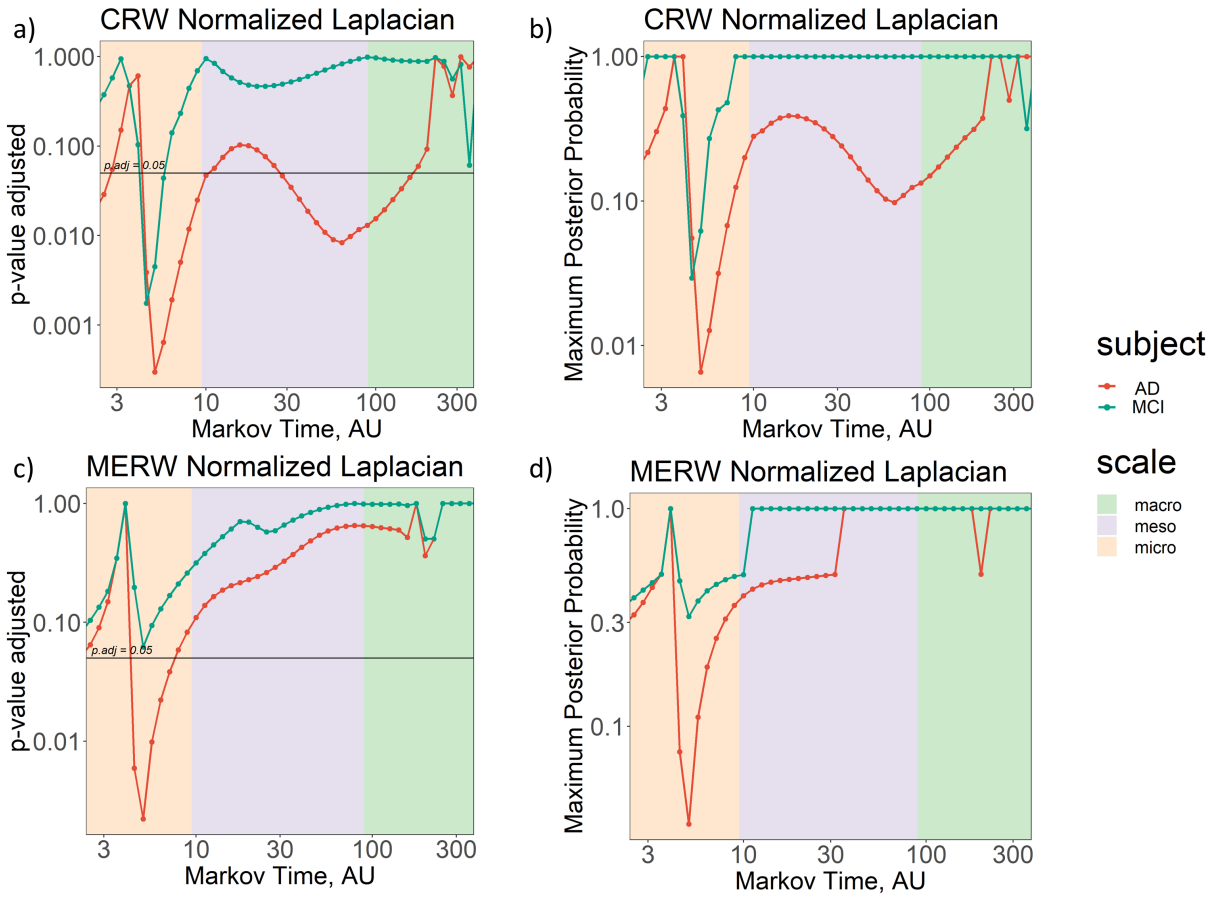

Figure 4.6: **Identifying significant differences between human brain networks in health and disease.** In a) and c) we display the adjusted p-value resulting from the t-test between different stage of dementia (MCI in teal and Alzheimer's disease in red) and healthy subjects for each value of spectral entropy varying with Markov time, τ, by considering the classic random walk (CRW) and the maximal entropy random walk (MERW) dynamics, respectively. Horizontal lines mark the p-value adjusted at 0.05. In b) and d) we display the values of maximum posterior probability recalibrated from the adjusted p-values. All the plots are expressed in log-log scale. Shaded areas represent in the order the micro, meso and macro-scale coincident with $\sqrt{N}$ (from micro to meso) and N from meso to macro-scale, with $N = 90$.

tural neuroimaging datasets [67, 262, 116, 115] that have established that brain regions have a modular functional organization and are also connected in a way that permits the emergence of whole-brain processes like attention, cognition and behavior. In other words, functionally distinct

brain areas have a hierarchical organization that permits integration at different topological scales [196, 35]. A typical example of a task that is implemented at different scales is invariant visual object recognition, that relies on a hierarchically organized set of visual cortical areas whose competition, biased by attention, is implemented locally but gradually increases thanks to the hierarchical nature of the network [98, 99]. In this context, to simultaneously capture the state of the network at different scales is crucial to fully understand a neural process. In this chapter we focused on resting state structural data but further works, investigating behavioral or cognitive functional tasks, can benefit from our approach. In particular, we could investigate how the functional role of brain regions changes in resting state with respect to specific behavioral or cognitive tasks, or how functional alterations are displayed at multiple brain scales in non-healthy subjects.

We exploited the information flow among system units restricted by the underlying connections to gain insights into the different functional role of brain regions at multiple scales. Here we used classical and maximal entropy random walk processes to explore the topological scale of the networks, but other types of dynamical processes (as synchronization processes) on the top of the system may be considered in further works, since the framework is very flexible. We first use our method to compare network models that have been widely used in the literature to describe brain organization and we found that at microscale, all the tested models are not suitable to describe real data. We hypothesize that, although MRI resolution preclude analysis about functional specialization within the dendritic tree or cortical macrocolumn [116] their layered structures could strongly affects the results at low spatial scale. On the contrary, the mesoscale is the most suitable resolution to compare network topologies. We found that real connectomes have features of stochastic block model and hyperbolic

model, where the former is representing the aforementioned brain modular organization of brain areas and the latter takes into account latent geometry in the communication flows among them.

Several previous studies have explored the mechanisms that control communication dynamics in brain networks [143, 25, 15]. Some models suggest that neural units have a knowledge of the whole network topology and convey information from a source to a predetermined target using (multiple) shortest paths [24, 132]. Other models, instead, do not make assumptions about global knowledge of network topology and propose that communication flows are ruled only by local knowledge of the distance between cortical regions [244]. In our work we explore both frameworks using two different diffusive processes to describe information flows among units: in the classical random walk we assume that communication dynamics only require local knowledge of the connectivity, whereas in the max-entropy random walk process we hypothesize that the walker uses global knowledge of the connectome to explore it. We found that the two approaches are compatible and that spectral entropy values are similar when we consider the two types of dynamics on top of stochastic block model and hyperbolic model. Those results are in agreement with the aforementioned study that shows how specific brain topological and geometrical properties lead to comparable efficiency in network communication with or without centralized knowledge.

Finally, our approach was used to investigated alterations in brain network topology in patients with Alzheimer's disease. Here we can avoid any assumption regarding the network generative model that better describe real data and we can focus on changes in information flows that characterize AD brain networks at different scales. Previous studies used standard networks analysis indicators to report abnormalities in the connectivity between different brain areas, and specifically found an increased connec-

tivity at spatial scales lower than brain lobe and postulated a mechanism of compensation associated with cognitive impairment [223, 300, 248, 233]. Our results are in agreement with the aforementioned studies, since they show a significant increase in persistence of information flows at microscopic scales in AD patients with respect healthy subjects. Furthermore, by taking simultaneously into account the whole network state, they suggest that compensation mechanisms may act at a smaller topological scale than previously hypothesized.

We conclude by outlining some limitations of our approach. Statistical physics of complex information dynamics has been shown to be a powerful framework to attack a range of problems in the domain of complex systems. Yet, it is worth mentioning that the computational cost for calculating the spectral entropy is still relatively high, being of the same order of the complexity of an eigenvalue problem. Therefore, our method would perform slower than more standard techniques in the case of very large networks, i.e. for sizes above 10,000 nodes: for smaller networks, the method is fast enough. The robustness of our analysis should be assessed also by analyzing other empirical data sets to further clarify how our entropy measures can be affected by the definition of distinct brain areas and can evolve when considering non-stationary (no resting state) brain activities. Finally, although the results presented in this work are promising for the investigation of dementia, the clinical usability of our approach requires further investigation.

In the next chapter, we will integrate the brain structure and functions with cognitive aspects, providing a new way of bridging between the human brain and the mind.

Chapter 5

A new framework towards the bridging between the human brain and the mind

In brief

In this chapter we propose a new framework to map the complex interplay between brain structure, function, and cognitive aspects, focusing on three different data sets in the MNI space. Nowadays, many studies are dedicated to the brain structure-function relationship, and its plausible mapping within the cerebral cortex. However, a clear understanding on such a relationship is still eluding us, because of its complexity. Here, we offer an integrated approach that capitalizes on neuroimaging, computational neuroscience and network science, to provide a novel mapping not only of the brain structure-function relationship but also of its cognitive counterpart, related to semantic aspects. Our result is an important preliminary step towards a better understanding of the human brain tradic nature. Notably, our mapping opens the door to the development of new integrated biomarkers for all diseases, such as AD, which strongly depends on the interplay between brain structure, function and cognition.

5.1 Introduction

There is evidence that damages to brain structure affect brain function and, as a consequence, cognitive aspects [243, 82]. As there is evidence of the other way around, i.e that brain structure might be affected by altered cognition [80]. The incomplete knowledge about the complex interplay between structure, function and cognitive capacity within the human brain has important clinical consequences, with obvious limitation to prevention and treatment of neurodegenerative disease and psychiatric disorders. Here, we offer a new way of mapping the triadic nature of the human brain, including its network structure, functional responses and semantic areas tiling cerebral cortex, the latter being specific areas of the human brain that get activated when a given concept is expressed, heard or perceived. This is possible thanks to an approach that integrates neuroimaging, computational neuroscience and network science, i.e network neuroscience.

The results of this chapter represent a novel attempt to bridge between brain and mind.

5.2 State of the Art

The human brain is structurally characterized by a heterogeneous pattern of evolving connections, giving rise to functional properties and supporting cognition. How matter operates within the human brain and how it relates to functional properties is still an open question, as is the implication of brain architecture and dynamics on cognitive aspects.

The brain, regarded as a complex system and thus modeled as a network, is a wide and intricated ensemble of neuronal hubs, connected by integrated, parallel and often even redundant axonal subcircuits [263]. The network of entities and connections creating the human brain is called the

human "connectome" [263]. The connectome is the setting of neurological functions. Such functions arise because of the multimodal interplay of key functional epicentres with each other, regulated by modulator areas [239]. Though, non-trivial relations exist between brain structure and functions. In this regards, a widely accepted idea is that the anatomy of the human brain has an impact on the dymanic of neural network [38, 44] although we cannot explain the observed functional connectivity by using only the anatomical information [44]. In fact, while the structural brain network represents the physical wiring of neural elements, to grasp brain mechanisms governing its functions we have to understand how the neural activity propagates, and how the information spreads, within the anatomical structure [185]. Secondly, a further less trivial relation appears if, in addiction to structure and function, we consider also the human cognition. In this case, the hypotheses at our disposal are at the edge of philosophy, physics and neuroscience. As discussed in the introduction of this thesis (Chap.1), the mind is expected to be an emergent process of the human brain, where cognition naturally emerges from interactions between brain areas, in multiple temporal and spatial domains [43, 38, 194, 72].

Thanks to neuroimaging tools, combining physics principle and neuroscience knowledge, we can gain unprecedented insight on brain components and on its inner functioning [185]. Brain activity mapping has clearly shown that are precisely the interactions between "hundreds or thousands of neurons" that give birth to mind's functional states [12]. Commonly, structural and functional connectivity are reconstructed from measurements of white matter (WM) tracts and regional brain activity, by means of neuroimaging techniques, such as MRI or DTI records for the brain structure and fMRI for functional connectivity [66, 168, 287]. On the one hand, structural connectivity is represented by an adjacency matrix obtained, for example, from DTI measurments of white matter tracts

between selected brain regions, and providing a proxy for real neural connections. On the other hand, functional connectivity is represented by similarity matrices obtained from fMRI records, for instance, and correlation measures or causal inference thereof, providing a proxy for real functional connections.

Clinically, the outputs given by the Direct Electrical Stimulation (DES) technique, adopted during resections of brain tumors for identifying and maintaining the eloquent structures – i.e brain areas that are identifiable with some neurologic function which, if injured, results in a neurologic deficit – has highlighted the pivotal role of brain connectivity for the functional processing [101, 239]. Using DES during intraoperative mapping of eloquent regions spurs a unique opportunity to assess the functional role of different brain pathways [101, 239]. This promising opportunity was seized by Sarubbo et al. which, in a study conducted in 2015 [239] on more than 100 patients who underwent awake surgery, provided a functional subcortical atlas of human white matter, summarizing the distribution of its essential sensorimotor, language and visual functions [239] (more on this atlas is reported below in Subsec.5.5.1). Specifically, they pointed out that while being DTI a powerful tool to enhance our understanding of white matter from an anatomical point of view, we were still lacking its functional information [239]. By stressing the need to define the pivotal role of WM in a more comprehensive way, Sarubbo et al. were able to provide a functional subcortical [239] and cortical [241, 240] atlas of human white matter, using DES.

A year after, in 2016, another important atlas was produced by Huth et al, providing a mapping of the semantic system that tiles human cerebral cortex [162], further strengthening the relation between the human brain and mind. In fact, this semantic atlas lists all brain areas that are selective to some specific concepts. Specifically, an area is considered

semantically selective if it activates when a given concept is expressed, heard or perceived. The semantic atlas groups concepts for which an area can be selective into 12 categories (tactile, visual, numeric, locational, abstract, temporal, professional, violent, communal, mental, emotional and social [162]). Each semantically selective area contains a combination of such categories, based on its 'sensitivity' to each category. If, for example, we heard the word 'love', selective areas for 'emotional' concepts will activate.

Worldwide, a common goal of mapping the human brain interactions is rising, motivating several brain initiatives (together with billion-dollar investments) [185], from the Human Connectome Project [286] in USA to the Blue Brain Project [190] in Europe, from the China Brain Project [224] to the Japan's Brain/ MINDS project [212].

5.3 The Problem

Nowadays, a complete knowledge on brain structure-function-mind relationship is still eluding us. As anticipated in the introduction of this thesis (Chap.1), the lack of this knowledge generates second-order gaps for example on the clinical side, where complex diseases such as AD, risk to be identified too late, with obvious limitation and prevention thereof. In this regard, the great challenge is to address the triadic nature of human brain, "with major implications for personalized mental health treatments" [185]. In general, aging – and AD in particular – is characterized by modification of brain morphology, in addition to a decline and impairment of cognitive aspects [44]. In this case, as clearly explained in [44], biomarkers based on both structural and functional (and cognitive, we claim) aspects would provide more meaningful biomarkers of Alzheimer's disease, with respect to those only relying on anatomical features measured by neuroimaging [44].

The first fundamental step to address this issue is to map crucial areas of the human brain, where multiple functions and cognitive aspects are manifest, bridging between brain and mind. This last chapter represents precisely our effort to this aim, proposing a new framework that accounts for structure, function and cognition. To this end, we have considered structural brain networks, cortical plus subcortical functional response errors and semantic areas tiling the human brain. Up an octave, this work constitutes our contribution to enhance *mapping* of the human brain.

5.4 The Proposed Approach

Here we take a step further in mapping the human brain triadic nature, by integrating three different data sets concerning the brain structure [3, 209], the brain functions [239, 240, 241] and the semantic systems tiling the human cerebral cortex [162]. As in chapter 2 where the exploration of concepts during a semantic task was considered part of the mental process, here the data set of semantic areas is intended as the "mental" layer of the mapping. This is a reasonable choice since the semantic areas are reconstructed from cerebral cortex sites which activate in the brains of individuals while listening to hours of narrative stories [162] with a given meaning. In other words, when a given concept or idea is expressed, heard or perceived certain areas get activated more than others. Here, these more active areas together constitute our "mental" layer.

Each data set is embedded into the MNI space. By considering the uncertainty σ on functional measurements and on the semantic selectivity of each area considered, we build three different "levels" of the brain map – from the finest grained possible to a more coarse-grained map – using two different type of assignment rules. In particular, a given functional and/or semantically selective area pertains to a structural node if their distance

is lower then a given threshold. How the threshold is defined depends on the assignment rule, which can be either geometric or hybrid, merging geometry and network information.

As the prime layer of the mapping, we took the structural connectivity network of the brain by randomly selecting one network from the same data set used in chapter 4 [209]. This data set consists of resting-state structural data, that represents the physical structure of brain networks of 196 healthy subjects not affected by mental or physical disorders. Then, we build upon this network, by enriching each node with functional and mental features provided by the studies of Sarubbo et al. [239, 240, 241] and Huth et al. [162], respectively. How? By considering the distance from functional and semantic areas' centroids to structural nodes and by setting a tolerance based on the uncertainty of measurements σ. Specifically, the way used to compute the distance defines the type of assignment rule. In fact, the distance can be a geometric one (geometric assignment) or a hybrid distance, merging geometry and network hops (hybrid assignment), more on that will be explained in Sec.5.5). For sake of clarity, we have reported a conceptual visualization of the assignment rules proposed for the mapping, in Fig.5.1.

We have considered an uncertainty range that spans from 1 to 3 standard deviations (σ) for both the functional and the mental data set. According to the selected σ, the results is a more or less fine-grained brain map, characterized by structural nodes having specific functional features (from sensorimotor to language and visual functions) and specific semantic selectivity. For semantic selectivity is meant the combination of semantic clusters, or group of concepts, to which one area is selective [162]. Specifically, we refer to the 12 distinct categories identified by Huth et al., which have been inspected and labelled by hand (i.e. tactile, visual, numeric, locational, abstract, temporal, professional, violent, communal, mental,

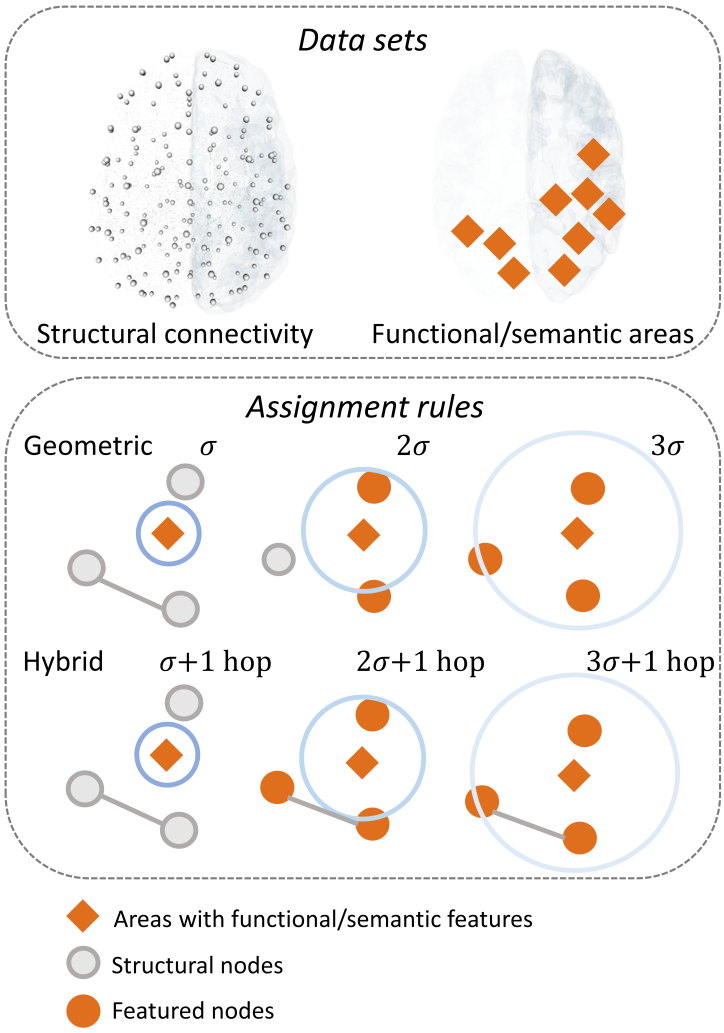

Figure 5.1: **Illustrating brain mapping** of functional and/or semantic features. Given the structural connectivity and the features data set either functional or semantic, the mapping is performed according to an assignment rule. The assignment can be either geometric or hybrid. In the case of geometric assignment, the structural node assumes the feature(s) of the closer functional/semantic areas depending on a distance corresponding to 1σ up to 3σ, where σ is the uncertainty of measurements. In the case of hybrid assignment, besides the distance between the structural node and feature areas, also the structural connectivity is considered. The structural node assumes the feature(s) of the closer functional/semantic areas depending i) on their distance and ii) on the features of the first nearest neighbor(s).

emotional and social [162]).

The so obtained mapping provides the basis for getting new insights on the brain-mind complex interplay. In fact, we can used it to measure the features-enriched structural connectivity, but also to assess whether specific concepts are potentially related to some brain functions, and more.

5.5 Materials and Methods

5.5.1 Dataset

In this work, we rely on three main data sets, representing the structure, the functions and the mental counterpart of the human brain. The three data sets are:

1. **A structural connectivity data set** provided by the Nathan S. Kline Institute - Rockland Sample (NKI-RS), consisting of 196 healthy subjects at rest without any mental or physical disorder [3]; For structural connectivity is intended the topological interconnection of brain regions as identified through diffusion tensor imaging (DTI) techniques and summarized in adjacency matrices according to some specific indicator (e.g., fractional anisotropy). This data set consists of resting-state structural data, representing physical structure of brain networks.

2. **A functional data set** at the cortical and subcortical level, provided by the study of Sarubbo et al. [239, 240, 241]; the data set provide the eloquent sites, intended as brain specific areas that are identifiable with some neurologic function which, if injured, results in a neurologic deficit. The eloquent sites are defined according to functional response errors, i.e. alterations in functional response in some specific sites, registered during intra-operative Direct Electrical Stimulation (DES). The study has been conducted at the cortical surface and subcortical white matter in more than 100 patients undergoing awake brain surgery [239, 240, 241]. Specifically, 1820 cortical and subcortical sites were registered in the MNI space, each one being eloquent for specific functions. The functions, reported in the data set are: Phonologic, Semantic, Anomia, Speech arrest, Language and

motor perseverations, Verbal apraxia, Motor, Movement arrest, Mentalizing, Eyes apraxia, Spatial perception, Sensorial, Visual, Alexia, Acustic and Asemantism.

3. **A semantic selectivity data set of cerebral cortex** provided by the study of Huth et al. [162]; For semantic selective area is intended an area which activates when a given concepts is heard, expressed or perceived. Concepts have been categorized in 12 semantic groups by Huth et al., the 12 categories are: tactile, visual, numeric, locational, abstract, temporal, professional, violent, communal, mental, emotional and social [162]. The data set consists of 140 semantic selective areas characterized by 20 meaningful words of that area and a measure of selectivity for each of the 12 semantic clusters.

Each data set is mapped into the Montreal Neurologic Institute (MNI) space.

5.5.2 Brain mapping

In previous sections, we have already anticipated what we meant by assignment rules and we provided a graphical representation of it in Fig.5.1. In the following, we better explain the mapping procedure for both the functional and the mental data set.

For what concerns the mapping of human brain triadic nature, we have considered two type of assignment rules: the geometric assignment and the hybrid assignment. However, results provided in the next section are mainly obtained via the geometric assignment. The geometric assignment considers the geometric distance, in the MNI space, between each structural node and each centroid of the features sites (weather functional or semantic). If such a distance is lower then a given tolerance, then the features site pertains to the structural node. The tolerance is equal to one

(up to three) standard deviation σ of the measurements, known a priori. In other words, a structural node is featured by the functional and/or semantic properties of a given site if it falls within one, two or three standard deviations from such site (see Fig.5.1). The standard deviation σ is defined a priori by the sensitivity of the measuring instrument (5mm) in the case of functional data set, or provided by the authors in the case of semantic atlas. The geometric assignment can be formalized as follow. Let us define the structural connectivity of the brain network as a finite connected graph of nodes $i = 1, ..., N$ whose connectivity is defined by the adjacency matrix $\mathbf{A}$. The element $a_{i,j}$ of $\mathbf{A}$ is equal to 1 if a link exists between node i and node j and 0 otherwise. Now let us arbitrarily choose a structural node i, and a functional (or semantic) site f, the node i is featured by the properties of f if:

$$dist(i, C_f) \leq b * \sigma \tag{5.1}$$

where $dist$ is the geometric distance, C_f is the centroid of the site f and b is a constant that can be equal to 1, 2, or 3. According to the value of b, the mapping is more or less coarse grained, since the higher the value of b, the wider the areas accounted for and the less specific the assignment. Finally, let us define the set of featured nodes F^{geom}, according to a geometric assignment rule:

$$F^{geom} = \{i \mid dist(i, C_f) \leq b * \sigma\} \tag{5.2}$$

The hybrid assignment merges the geometric distance, of the previous case, and the network distance (see Fig.5.1). Specifically, the structural nodes can be featured ii) by the functional and/or semantic properties of nearby areas according to a tolerance (geometric assignment) and ii) by the features of the nearest neighbor(s) in the structural network, i.e the

nodes within one hop (or more, according to the order of nearest neighbor we want to account for, here we have considered just one hop). The hybrid assignment can be formalized as follow. Let us define the set of nearest neighbors of node i, K_i as:

$$K_i = \{j \mid a_{i,j} = 1, i \neq j\} \tag{5.3}$$

We can now define the set of featured nodes in the case of hybrid assignment, F^{hyb}:

$$F^{hyb} = \{i \in F^{geom} \cup j \in K_i, j \notin F^{geom}\} \tag{5.4}$$

It must be noticed that while the values of σ are constant for each site and within the three dimensions for the functional data set, the same is not true for the semantic atlas. In fact, in the semantic atlas the standard deviation is different for each semantic tile and it also changes in the three dimension x, y, z. However, for each tile of the semantic atlas, the values of σ are positively correlated within the three dimensions (all p-values of Pearson's correlation lower than 0.0007). For this reason, we aggregated the standard deviations of each semantic tile on the three dimensions as follow:

$$\sigma = \sqrt{\frac{\sigma_x^2 + \sigma_y^2 + \sigma_z^2}{3}} \tag{5.5}$$

5.6 Experimental results

Since we provide a new framework to map the brain-mind relation, the main result of our work is precisely the mapping of the human brain, which integrates the structural, the functional and the mental counterparts. We proposed two different assignments rules – geometric and hybrid – to obtain the brain mapping. In Fig.5.2 we show a representative result of our work,

i.e. the brain mapping obtained using the geometric assignment rule. A similar result can be provided using the hybrid approach as well.

In Fig.5.2 we offer different perspectives of the brain mapping, highlighting the salient layouts that can be obtained with our approach. Let us explore them in details in the following.

Firstly, we show a general brain map in Fig.5.2 a), reporting the structural connectivity network (grey nodes) enriched by i) the presence or not of semantic selectivity (nodes with green halo are semantically selective) and ii) the total amount of functional features expressed by each node (color ramp from grey to blue), varying σ. It is to be noticed that for what concerns the semantic selectivity, here we have only indicated whether or not a node is semantically selective, and not to what extent each of the 12 semantic categories is expressed by the node (this information will be shown later in Fig.5.2 c)). For functional features, we have indicated the total amount of features expressed by the nodes. To give an example, a node can be eloquent for movement arrest, semantic, anomia and verbal apraxia functions, concomitantly. To avoid possible misunderstanding, we would like to stress the fact that the function 'semantic' and the semantic selectivity are two distinct things. In fact, the function 'semantic' comes from the functional data set and indicates our ability to call something with its proper name (e.g. when we see a horse, we are able to call it 'horse' and not 'cow' [240]). The semantic selectivity, instead, comes from the mental data set, and defines the category of concepts to which an area of the brain is selective for (e.g. if you are a professional horse rider and you hear the word 'horse' then the brain regions selective for those concepts evoked by the word 'horse' will get activated, e.g. brain areas selective for emotional, professional or even social concepts). Not surprisingly, the higher the value of σ the higher the number of nodes featured by both semantic and functional properties. These maps are useful to grasp a general overview of the

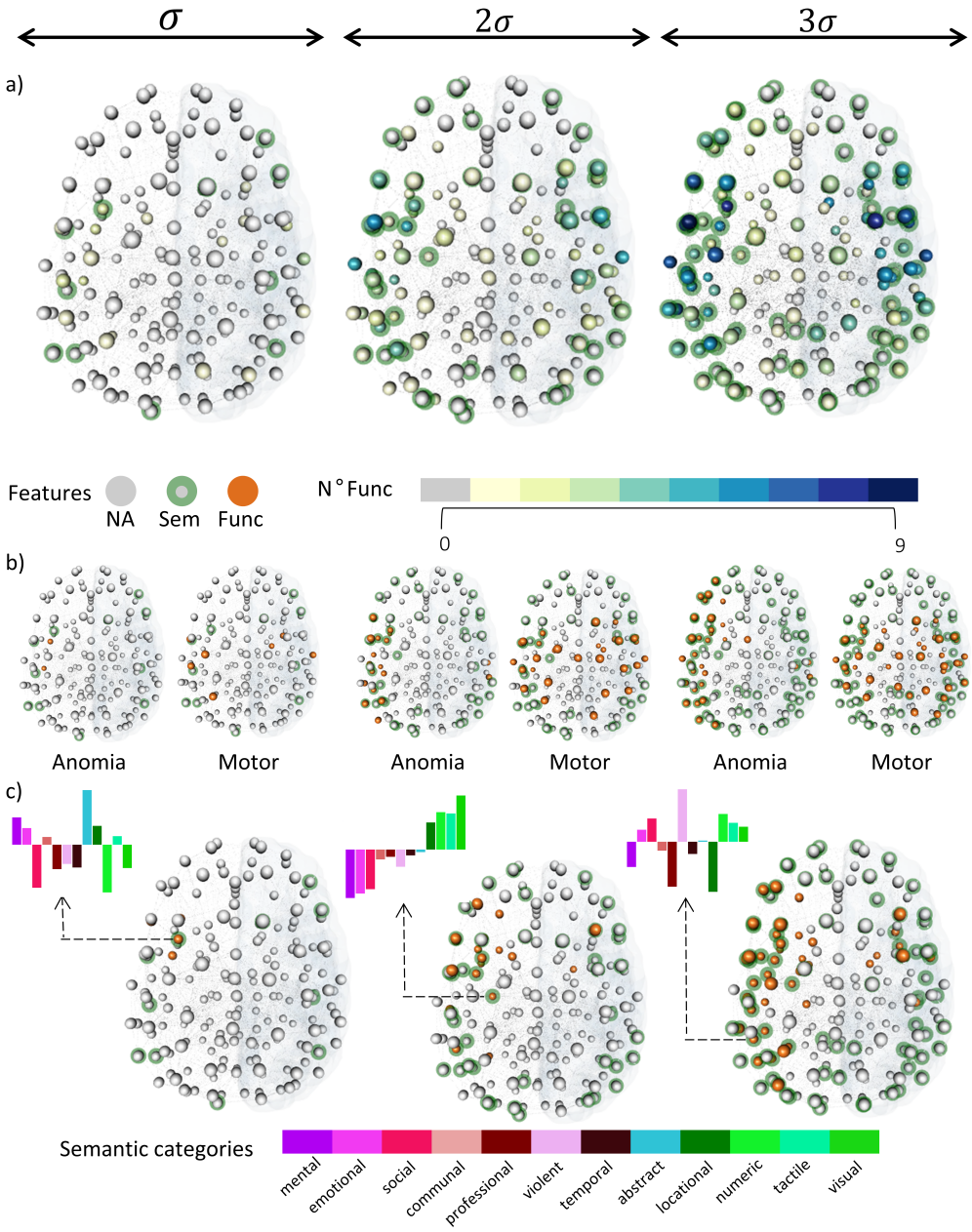

Figure 5.2: **Brain mapping via geometric assignment.** a) Brain mapping of structural connectivity network (grey nodes) enriched by semantic selectivity (nodes with green halo) and the total amount of functional features (color ramp) expressed by that node, varying σ. b) Example of mapping of eloquent sites for anomia and motor functions (orange nodes) together with semantic selective nodes, varying σ. c) as b) but considering the eloquent sites for semantic functions (orange nodes), and the semantic selectivity of three nodes expressed according to the 12 categories provided by Huth et al. (color ramp) [162].

fraction of nodes featured increasing σ. Moreover, with these maps we can gain information about the correlation between the number of functional features expressed by the node and the presence of a semantic (mental) selectivity. Also, we can assess the correlation between the node centrality in the structural network and the number of functions expressed by such a node.

Secondly, in Fig.5.2 b) we report examples of specific eloquent sites mapped for anomia and motor functions (orange nodes), together with semantic selective nodes (nodes with green halo), varying σ. Also in this case, the higher the value of σ the higher the number of nodes featured by both semantic and functional properties. These maps are useful to understand which network nodes express some specific functional features, and weather these nodes match with the ones featured by mental characteristics. It is to be noticed that here we just reported plots for anomia and motor functions but a equivalent plot can be obtained for all other functions (i.e. phonologic, semantic, speech arrest, language and motor perseverations, verbal apraxia, movement arrest, mentalizing, eyes apraxia, spatial perception, sensorial, visual, alexia, acustic and asemantism).

Finally, in Fig.5.2 c) we provide a more specific characterization of semantic selectivity for three nodes (green halo), randomly chosen in the network, where also the semantic functions were active (orange nodes). We chose the semantic functions just for sake of congruence but all other functions can be shown. Here the semantic selectivity of the three different nodes is characterized according to the 12 semantic categories provided by Huth et al. [162] and it is represented with colored barplots. To give an idea, from the barplot in the first map of Fig.5.2 c) we can see that the chosen node is more selective for mental, emotional, abstract and locational concepts, with a maximum for the abstract one. Again, increasing σ the fraction of included nodes increases. These maps could be useful to

gain an insight about what and where are the nodes which are semantically selective for a given category of concepts, e.g. for emotional or social concepts. In other words, what are the nodes that could activate when a given concepts is expressed, heard or perceived in the outer world, and eventually which are the functions concomitantly expressed by that node.

In the following, we inspect a couple of analyses conducted on our brain maps to give a glimpse of what can be done with our approach. Again, the results are provided for the maps obtained via geometric assignment, but the same analyses can be conducted on maps obtained via hybrid assignment.

In general, considering one σ, 10% of the nodes has at least one functional feature, with 2σ up to 44% of nodes has at least one functional feature, while when we set the threshold to 3σ we have the 62%. Interestingly, if we only look at the nodes with a semantic function, 25% of them has also a semantic selectivity when we set the lower σ, the percentage of nodes grows up to 65% considering 3σ.

To start, we wonder if the most central nodes in the structural network in terms of degree, betweenness and PageRank are also those ones that express the largest number of functions. To this aim, we computed the Pearson correlation coefficient and the Spearman's rank correlation coefficient between the centrality and the number of functions expressed by each node. We found out that there is no correlation between the node centrality and the number of functions expressed by the node, whatever the value of σ (see table 5.1). Hence, for example, the most connected nodes in the structural network (hubs) are not the ones with higher functionality.

Similarly, we wonder if the most central nodes in the structural network (in terms of degree, betweenness and PageRank) are also those that express a semantic selectivity. Also in this case we observed that there is no correlation between the node centrality and the expression of semantic

metric	σ	Pear corr coeff	p-val	Spear rank corr coeff	p-val
deg	1	-0.006929106	0.9248	-0.004923216	0.9465
deg	2	-0.1452506	0.04672	-0.1356933	0.06335
deg	3	-0.114692	0.1171	-0.1386297	0.05779
bet	1	0.05332937	0.4673	0.05231594	0.4758
bet	2	-0.03394414	0.6438	-0.04739452	0.5184
bet	3	0.002122603	0.9769	-0.03074136	0.6754
PR	1	0.00547763	0.9405	0.004891847	0.9469
PR	2	-0.1109739	0.1295	-0.09438166	0.1976
PR	3	-0.06538622	0.3727	-0.08617088	0.2397

Table 5.1: **Correlation results** between node centality in terms of degree (deg), betweenness (bet) and PageRank (PR) and the number of functional features expressed by the node. Null hypothesis: correlation is equal to zero.

selectivity by the node, at lower values of σ, while increasing σ the correlation becomes negative (see table 5.2). Hence, the semantic selectivity (in terms of presence/absence) of the node is not related to the centrality of the node itself (or poorly negatively correlated).

Finally, we concentrate only on those nodes which have both functional and mental features. We wonder if there is a match between the expression of a given functional feature and the selectiveness to a group of concepts. For example, to which concepts are selective the nodes that express functions related to the language (e.g. semantic, phonemic, anomia, speech arrest) or related to motor skills (e.g. motor, movement arrest) or again related to a combination of language and motor (e.g. alexia, language and motor perseverations). To investigate this functional-mental relation we provide its representation in terms of a bipartite network (see Fig.5.3). In this bipartite network we see how increasing the value of σ, the number of nodes with both functional and mental features increases. Each bipartite network of Fig.5.3 maps the relation between a given function expressed by the node and its semantic selectivity, in terms of maximum cluster ex-

metric	σ	Pear corr coeff	p-val	Spear rank corr coeff	p-val
deg	1	-0.1234285	0.0915	-0.1197264	0.1017
deg	2	-0.2023753	0.005349	-0.1524907	0.0367
deg	3	-0.371698	1.506e-07	-0.3616458	3.411e-07
bet	1	-0.06984917	0.3408	-0.07245287	0.3231
bet	2	-0.141635	0.05252	-0.05705579	0.4367
bet	3	-0.2546259	0.0004215	-0.256737	0.0003758
PR	1	-0.09277222	0.2054	-0.08915667	0.2237
PR	2	-0.1682046	0.02103	-0.1139949	0.1193
PR	3	-0.3390821	1.936e-06	-0.3263068	4.878e-06

Table 5.2: **Correlation results** between node centality in terms of degree (deg), betweenness (bet) and PageRank (PR) and the presence or not of a semantic selectivity in the node. Null hypothesis: correlation is equal to zero.

pressed by the node. The scale color is the same for all the network, the colored link encodes the number of nodes which share that combination of functional-conceptual expression. As well for the thickness of the links, but the scale is proper to each network. Considering one σ (Fig.5.3 a)), we can see that the nodes having a 'semantic' or a 'speech arrest' function are maximally selective for abstract concepts. It is interesting to note that in this case just one out of 12 semantic categories is maximally selective. Increasing σ, we have up to 8 semantic categories (out of 12) to which the nodes are maximally selective. Intriguingly, nodes that have functional features related to language skills are highly selective for social, abstract, violent and visual concepts. While the nodes with motor functions are particularly selective for abstract and social concepts. Finally, the nodes featured with functions related to both language and motor (together) are highly selective for abstract, social and violent concepts. Curiously, nodes which exhibits the function 'Semantic' or 'Anomia' are especially selective for social concepts.

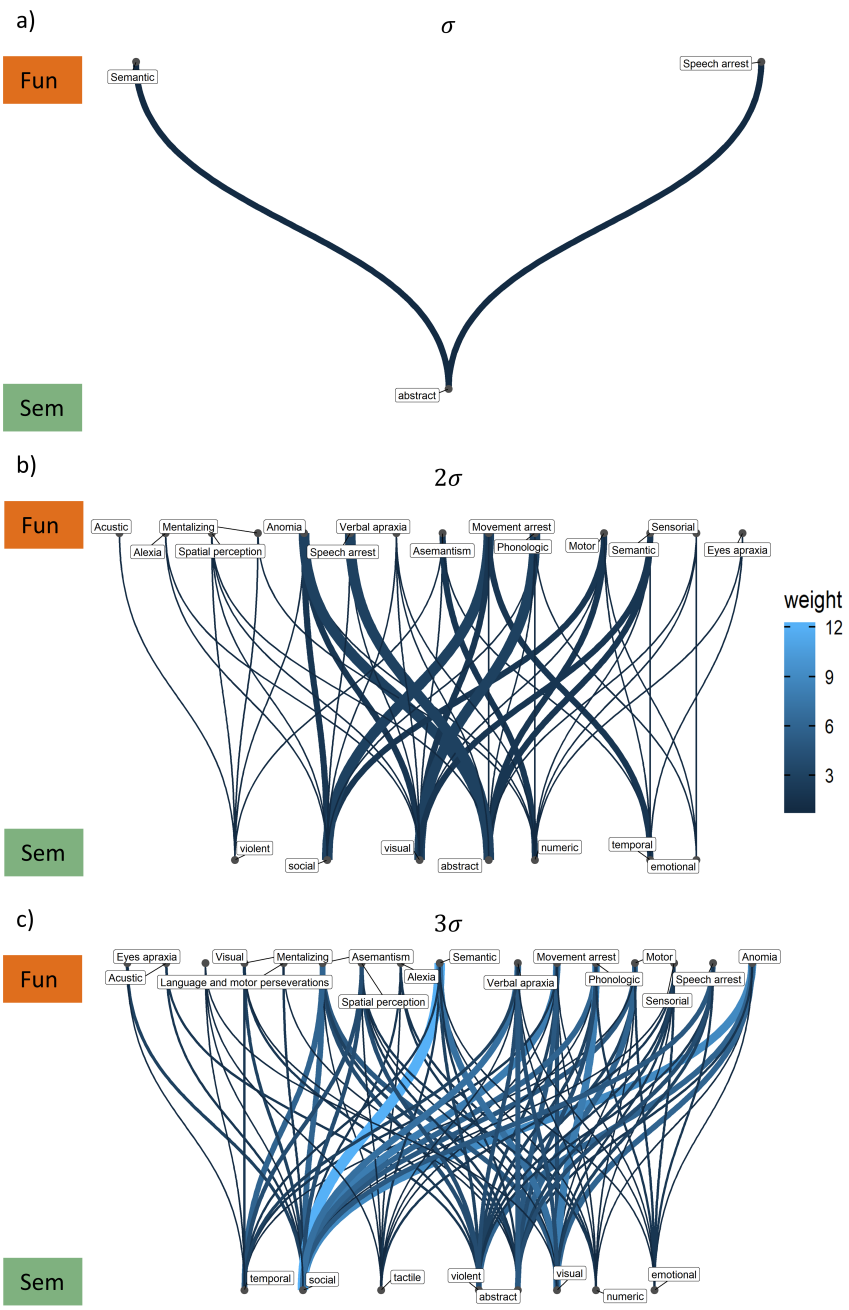

Figure 5.3: **Bridging functional and mental features.** Bipartite networks of nodes featured by both functional and mental features, concomitantly, varying σ. Each bipartite network maps the relation between a given function expressed by the nodes and their semantic selectivity, in terms of maximum cluster expressed. The scale color is the same for all the network, the colored link encodes the number of nodes which share that combination of functional-conceptual expression. As well for the thickness of the link, but the scale is proper to each network. a) Considering one σ, the nodes having a 'semantic' or a 'speech arrest' function are maximally selective for abstract concepts. A similar reasoning can be done for for b) and c).

5.7 Concluding Remarks

In this chapter, we provided a new framework to map the triadic nature of the human brain, including structure, function and cognition. We proposed two different types of assignment rules – geometric and hybrid – to match

structural nodes, functional areas and the semantic system tiling the human cerebral cortex. Relying on three data sets, i.e the brain connectome, the brain functions at cortical and subcortical levels and a semantic atlas, we provide different levels and layouts of brain mapping in the MNI space.

We found out that both the functional and the semantic richness of a node does not correlate (or poorly negatively correlates) with its centrality in terms of degree, betweenness and page rank in the brain structural network, whatever the uncertainty considered in the assignment rule. These findings suggest that structural hubs related to brain anatomy do not correspond to functional hubs related to brain activity, fostering the idea that brain anatomy is impactful although not determinant for the dymanic of neural network [38, 44] and we cannot explain the functional connectivity by limiting the view at the anatomical counterpart [44]. Moreover, not even the nodes exhibiting a semantic selectivity are the most central in terms of degree, betweenness and page rank. Future developments of this work should consider extracting more targeted sub-networks (e.g.: one network for each functional feature and/or one network for each semantic cluster) and build a multilayer network of the human brain. Specifically, a straightforward approach would be to extract each layer directly from the structural connectivity network, considering the active nodes for each function (and/or for each semantic cluster) and the link among them, to assess their versatility in such a multilayer (e.g. layer-layer correlation, pairwise multiplexity,...) and eventually gain new understanding about the relation between brain structure, functions and mental aspects. Our preliminary results on this matter indicated a positive interlayer degree correlation between the nodes of the induced functional network (considering all functions) and in the structural network and a zero correlation between the nodes in the induced semantic network and in the structural network. This preliminary finding could point out the possible networked

nature of the functional system and the plausible non-networked nature of the semantic system within the human brain; however a deeper analysis should be carried out.

Considering only the fraction of nodes featured by both functional and mental properties, we assessed whether a pattern exists between the expression of a given functional feature and the selectiveness to a group of concepts. Intriguingly, it turns out that nodes having functional features related to language skills are highly selective for social, abstract, violent and visual concepts. While the nodes with motor functions are particularly selective for abstract and social concepts. Finally, the nodes featured with a combination of motor and language functions are highly selective for concepts related to abstract, social and violent meaning. The fact that a node featured with movement functions is also semantically selective is in agreement with previous studies indicating that even just reading a word somehow linked to the movement (e.g. dance) actives areas dedicated to motor skills [94, 145, 285]. Moreover, it has been shown that subjects listening to the lip- or tongue-related phonemes, activate motor regions related to lips and tongue movements [227], pointing out a relation between the cognitive perception of *something* and the activation of motor circuits prone to that *something*, further strengthening the complex interplay between brain and mind.

The brain maps obtained through our approach provide a promising contribution towards the bridging between human brain and mind, in all its aspects. Unraveling candidate brain areas that are likely to be implicated in particular structural, functional or cognitive decline, maybe concomitantly, would be of tremendous helps for those diseases, such as AD, strongly related to the complex interplay between brain and mind. In other words, knowing the triadic nature of such candidate brain areas could potentially improve the discovery of early warning signals of neurodegenerative disease

affecting the human brain on all fronts: structural, functional and mental.

Our mapping provides a promising fundamental basis for conducting integrated analyses on the brain-mind interplay. Above all, our mapping approach opens the doors for developing complex integrated biomarkers for Alzheimer's disease, overcoming those indicators merely relying on anatomical features registered by neuroimaging [44].

Whether the functional or mental areas considered for our study fall into the default mode network – a part of the brain which is active at the wakeful rest, e.g. when daydreaming or mind wandering – should be investigated in further developments of this work.

In the next and last chapter, we draw the overall conclusions of this thesis, presenting also its limitations but mostly its possible future directions.

Chapter 6

Conclusions and new directions

How does the brain work? How do brain architecture and activity concur in creating the mind? And finally, is it possible to tackle these issues with the currently available tools from neuroscience?

We started our journey with these enthralling questions and it took us three years of research to advance towards an answer. Our first definitely concise – yet meaningful – answer can be summarized as: *it is complex*.

The understanding of human brain mechanisms has captured the imagination and efforts of scientists and clinicians for ages. In this thesis, we aimed at enhancing our knowledge of human brain by means of an integrated and data-driven approach, with a particular focus on possible important implications for the prevention and treatments of brain diseases, especially dementia and Alzheimer's disease, which have constituted the motivation and the case study of our work. To this aim, we have investigated the complex interplay between the human brain and the mind with sharp attention to such a relation in health and disease, by adopting a systemic perspective and leveraging on tools from computational and network neuroscience.

The study of human brain cannot prescind from the acknowledgement of its triadic nature, i.e. i) the structure, ii) the multiple functions and iii)

the cognitive aspects, and it cannot disregard the interplay among them. We have inspected human cognition by focusing on the geometric exploration of concepts in the human mind to build new data-driven metrics to complement the neurological assessment and to confirm Alzheimer's disease diagnosis (chapter 2). We realized that non-trivial patterns emerging from the analysis of information flows in interconnected real-world systems, such as the human brain, were not captured by existing routing protocols. In this regards, we have formalized a new stochastic process, the potential-driven random walk, able to model the trade-off between exploitation and exploration of network structure, by accounting for local and global information, providing a flexible tool to span from random walk and shortest-path based navigation (chapter 3). Probing the interplay between brain structure and dynamics by means of its Von Neumann entropy, we develop a new framework for the multiscale analysis of the human connectome, which is effective for discerning between healthy conditions and Alzheimer's disease (chapter 4). Finally, by integrating data from the human brain structural connectivity, its functional response errors as measured by Direct Electrical Stimulation and semantic selectivity, we propose a new procedure for mapping the human brain triadic nature, thus providing a model-oriented bridge between the human brain and mind (chapter 5). And thus, how does the brain work? Exhaustively, we still don't know. Promisingly, our findings could help advance one step ahead. Here is the detailed summary of findings of the present thesis, representing our contribution to shed more light on the scientific understanding of human brain functioning:

- probing the exploration of concepts in the human mind, we have unraveled the plausible latent geometry of its semantic space, providing a set of new metrics able to measure such a navigation. Our indicators can capture significant differences between healthy and non-healthy

brains when considering patients suffering of Alzheimer's disease and its precursor, the mild cognitive impairment. This has been possible especially thanks to the access to an exclusive data set about records of verbal fluency test (chapter 2);

- we have formalized a new stochastic process, the potential-driven random walk, enabling for a continuous exploration of interconnected systems, such as the human brain. The potential-driven random walk interpolates between shortest path and random walk, two extreme and well-known routing strategies, by minimizing distances (like a shortest path; a global feature) while keeping some flexibility in random exploration (like a random walk; a local feature). Remarkably, the potential-driven random walk models the inevitable trade-off between exploitation and exploration, which can be found in space, mind and society. This has been possible using data of both human and animal mobility, and especially by taking inspiration from animal behaviors (i.e of the slime mold and ant colonies) and from human brain plasticity (chapter 3);

- We have provided a new information-theoretic approach based on spectral entropy to assess the persistence of information flow within the human brain at different scales. In this regards, we have found out that the spectral entropy of real connectome lies between two generative models, indicating an interpolation between modular and geometry-driven structural features. Moreover, we have noticed that significant differences between healthy individuals and the ones affected by Alzheimer's disease arise at the microscale and that such differences emerge as long as we acknowledge for the interplay between the underlying structure and a dynamical process on the top of it. In fact, significant differences between healthy brain and the patho-

logical ones are absent when considering solely the structural aspects of the two types of connectomes. This has been possible thanks to a data set of empirical connectomes at different stages of dementia and to a previously proposed method inspired by quantum statistical physics (chapter 4);

- We have proposed a promising approach to bridge between the human brain and the mind. Specifically, we offer several layouts of brain mapping in the MNI space, integrating the structure, the functions and the mental aspects related to word meaning. We have listed possible ways to gain insights about the complex relation among brain structure, function and mind when using our mapping. This has been possible thanks to three data sets related to structural connectivity, a cortical and subcortical functional atlas and a semantic atlas of the human brain. We have observed that structural hubs related to brain anatomy do not correspond neither to functional hubs related to brain activity or semantically selective hubs. Remarkably, our brain maps evidenced a match between the expression of motor functions and the semantic selectivity to specific clusters of concepts, pointing out a relation between the cognitive perception of a given action and the activation of motor areas prone to that action, in agreement with previous studies, further strengthening the complex interplay between brain and mind (chapter 5).

To sum up, besides shedding more light on human brain functioning, our findings offer original and promising clues to develop integrated biomarkers for Alzheimer's disease detection, with the potential of extension for applications to other neurodegenerative diseases and psychiatric disorders.

How do brain architecture and activity concur in creating the mind? According to a complex systems perspective, the mind is an emergent pro-

cess resulting from brain interactions, but a final response is still missing. Following the systemic paradigm, we have investigated such interactions on multiple levels and scales, with the intention of gaining momentum towards a clearer vision of the human mind. Our findings stress the need for a systemic approach when defining biomarkers for brain diseases involving cognitive aspects. We are confident that our results can offer original and practical clues on this matter, fostering integrated, personalized and data-driven treatments as health-care options. Specifically, we are referring to our new metrics for measuring mental navigation, but also to the mutliscale characterization of the human brain through spectral entropy and finally to our brain mapping that accounts for relations between structure, functions and semantic aspects, which are crucial for Alzheimer's disease.

Besides knowledge gained from our work, its limitations have to be mentioned. Our metrics on mental navigation represents the very first step to provide a new data-driven framework to eventually predict the diagnoses from fluency data in a future, when more of such clinical data will be available. In addition, a Bayesian mixed effects model would be a powerful tool to get a grounded and much informative inference on the relationship between different key variables, such as the diagnosis label, the population class demographic (age, sex, education) that we have neglected, the semantic space (itwac, twitter, wikipedia) and the value of the metrics in each semantic space. The potential-driven random walk should be tested also on real data about brain neuroplasticity, if ever available. It is worth mentioning that the computational cost for calculating the spectral entropy is still relatively high, being of the same order of the complexity of an eigenvalue problem. Even though it is fast for small network, our method would perform slower than more standard techniques in the case of very large networks (i.e. above 10,000 nodes). Finally, our brain mapping should be enhanced for example considering the true values of the

standard deviation σ of the semantic tiles, and not their average.

From our results, two natures of possible future developments emerge: i) academic and ii) practical for the clinical side. On the one hand, possible further researches should corroborate the robustness of our method for the brain mapping with other data sets and studies. Moreover, a recent research on altered outdoor spatial navigation of Alzheimer's disease patients [128] has triggered our attention, making us envisioning potential parallelisms between our metrics, obtained from the navigation in the human mind, and their results in open space. This might spur the generation of multi-domain biomarkers for Alzheimer's Disease pathophysiology. On the other hand, our results lay a solid foundation for the development of a mobile app designed for computing the above discussed metrics from verbal fluency records, with the goal of possibly detecting early warning signals of dementia, essential to develop a personalized plan of cognitive capacity maintenance. In this regard, we are going to begin an informal dialogue with a new born start-up whose goal is to improve the life quality of people with dementia and their caregiver, possibly igniting a new fruitful collaboration.

To conclude, is it possible to tackle the brain-mind issue with current tools from neuroscience? Our answer is no, the tools currently available to neuroscientists are not enough. We have demonstrated that adopting a complex systems perspective able to integrate theoretical, computational, data-driven, clinical and even philosophical aspects, is imperative. We firmly believe that investing on multidisciplinary and collaborative efforts would lead us to new discoveries about the brain-mind still unsolved puzzle, signaling the beginning of an era where complexity is not avoided but rather, embraced.

Bibliography

[1] Network geometry - mercator. https://github.com/networkgeometry/mercator.

[2] Retrieved on February 2020 from Italian Word Embeddings. http://hlt.isti.cnr.it/wordembeddings/.

[3] Usc multimodal connectivity database, accessed 2011. http://umcd.humanconnectomeproject.org/.

[4] Joshua T Abbott, Joseph L Austerweil, and Thomas L Griffiths. Human memory search as a random walk in a semantic network. In *NIPS*, pages 3050–3058, 2012.

[5] Joshua T Abbott, Joseph L Austerweil, and Thomas L Griffiths. Random walks on semantic networks can resemble optimal foraging. In *Neural Information Processing Systems Conference; A preliminary version of this work was presented at the aforementined conference.*, volume 122, page 558. American Psychological Association, 2015.

[6] LF Abbott and Wade G Regehr. Synaptic computation. *Nature*, 431(7010):796–803, 2004.

[7] Meisam Akbarzadeh and Ernesto Estrada. Communicability geometry captures traffic flows in cities. *Nature human behaviour*, 2(9):645–652, 2018.

[8] Réka Albert and Albert-László Barabási. Statistical mechanics of complex networks. *Reviews of modern physics*, 74(1):47, 2002.

[9] Réka Albert, Hawoong Jeong, and Albert-László Barabási. Diameter of the world-wide web. *nature*, 401(6749):130–131, 1999.

[10] Aaron Alexander-Bloch, Renaud Lambiotte, Ben Roberts, Jay Giedd, Nitin Gogtay, and Ed Bullmore. The discovery of population differences in network community structure: new methods and applications to brain functional networks in schizophrenia. *Neuroimage*, 59(4):3889–3900, 2012.

[11] Aaron F Alexander-Bloch, Petra E Vértes, Reva Stidd, François Lalonde, Liv Clasen, Judith Rapoport, Jay Giedd, Edward T Bullmore, and Nitin Gogtay. The anatomical distance of functional connections predicts brain network topology in health and schizophrenia. *Cerebral cortex*, 23(1):127–138, 2013.

[12] A Paul Alivisatos, Anne M Andrews, Edward S Boyden, Miyoung Chun, George M Church, Karl Deisseroth, John P Donoghue, Scott E Fraser, Jennifer Lippincott-Schwartz, Loren L Looger, et al. Nanotools for neuroscience and brain activity mapping. *ACS nano*, 7(3):1850–1866, 2013.

[13] Antoine Allard and M Ángeles Serrano. Navigable maps of structural brain networks across species. *PLoS computational biology*, 16(2):e1007584, 2020.

[14] Alois Alzheimer. Uber eine eigenartige erkrankung der hirnrinde. *Zentralbl. Nervenh. Psych.*, 18:177–179, 1907.

[15] Enrico Amico, Kausar Abbas, Duy Anh Duong-Tran, Uttara Tipnis, Meenusree Rajapandian, Evgeny Chumin, Mario Ventresca, Jaroslaw

Harezlak, and Joaquín Goñi. Toward an information theoretical description of communication in brain networks. *Netw. Neurosci.*, pages 1–20, apr 2021.

[16] Enrico Amico and Joaquín Goñi. Mapping hybrid functional-structural connectivity traits in the human connectome. *Network Neuroscience*, 2(3):306–322, 2018.

[17] Philip W Anderson. More is different. *Science*, 177(4047):393–396, 1972.

[18] Julian Appell, Andrew Kertesz, and Michael Fisman. A study of language functioning in alzheimer patients. *Brain and language*, 17(1):73–91, 1982.

[19] Thomas Arendt. Alzheimer's disease as a disorder of mechanisms underlying structural brain self-organization. *Neuroscience*, 102(4):723–765, 2001.

[20] Oriol Artime and Manlio De Domenico. From the origin of life to pandemics: emergent phenomena in complex systems, 2022.

[21] Ulf Aslak and Laura Alessandretti. Infostop: Scalable stop-location detection in multi-user mobility data. *arXiv preprint arXiv:2003.14370*, 2020.

[22] Yaniv Assaf and Ofer Pasternak. Diffusion tensor imaging (DTI)-based white matter mapping in brain research: A review. *Journal of Molecular Neuroscience*, 34(1):51–61, September 2007.

[23] Alzheimer's Association et al. 2018 alzheimer's disease facts and figures. *Alzheimer's & Dementia*, 14(3):367–429, 2018.

[24] Andrea Avena-Koenigsberger, Bratislav Mišić, Robert X.D. Hawkins, Alessandra Griffa, Patric Hagmann, Joaquín Goñi, and Olaf Sporns. Path ensembles and a tradeoff between communication efficiency and resilience in the human connectome. *Brain Struct. Funct.*, 222(1):603–618, 2017.

[25] Andrea Avena-Koenigsberger, Bratislav Misic, and Olaf Sporns. Communication dynamics in complex brain networks. *Nat Rev Neurosci*, 19(1):17–33, 2018.

[26] Andrea Avena-Koenigsberger, Xiaoran Yan, Artemy Kolchinsky, Martijn van den Heuvel, Patric Hagmann, and Olaf Sporns. A spectrum of routing strategies for brain networks. *PLoS computational biology*, 15(3):e1006833, 2019.

[27] Lars Bäckman, Brent J Small, and Laura Fratiglioni. Stability of the preclinical episodic memory deficit in alzheimer's disease. *Brain*, 124(1):96–102, 2001.

[28] Alex Bahar-Fuchs, Anthony Martyr, Anita MY Goh, Julieta Sabates, and Linda Clare. Cognitive training for people with mild to moderate dementia. *Cochrane Database of Systematic Reviews*, (3), 2019.

[29] Frank B Baker. Stability of two hierarchical grouping techniques case i: Sensitivity to data errors. *Journal of the American Statistical Association*, 69(346):440–445, 1974.

[30] Philip Ball. *The self-made tapestry: pattern formation in nature*. Oxford University Press, Inc., 2001.

[31] Andrea Baronchelli, Ramon Ferrer-i Cancho, Romualdo Pastor-Satorras, Nick Chater, and Morten H Christiansen. Networks in cognitive science. *Trends in cognitive sciences*, 17(7):348–360, 2013.

[32] Frederic Bartumeus, Jordi Catalan, GM Viswanathan, EP Raposo, and MGE Da Luz. The influence of turning angles on the success of non-oriented animal searches. *Journal of Theoretical Biology*, 252(1):43–55, 2008.

[33] Lasko Basnarkov, Miroslav Mirchev, and Ljupco Kocarev. Random walk with memory on complex networks. *Physical Review E*, 102(4):042315, 2020.

[34] Danielle S Bassett, Jesse A Brown, Vibhas Deshpande, Jean M Carlson, and Scott T Grafton. Conserved and variable architecture of human white matter connectivity. *Neuroimage*, 54(2):1262–1279, 2011.

[35] Danielle S. Bassett, Edward Bullmore, Beth A. Verchinski, Venkata S. Mattay, Daniel R. Weinberger, and Andreas Meyer-Lindenberg. Hierarchical organization of human cortical networks in health and Schizophrenia. *J. Neurosci.*, 28(37):9239–9248, 2008.

[36] Danielle S Bassett and Edward T Bullmore. Human brain networks in health and disease. *Current opinion in neurology*, 22(4):340, 2009.

[37] Danielle S. Bassett and Edward T. Bullmore. Small-world brain networks revisited. *The Neuroscientist*, 23(5):499–516, September 2016.

[38] Danielle S Bassett and Michael S Gazzaniga. Understanding complexity in the human brain. *Trends in cognitive sciences*, 15(5):200–209, 2011.

[39] Danielle S Bassett and Olaf Sporns. Network neuroscience. *Nature neuroscience*, 20(3):353–364, 2017.

[40] Danielle S Bassett, Nicholas F Wymbs, Mason A Porter, Peter J Mucha, Jean M Carlson, and Scott T Grafton. Dynamic reconfigu-

ration of human brain networks during learning. *Proceedings of the National Academy of Sciences*, 108(18):7641–7646, 2011.

[41] Danielle Smith Bassett and ED Bullmore. Small-world brain networks. *The neuroscientist*, 12(6):512–523, 2006.

[42] Aleix Bassolas, Riccardo Gallotti, Fabio Lamanna, Maxime Lenormand, and José J Ramasco. Scaling in the recovery of urban transportation systems from massive events. *Scientific reports*, 10(1):1–13, 2020.

[43] Gregory Bateson. *Steps to an ecology of mind: Collected essays in anthropology, psychiatry, evolution, and epistemology.* University of Chicago Press, 2000.

[44] Karla Batista-García-Ramó and Caridad Ivette Fernández-Verdecia. What we know about the brain structure–function relationship. *Behavioral Sciences*, 8(4):39, 2018.

[45] Edward Batschelet. Circular statistics in biology. *ACADEMIC PRESS, 111 FIFTH AVE., NEW YORK, NY 10003, 1981, 388*, 1981.

[46] Federico Battiston, Jeremy Guillon, Mario Chavez, Vito Latora, and Fabrizio de Vico Fallani. Multiplex core–periphery organization of the human connectome. *Journal of the Royal Society Interface*, 15(146):20180514, 2018.

[47] François Bavaud and Guillaume Guex. Interpolating between random walks and shortest paths: a path functional approach. In *International conference on social informatics*, pages 68–81. Springer, 2012.

[48] Mark Bedau. Downward causation and the autonomy of weak emergence. *Principia: an international journal of epistemology*, 6(1):5–50, 2002.

[49] Barbara Benigni, Monica Dallabona, Elena Bravi, Stefano Merler, and Manlio De Domenico. Supplementary materials for navigating concepts in the human mind unravels the la-tent geometry of its semantic space.

[50] Barbara Benigni, Monica Dallabona, Elena Bravi, Stefano Merler, and Manlio De Domenico. Navigating concepts in the human mind unravels the latent geometry of its semantic space. *Complexity*, 2021, 2021.

[51] Barbara Benigni, Riccardo Gallotti, and Manlio De Domenico. Potential-driven random walks on interconnected systems. *Physical Review E*, 104(2):024120, 2021.

[52] Barbara Benigni, Arsham Ghavasieh, Alessandra Corso, Valeria d'Andrea, and Manlio De Domenico. Persistence of information flow: A multiscale characterization of human brain. *Network Neuroscience*, 5(3):831–850, 2021.

[53] Laiss Bertola, Natália B Mota, Mauro Copelli, Thiago Rivero, Breno Satler Diniz, Marco A Romano-Silva, Sidarta Ribeiro, and Leandro F Malloy-Diniz. Graph analysis of verbal fluency test discriminate between patients with alzheimer's disease, mild cognitive impairment and normal elderly controls. *Frontiers in aging neuroscience*, 6:185, 2014.

[54] Maxwell A. Bertolero, B. T. Thomas Yeo, Danielle S. Bassett, and Mark D'Esposito. A mechanistic model of connector hubs, modular-

ity and cognition. *Nature Human Behaviour*, 2(10):765–777, September 2018.

[55] Richard F Betzel. Community detection in network neuroscience. *arXiv preprint arXiv:2011.06723*, 2020.

[56] Richard F Betzel, Andrea Avena-Koenigsberger, Joaquín Goñi, Ye He, Marcel A De Reus, Alessandra Griffa, Petra E Vértes, Bratislav Mišic, Jean-Philippe Thiran, Patric Hagmann, et al. Generative models of the human connectome. *Neuroimage*, 124:1054–1064, 2016.

[57] Richard F. Betzel and Danielle S. Bassett. Generative models for network neuroscience: prospects and promise. *Journal of the Royal Society Interface*, 14, 2017.

[58] Richard F Betzel and Danielle S Bassett. Specificity and robustness of long-distance connections in weighted, interareal connectomes. *Proceedings of the National Academy of Sciences*, 115(21):E4880–E4889, 2018.

[59] David Blitz. *Emergent evolution: Qualitative novelty and the levels of reality*, volume 19. Springer Science & Business Media, 2013.

[60] Marian Boguna, Dmitri Krioukov, and Kimberly C Claffy. Navigability of complex networks. *Nature Physics*, 5(1):74–80, 2009.

[61] Moreno Bonaventura, Vincenzo Nicosia, and Vito Latora. Characteristic times of biased random walks on complex networks. *Physical Review E*, 89(1):012803, 2014.

[62] Javier Borge-Holthoefer and Alex Arenas. Categorizing words through semantic memory navigation. *The European Physical Journal B*, 74(2):265–270, 2010.

[63] Javier Borge-Holthoefer, Yamir Moreno, and Alex Arenas. Modeling abnormal priming in alzheimer's patients with a free association network. *PloS one*, 6(8), 2011.

[64] Ulrik Brandes. A faster algorithm for betweenness centrality. *Journal of mathematical sociology*, 25(2):163–177, 2001.

[65] Javier M. Buldú and Mason A. Porter. Frequency-based brain networks: From a multiplex framework to a full multilayer description. *Network Neuroscience*, 2(4):418–441, October 2018.

[66] Ed Bullmore, Anna Barnes, Danielle S Bassett, Alex Fornito, Manfred Kitzbichler, David Meunier, and John Suckling. Generic aspects of complexity in brain imaging data and other biological systems. *Neuroimage*, 47(3):1125–1134, 2009.

[67] Ed Bullmore and Olaf Sporns. Complex brain networks: graph theoretical analysis of structural and functional systems. *Nature reviews neuroscience*, 10(3):186–198, 2009.

[68] Ed Bullmore and Olaf Sporns. The economy of brain network organization. *Nature Reviews Neuroscience*, 13(5):336–349, 2012.

[69] Zdzislaw Burda, Jarek Duda, Jean-Marc Luck, and Bartek Waclaw. Localization of the maximal entropy random walk. *Physical review letters*, 102(16):160602, 2009.

[70] Scott Camazine, Jean-Louis Deneubourg, Nigel R Franks, James Sneyd, Guy Theraula, and Eric Bonabeau. *Self-organization in biological systems*. Princeton university press, 2020.

[71] Fritjof Capra. Complexity and life. *Emergence*, 4(1-2):15–33, 2002.

[72] Fritjof Capra and Pier Luigi Luisi. *The systems view of life: A unifying vision*. Cambridge University Press, 2014.

[73] F Xavier Castellanos and Erika Proal. Large-scale brain systems in adhd: beyond the prefrontal–striatal model. *Trends in cognitive sciences*, 16(1):17–26, 2012.

[74] Agnes S Chan, Nelson Butters, Jane S Paulsen, David P Salmon, Michael R Swenson, and Laurence T Maloney. An assessment of the semantic network in patients with alzheimer's disease. *Journal of Cognitive Neuroscience*, 5(2):254–261, 1993.

[75] Eric L Charnov et al. Optimal foraging, the marginal value theorem. 1976.

[76] Alexander P Christensen, Yoed N Kenett, Katherine N Cotter, Roger E Beaty, Paul J Silvia, and René Mõttus. Remotely close associations: Openness to experience and semantic memory structure. *European Journal of Personality*, 32(4):480–492, 2018.

[77] Andrea Cimino, Lorenzo De Mattei, and Felice Dell'Orletta. Multi-task learning in deep neural networks at evalita 2018. *Proceedings of the 6th evaluation campaign of Natural Language Processing and Speech tools for Italian (EVALITA'18)*, pages 86–95, 2018.

[78] Edward A Codling, Michael J Plank, and Simon Benhamou. Random walk models in biology. *Journal of the Royal society interface*, 5(25):813–834, 2008.

[79] Allan M Collins, M Ross Quillian, et al. Retrieval time from semantic memory. 1969.

[80] Roberto Colom, Xue Hua, Kenia Martínez, Miguel Burgaleta, Francisco J Román, Jeffrey L Gunter, Susanna Carmona, Susanne M Jaeggi, and Paul M Thompson. Brain structural changes following

adaptive cognitive training assessed by tensor-based morphometry (tbm). *Neuropsychologia*, 91:77–85, 2016.

[81] Peter A Corning. The re-emergence of "emergence": A venerable concept in search of a theory. *Complexity*, 7(6):18–30, 2002.

[82] Irene Cristofori and Harvey S Levin. Traumatic brain injury and cognition. *Handbook of clinical neurology*, 128:579–611, 2015.

[83] Paolo Crucitti, Vito Latora, and Sergio Porta. Centrality measures in spatial networks of urban streets. *Physical Review E*, 73(3):036125, 2006.

[84] Jesper Dall and Michael Christensen. Random geometric graphs. *Physical review E*, 66(1):016121, 2002.

[85] Antonio R Damasio. How the brain creates the mind. *Scientific American*, 281(6):112–117, 1999.

[86] Manlio De Domenico. Diffusion geometry unravels the emergence of functional clusters in collective phenomena. *Physical review letters*, 118(16):168301, 2017.

[87] Manlio De Domenico. Multilayer modeling and analysis of human brain networks. *Giga Science*, 6(5):gix004, 2017.

[88] Manlio De Domenico and Jacob Biamonte. Spectral entropies as information-theoretic tools for complex network comparison. *Physical Review X*, 6(4):041062, 2016.

[89] Manlio De Domenico, Dirk Brockmann, CQ Camargo, Carlos Gershenson, Daniel Goldsmith, Sabine Jeschonnek, Lorren Kay, Stefano Nichele, J Nicolás, Thomas Schmickl, et al. Complexity explained. 2019.

[90] Manlio De Domenico, Antonio Lima, Marta C González, and Alex Arenas. Personalized routing for multitudes in smart cities. *EPJ Data Science*, 4(1):1–11, 2015.

[91] Manlio De Domenico, Shuntaro Sasai, and Alex Arenas. Mapping multiplex hubs in human functional brain networks. *Frontiers in neuroscience*, 10:326, 2016.

[92] Manlio De Domenico, Albert Solé-Ribalta, Emanuele Cozzo, Mikko Kivelä, Yamir Moreno, Mason A Porter, Sergio Gómez, and Alex Arenas. Mathematical formulation of multilayer networks. *Physical Review X*, 3(4):041022, 2013.

[93] Willem De Haan, Yolande AL Pijnenburg, Rob LM Strijers, Yolande van der Made, Wiesje M van der Flier, Philip Scheltens, and Cornelis J Stam. Functional neural network analysis in frontotemporal dementia and alzheimer's disease using eeg and graph theory. *BMC neuroscience*, 10(1):1–12, 2009.

[94] Victor de Lafuente and Ranulfo Romo. Language abilities of motor cortex. *Neuron*, 41(2):178–180, 2004.

[95] Fabrizio de Vico Fallani, Jonas Richiardi, Mario Chavez, and Sophie Achard. Graph analysis of functional brain networks: practical issues in translational neuroscience. *Philosophical Transactions of the Royal Society B: Biological Sciences*, 369(1653):20130521, 2014.

[96] Tom De Wolf and Tom Holvoet. Emergence and self-organisation: a statement of similarities and differences. In *Proceedings of the International Workshop on Engineering Self-Organising Applications 2004*, pages 96–110, 2004.

[97] Gustavo Deco, Viktor K. Jirsa, and Anthony R. McIntosh. Emerging concepts for the dynamical organization of resting-state activity in the brain. *Nature Reviews Neuroscience*, 12(1):43–56, December 2010.

[98] Gustavo Deco and Edmund T. Rolls. A Neurodynamical cortical model of visual attention and invariant object recognition. *Vision Res.*, 44(6):621–642, 2004.

[99] Gustavo Deco and Edmund T. Rolls. Attention, short-term memory, and action selection: A unifying theory. *Prog. Neurobiol.*, 76(4):236–256, 2005.

[100] Gustavo Deco, Giulio Tononi, Melanie Boly, and Morten L. Kringelbach. Rethinking segregation and integration: contributions of whole-brain modelling. *Nature Reviews Neuroscience*, 16(7):430–439, June 2015.

[101] Hugues Duffau. The anatomo-functional connectivity of language revisited: new insights provided by electrostimulation and tractography. *Neuropsychologia*, 46(4):927–934, 2008.

[102] David Eagleman. *The brain: The story of you.* Canongate Books, 2015.

[103] Gerald M Edelman and Giulio Tononi. Reentry and the dynamic core: neural correlates of conscious experience. *Neural correlates of consciousness: Empirical and conceptual questions*, pages 139–151, 2000.

[104] Dorothy F Edwards, Carolyn M Baum, and Ruthmary K Deuel. Constructional apraxia in alzheimer's disease: Contributions to func-

tional loss. *Physical & Occupational Therapy In Geriatrics*, 9(3-4):53–68, 1991.

[105] Zoltán Eisler and János Kertész. Random walks on complex networks with inhomogeneous impact. *Physical Review E*, 71(5):057104, 2005.

[106] P. Erdős and A. Rényi. On random graphs. *Publicationes Mathematicae*, 6:290–297, 1959.

[107] Ernesto Estrada. Informational cost and networks navigability. *Applied Mathematics and Computation*, 397:125914, 2021.

[108] Damien A Fair, Nico UF Dosenbach, Amy H Moore, Theodore Satterthwaite, and Michael P Milham. Developmental cognitive neuroscience in the era of networks and big data: Strengths, weaknesses, opportunities, and threats. *Annual Review of Developmental Psychology*, 3, 2021.

[109] Joshua Faskowitz, Farnaz Zamani Esfahlani, Youngheun Jo, Olaf Sporns, and Richard F Betzel. Edge-centric functional network representations of human cerebral cortex reveal overlapping system-level architecture. *Nature neuroscience*, 23(12):1644–1654, 2020.

[110] Alex Fornito and Edward T Bullmore. Reconciling abnormalities of brain network structure and function in schizophrenia. *Current opinion in neurobiology*, 30:44–50, 2015.

[111] Alex Fornito, Andrew Zalesky, and Michael Breakspear. The connectomics of brain disorders. *Nature Reviews Neuroscience*, 16(3):159–172, 2015.

[112] Santo Fortunato. Community detection in graphs. *Physics Reports*, 486(3-5):75–174, February 2010.

[113] M. D. Fox, A. Z. Snyder, J. L. Vincent, M. Corbetta, D. C. Van Essen, and M. E. Raichle. From the cover: The human brain is intrinsically organized into dynamic, anticorrelated functional networks. *Proceedings of the National Academy of Sciences*, 102(27):9673–9678, June 2005.

[114] William J Freed, Luis De Medinaceli, and Richard Jed Wyatt. Promoting functional plasticity in the damaged nervous system. *Science*, 227(4694):1544–1552, 1985.

[115] K. Friston, J Kahan, A Razi, K E Stephan, and O Sporns. On nodes and modes in resting state fmri. *Neuroimage*, 99:533–547, 2014.

[116] Karl J. Friston. Modalities, modes, and models in functional neuroimaging. *Science (80-.).*, 326(5951):399–403, 2009.

[117] Agata Fronczak and Piotr Fronczak. Biased random walks in complex networks: The role of local navigation rules. *Physical Review E*, 80(1):016107, 2009.

[118] Riccardo Gallotti, Armando Bazzani, and Sandro Rambaldi. Towards a statistical physics of human mobility. *Int. J. Mod. Phys. C*, 23(arXiv: 1207.5698):1250061, 2012.

[119] Riccardo Gallotti, Mason A Porter, and Marc Barthelemy. Lost in transportation: Information measures and cognitive limits in multilayer navigation. *Science advances*, 2(2):e1500445, 2016.

[120] Guillermo García-Pérez, Antoine Allard, M. Ángeles Serrano, and Marián Boguñá. Mercator: uncovering faithful hyperbolic embeddings of complex networks. *New Journal of Physics*, 21(12):123033, 2019.

[121] Peter Garrard, Matthew A Lambon Ralph, Karalyn Patterson, Katherine H Pratt, and John R Hodges. Semantic feature knowledge and picture naming in dementia of alzheimer's type: a new approach. *Brain and language*, 93(1):79–94, 2005.

[122] Michael S Gazzaniga. Neuroscience and the correct level of explanation for understanding mind. *Trends in Cognitive Sciences*, 14(7):297, 2010.

[123] MS Gazzaniga, K Doron, and C Funk. Looking toward the future: Perspectives on examining the architecture and function of the human brain as a complex system. *The cognitive neurosciences IV*, pages 1245–1252, 2010.

[124] Arsham Ghavasieh, Giulia Bertagnolli, and Manlio De Domenico. Dismantling the information flow in complex interconnected systems. *arXiv preprint arXiv:2202.09692*, 2022.

[125] Arsham Ghavasieh, Sebastiano Bontorin, Oriol Artime, Nina Verstraete, and Manlio De Domenico. Multiscale statistical physics of the pan-viral interactome unravels the systemic nature of SARS-CoV-2 infections. *Communications Physics*, 4(1), April 2021.

[126] Arsham Ghavasieh and Manlio De Domenico. Enhancing transport properties in interconnected systems without altering their structure. *Physical Review Research*, 2(1), February 2020.

[127] Arsham Ghavasieh, Carlo Nicolini, and Manlio De Domenico. Statistical physics of complex information dynamics. *Physical Review E*, 102(5):052304, 2020.

[128] Abhirup Ghosh, Vaisakh Puthusseryppady, Dennis Chan, Cecilia Mascolo, and Michael Hornberger. Machine learning detects altered

spatial navigation features in outdoor behaviour of alzheimer's disease patients. *Scientific Reports*, 12(1):1–13, 2022.

[129] James B Glattfelder. *Information—consciousness—reality: how a new understanding of the universe can help answer age-old questions of existence*. Springer Nature, 2019.

[130] Jesús Gómez-Gardenes and Vito Latora. Entropy rate of diffusion processes on complex networks. *Physical Review E*, 78(6):065102, 2008.

[131] Joaquín Goñi, Iñigo Martincorena, Bernat Corominas-Murtra, Gonzalo Arrondo, Sergio Ardanza-Trevijano, and Pablo Villoslada. Switcher-random-walks: A cognitive-inspired mechanism for network exploration. *International Journal of Bifurcation and Chaos*, 20(03):913–922, 2010.

[132] Joaquin Goni, Martijn P. Van Den Heuvel, Andrea Avena-Koenigsberger, Nieves Velez De Mendizabal, Richard F. Betzel, Alessandra Griffa, Patric Hagmann, Bernat Corominas-Murtra, Jean Philippe Thiran, and Olaf Sporns. Resting-brain functional connectivity predicted by analytic measures of network communication. *Proc. Natl. Acad. Sci. U. S. A.*, 111(2):833–838, 2014.

[133] John DW Greene, Alan D Baddeley, and John R Hodges. Analysis of the episodic memory deficit in early alzheimer's disease: evidence from the doors and people test. *Neuropsychologia*, 34(6):537–551, 1996.

[134] Kristi R Griffiths, Taylor A Braund, Michael R Kohn, Simon Clarke, Leanne M Williams, and Mayuresh S Korgaonkar. Structural brain network topology underpinning adhd and response to

methylphenidate treatment. *Translational psychiatry*, 11(1):1–9, 2021.

[135] Thomas L Griffiths, Mark Steyvers, and Alana Firl. Google and the mind: Predicting fluency with pagerank. *Psychological Science*, 18(12):1069–1076, 2007.

[136] Thomas L Griffiths, Mark Steyvers, and Joshua B Tenenbaum. Topics in semantic representation. *Psychological review*, 114(2):211, 2007.

[137] Charles Grinstead and Laurie J Snell. *Introduction to probability*. 2006.

[138] Jérémy Guillon, Yohan Attal, Olivier Colliot, Valentina La Corte, Bruno Dubois, Denis Schwartz, Mario Chavez, and F De Vico Fallani. Loss of brain inter-frequency hubs in alzheimer's disease. *Scientific reports*, 7(1):1–13, 2017.

[139] Jeremy Guillon, Mario Chavez, Federico Battiston, Yohan Attal, Valentina La Corte, Michel Thiebaut de Schotten, Bruno Dubois, Denis Schwartz, Olivier Colliot, and Fabrizio de Vico Fallani. Disrupted core-periphery structure of multimodal brain networks in alzheimer's disease. *Network Neuroscience*, 3(2):635–652, 2019.

[140] Roger Guimera and Luis A Nunes Amaral. Modeling the world-wide airport network. *The European Physical Journal B*, 38(2):381–385, 2004.

[141] Fritz Günther, Luca Rinaldi, and Marco Marelli. Vector-space models of semantic representation from a cognitive perspective: A discussion of common misconceptions. *Perspectives on Psychological Science*, 14(6):1006–1033, 2019.

[142] Patric Hagmann, Leila Cammoun, Xavier Gigandet, Reto Meuli, Christopher J Honey, Van J Wedeen, and Olaf Sporns. Mapping the structural core of human cerebral cortex. *PLoS biology*, 6(7):e159, 2008.

[143] Gerald Hahn, Adrian Ponce-Alvarez, Gustavo Deco, Ad Aertsen, and Arvind Kumar. Portraits of communication in neuronal networks. *Nat. Rev. Neurosci.*, 20(2):117–127, 2019.

[144] Julianne D Halley and David A Winkler. Classification of emergence and its relation to self-organization. *Complexity*, 13(5):10–15, 2008.

[145] Olaf Hauk, Ingrid Johnsrude, and Friedemann Pulvermüller. Somatotopic representation of action words in human motor and premotor cortex. *Neuron*, 41(2):301–307, 2004.

[146] Victor W Henderson, Wendy Mack, and Betsy White Williams. Spatial disorientation in alzheimer's disease. *Archives of neurology*, 46(4):391–394, 1989.

[147] Holland John Henry et al. Adaptation in natural and artificial systems: an introductory analysis with applications to biology, control, and artificial intelligence, 1992.

[148] Julie D Henry, John R Crawford, and Louise H Phillips. Verbal fluency performance in dementia of the alzheimer's type: a meta-analysis. *Neuropsychologia*, 42(9):1212–1222, 2004.

[149] Miguel A Hernán, John Hsu, and Brian Healy. A second chance to get causal inference right: a classification of data science tasks. *Chance*, 32(1):42–49, 2019.

[150] Leanna M Hernandez, Jeffrey D Rudie, Shulamite A Green, Susan Bookheimer, and Mirella Dapretto. Neural signatures of autism spec-

trum disorders: insights into brain network dynamics. *Neuropsychopharmacology*, 40(1):171–189, 2015.

[151] Francis Heylighen, Paul Cilliers, and Carlos Gershenson. Complexity and philosophy. *arXiv preprint cs/0604072*, 2006.

[152] Thomas T Hills, Michael N Jones, and Peter M Todd. Optimal foraging in semantic memory. *Psychological review*, 119(2):431, 2012.

[153] Thomas T Hills, Peter M Todd, and Michael N Jones. Foraging in semantic fields: How we search through memory. *Topics in Cognitive Science*, 7(3):513–534, 2015.

[154] Thomas T Hills, Peter M Todd, David Lazer, A David Redish, Iain D Couzin, Cognitive Search Research Group, et al. Exploration versus exploitation in space, mind, and society. *Trends in cognitive sciences*, 19(1):46–54, 2015.

[155] John H Holland. *Emergence: From chaos to order*. OUP Oxford, 2000.

[156] Paul W. Holland, Kathryn Vlackmond Laskey, and Samuel Leinhardt. Stochastic blockmodels: First steps. *Social Networks*, 5(2):109–137, 1983.

[157] Christopher J Honey, Rolf Kötter, Michael Breakspear, and Olaf Sporns. Network structure of cerebral cortex shapes functional connectivity on multiple time scales. *Proceedings of the National Academy of Sciences*, 104(24):10240–10245, 2007.

[158] Christopher J. Honey, Rolf Kötter, Michael Breakspear, and Olaf Sporns. Network structure of cerebral cortex shapes functional connectivity on multiple time scales. *Proc. Natl. Acad. Sci. U. S. A.*, 104(24):10240–10245, 2007.

[159] Liu Hui. Assessment of the role of ageing and non-ageing factors in death from non-communicable diseases based on a cumulative frequency model. *Scientific reports*, 7(1):1–7, 2017.

[160] Edmund R Hunt, Roland J Baddeley, Alan Worley, Ana B Sendova-Franks, and Nigel R Franks. Ants determine their next move at rest: motor planning and causality in complex systems. *Royal Society open science*, 3(1):150534, 2016.

[161] Jeffrey J Hunter. Variances of first passage times in a markov chain with applications to mixing times. *Linear Algebra and its Applications*, 429(5-6):1135–1162, 2008.

[162] Alexander G Huth, Wendy A De Heer, Thomas L Griffiths, Frédéric E Theunissen, and Jack L Gallant. Natural speech reveals the semantic maps that tile human cerebral cortex. *Nature*, 532(7600):453–458, 2016.

[163] Kai Hwang, Michael N. Hallquist, and Beatriz Luna. The development of hub architecture in the human functional brain network. *Cerebral Cortex*, 23(10):2380–2393, August 2012.

[164] William Jagust. Imaging the evolution and pathophysiology of alzheimer disease. *Nature Reviews Neuroscience*, 19(11):687–700, 2018.

[165] Michael N Jones, Thomas T Hills, and Peter M Todd. Hidden processes in structural representations: A reply to abbott, austerweil, and griffiths (2015). 2015.

[166] JA Scott Kelso. *Dynamic patterns: The self-organization of brain and behavior*. MIT press, 1995.

[167] Daniel Kempler. Language changes in dementia of the alzheimer type. *Dementia and communication*, pages 98–114, 1995.

[168] Manfred G Kitzbichler, Marie L Smith, Søren R Christensen, and Ed Bullmore. Broadband criticality of human brain network synchronization. *PLoS computational biology*, 5(3):e1000314, 2009.

[169] Ilkka Kivimäki, Bram Van Moorter, Manuela Panzacchi, Jari Saramäki, and Marco Saerens. Maximum likelihood estimation for randomized shortest paths with trajectory data. *Journal of Complex Networks*, 8(4):cnaa024, 2020.

[170] Jon Kleinberg. Complex networks and decentralized search algorithms. In *Proceedings of the International Congress of Mathematicians (ICM)*, volume 3, pages 1019–1044, 2006.

[171] Jon M Kleinberg. Navigation in a small world. *Nature*, 406(6798):845–845, 2000.

[172] Blanka Klimova, Petra Maresova, Martin Valis, Jakub Hort, and Kamil Kuca. Alzheimer's disease and language impairments: social intervention and medical treatment. *Clinical interventions in aging*, 10:1401, 2015.

[173] Jerzy Konorski. Conditioned reflexes and neuron organization. 1948.

[174] Andrea Lancichinetti, Santo Fortunato, and Filippo Radicchi. Benchmark graphs for testing community detection algorithms. *Physical review E*, 78(4):046110, 2008.

[175] Shaun Larcom, Ferdinand Rauch, and Tim Willems. The benefits of forced experimentation: striking evidence from the london underground network. *The Quarterly Journal of Economics*, 132(4):2019–2055, 2017.

[176] S Lee, S-H Yook, and Y Kim. Centrality measure of complex networks using biased random walks. *The European Physical Journal B*, 68(2):277–281, 2009.

[177] Eufemia Lella and Ernesto Estrada. Communicability distance reveals hidden patterns of alzheimer's disease. *Network Neuroscience*, 4(4):1007–1029, 2020.

[178] Alan J Lerner, Paula K Ogrocki, and Peter J Thomas. Network graph analysis of category fluency testing. *Cognitive and Behavioral Neurology*, 22(1):45–52, 2009.

[179] Wei Liao, Jurong Ding, Daniele Marinazzo, Qiang Xu, Zhengge Wang, Cuiping Yuan, Zhiqiang Zhang, Guangming Lu, and Huafu Chen. Small-world directed networks in the human brain: multivariate granger causality analysis of resting-state fmri. *Neuroimage*, 54(4):2683–2694, 2011.

[180] Antonio Lima, Rade Stanojevic, Dina Papagiannaki, Pablo Rodriguez, and Marta C González. Understanding individual routing behaviour. *Journal of The Royal Society Interface*, 13(116):20160021, 2016.

[181] Shih-Yen Lin, Chen-Pei Lin, Tsung-Jen Hsieh, Chung-Fen Lin, Sih-Huei Chen, Yi-Ping Chao, Yong-Sheng Chen, Chih-Cheng Hsu, and Li-Wei Kuo. Multiparametric graph theoretical analysis reveals altered structural and functional network topology in alzheimer's disease. *NeuroImage: Clinical*, 22:101680, 2019.

[182] Nicklas Linz, Johannes Tröger, Jan Alexandersson, and Alexandra König. Using neural word embeddings in the analysis of the clinical semantic verbal fluency task. In *IWCS 2017—12th International Conference on Computational Semantics—Short papers*, 2017.

[183] Gabriele Lohmann, Daniel S. Margulies, Annette Horstmann, Burkhard Pleger, Joeran Lepsien, Dirk Goldhahn, Haiko Schloegl, Michael Stumvoll, Arno Villringer, and Robert Turner. Eigenvector centrality mapping for analyzing connectivity patterns in fMRI data of the human brain. *PLoS ONE*, 5(4):e10232, April 2010.

[184] Donghuan Lu, Karteek Popuri, Gavin Weiguang Ding, Rakesh Balachandar, and Mirza Faisal Beg. Multimodal and multiscale deep neural networks for the early diagnosis of alzheimer's disease using structural mr and fdg-pet images. *Scientific reports*, 8(1):1–13, 2018.

[185] Christopher W Lynn and Danielle S Bassett. The physics of brain network structure, function and control. *Nature Reviews Physics*, 1(5):318–332, 2019.

[186] Paweł Mandera, Emmanuel Keuleers, and Marc Brysbaert. Explaining human performance in psycholinguistic tasks with models of semantic similarity based on prediction and counting: A review and empirical validation. *Journal of Memory and Language*, 92:57–78, 2017.

[187] Ed Manley and Tao Cheng. Exploring the role of spatial cognition in predicting urban traffic flow through agent-based modelling. *Transportation Research Part A: Policy and Practice*, 109:14–23, 2018.

[188] EJ Manley, Shepley W Orr, and Tao Cheng. A heuristic model of bounded route choice in urban areas. *Transportation Research Part C: Emerging Technologies*, 56:195–209, 2015.

[189] L Manubens-Gil, J Swoger, B Sancristóbal, Q Serra, T Gener, L Hernández, J Soriano-Fradera, J Sharpe, and M Dierssen. Neuromorphological and wiring pattern alterations effects on brain function: a mixed experimental and computational approach. In *Front.*

Syst. Neurosci. Conference Abstract: B· DEBATE— A Dialogue with the Cerebral Cortex: Cortical Function and Interfacing (Workshop). doi: 10.3389/conf. fnsys, volume 10, 2015.

[190] Henry Markram, Eilif Muller, Srikanth Ramaswamy, Michael W Reimann, Marwan Abdellah, Carlos Aguado Sanchez, Anastasia Ailamaki, Lidia Alonso-Nanclares, Nicolas Antille, Selim Arsever, et al. Reconstruction and simulation of neocortical microcircuitry. *Cell*, 163(2):456–492, 2015.

[191] Sergei Maslov and Kim Sneppen. Specificity and stability in topology of protein networks. *Science*, 296(5569):910–913, 2002.

[192] Naoki Masuda, Mason A Porter, and Renaud Lambiotte. Random walks and diffusion on networks. *Physics reports*, 716:1–58, 2017.

[193] Naoki Masuda, Mason A. Porter, and Renaud Lambiotte. Random walks and diffusion on networks. *Physics Reports*, 716-717:1–58, 2017.

[194] Humberto R Maturana and Francisco J Varela. *Autopoiesis and cognition: The realization of the living*, volume 42. Springer Science & Business Media, 2012.

[195] David Meunier, Renaud Lambiotte, and Edward T Bullmore. Modular and hierarchically modular organization of brain networks. *Frontiers in neuroscience*, 4:200, 2010.

[196] David Meunier, Renaud Lambiotte, Alex Fornito, Karen Ersche, and Edward T Bullmore. Hierarchical modularity in human brain functional networks. *Frontiers in neuroinformatics*, 3:37, 2009.

[197] Rada Mihalcea, Paul Tarau, and Elizabeth Figa. Pagerank on semantic networks, with application to word sense disambiguation. In

COLING 2004: Proceedings of the 20th International Conference on Computational Linguistics, pages 1126–1132, 2004.

[198] Tomas Mikolov, Ilya Sutskever, Kai Chen, Greg S Corrado, and Jeff Dean. Distributed representations of words and phrases and their compositionality. In *Advances in neural information processing systems*, pages 3111–3119, 2013.

[199] John H Miller, Scott E Page, and Scott Page. *Complex adaptive systems*. Princeton university press, 2009.

[200] Melanie Mitchell. *Complexity: A guided tour*. Oxford University Press, 2009.

[201] Natalia B Mota, Nivaldo AP Vasconcelos, Nathalia Lemos, Ana C Pieretti, Osame Kinouchi, Guillermo A Cecchi, Mauro Copelli, and Sidarta Ribeiro. Speech graphs provide a quantitative measure of thought disorder in psychosis. *PloS one*, 7(4):e34928, 2012.

[202] Lennart Mucke. Alzheimer's disease. *Nature*, 461(7266):895–897, 2009.

[203] Sarah Feldt Muldoon, Eric W. Bridgeford, and Danielle S. Bassett. Small-world propensity and weighted brain networks. *Scientific Reports*, 6(1), February 2016.

[204] Bruce E Murdoch, Helen J Chenery, Vicki Wilks, and Richard S Boyle. Language disorders in dementia of the alzheimer type. *Brain and language*, 31(1):122–137, 1987.

[205] Carolin Nerlich et al. The 2018 ageing report: population ageing poses tough fiscal challenges. *Economic Bulletin Boxes*, 4, 2018.

[206] M. E. J. Newman. *Networks An Introduction*. Oxford University Press, 2017.

[207] M.E. J. Newman. A measure of betweenness centrality based on random walks. *Social Networks*, 27(1):39–54, 2005.

[208] Jae Dong Noh and Heiko Rieger. Random walks on complex networks. *Physical review letters*, 92(11):118701, 2004.

[209] Kate Nooner, Stanley Colcombe, Russell Tobe, Maarten Mennes, Melissa Benedict, Alexis Moreno, Laura Panek, Shaquanna Brown, Stephen Zavitz, Qingyang Li, Sharad Sikka, David Gutman, Saroja Bangaru, Rochelle Tziona Schlachter, Stephanie Kamiel, Ayesha Anwar, Caitlin Hinz, Michelle Kaplan, Anna Rachlin, Samantha Adelsberg, Brian Cheung, Ranjit Khanuja, Chaogan Yan, Cameron Craddock, Vincent Calhoun, William Courtney, Margaret King, Dylan Wood, Christine Cox, Clare Kelly, Adriana DiMartino, Eva Petkova, Philip Reiss, Nancy Duan, Dawn Thompsen, Bharat Biswal, Barbara Coffey, Matthew Hoptman, Daniel Javitt, Nunzio Pomara, John Sidtis, Harold Koplewicz, Francisco Castellanos, Bennett Leventhal, and Michael Milham. The nki-rockland sample: a model for accelerating the pace of discovery science in psychiatry. *Frontiers in Neuroscience*, 6:152, 2012.

[210] Rachel Nugent, Melanie Y Bertram, Stephen Jan, Louis W Niessen, Franco Sassi, Dean T Jamison, Eduardo González Pier, and Robert Beaglehole. Investing in non-communicable disease prevention and management to advance the sustainable development goals. *The Lancet*, 391(10134):2029–2035, 2018.

[211] Ziad Obermeyer and Ezekiel J Emanuel. Predicting the future—big data, machine learning, and clinical medicine. *The New England journal of medicine*, 375(13):1216, 2016.

[212] Hideyuki Okano, Atsushi Miyawaki, and Kiyoto Kasai. Brain/minds:

brain-mapping project in japan. *Philosophical Transactions of the Royal Society B: Biological Sciences*, 370(1668):20140310, 2015.

[213] Vasiliki Orgeta, Phuong Leung, Lauren Yates, Sujin Kang, Zoe Hoare, Catherine Henderson, Christopher Whitaker, Alistair Burns, Martin Knapp, Iracema Leroi, et al. Individual cognitive stimulation therapy for dementia: a clinical effectiveness and cost-effectiveness pragmatic, multicentre, randomised controlled trial. *Health Technology Assessment*, 19(64):1–108, 2015.

[214] Lawrence Page, Sergey Brin, Rajeev Motwani, and Terry Winograd. The pagerank citation ranking: Bringing order to the web. Technical report, Stanford InfoLab, 1999.

[215] Fragkiskos Papadopoulos, Maksim Kitsak, M. Ángeles Serrano, Marián Boguñá, and Dmitri Krioukov. Popularity versus similarity in growing networks. *Nature*, 489:537–540, 2012.

[216] David Papo, Javier M. Buldú, Stefano Boccaletti, and Edward T. Bullmore. Complex network theory and the brain. *Philosophical Transactions of the Royal Society B: Biological Sciences*, 369(1653):20130520, October 2014.

[217] Hae-Jeong Park and Karl Friston. Structural and functional brain networks: from connections to cognition. *Science*, 342(6158), 2013.

[218] Alvaro Pascual-Leone, Amir Amedi, Felipe Fregni, and Lotfi B Merabet. The plastic human brain cortex. *Annu. Rev. Neurosci.*, 28:377–401, 2005.

[219] Alvaro Pascual-Leone, Catarina Freitas, Lindsay Oberman, Jared C Horvath, Mark Halko, Mark Eldaief, Shahid Bashir, Marine Vernet,

Mouhshin Shafi, Brandon Westover, et al. Characterizing brain cortical plasticity and network dynamics across the age-span in health and disease with tms-eeg and tms-fmri. *Brain topography*, 24(3-4):302, 2011.

[220] Christina Patterson. World alzheimer report 2018 the state of the art of dementia research: New frontiers. 2018.

[221] Tiago P Peixoto. Hierarchical block structures and high-resolution model selection in large networks. *Physical Review X*, 4(1):011047, 2014.

[222] Tiago P. Peixoto. *Bayesian Stochastic Blockmodeling*, chapter 11, pages 289–332. John Wiley & Sons, Ltd, 2019.

[223] Will Penny, Jorge Iglesias-Fuster, Yakeel T. Quiroz, Francisco Javier Lopera, and Maria A. Bobes. Dynamic causal modeling of preclinical autosomal-dominant Alzheimer's disease. *J. Alzheimer's Dis.*, 65(3):697–711, 2018.

[224] Mu-ming Poo, Jiu-lin Du, Nancy Y Ip, Zhi-Qi Xiong, Bo Xu, and Tieniu Tan. China brain project: basic neuroscience, brain diseases, and brain-inspired computing. *Neuron*, 92(3):591–596, 2016.

[225] Charley Presigny and Fabrizio De Vico Fallani. Multiscale modeling of brain network organization. *arXiv preprint arXiv:2111.13473*, 2021.

[226] Andrea Puglisi, Andrea Baronchelli, and Vittorio Loreto. Cultural route to the emergence of linguistic categories. *Proceedings of the National Academy of Sciences*, 105(23):7936–7940, 2008.

[227] Friedemann Pulvermüller, Martina Huss, Ferath Kherif, Fermin Moscoso del Prado Martin, Olaf Hauk, and Yury Shtyrov. Motor

cortex maps articulatory features of speech sounds. *Proceedings of the National Academy of Sciences*, 103(20):7865–7870, 2006.

[228] Ming-guo Qiu, Zhang Ye, Qi-yu Li, Guang-jiu Liu, Bing Xie, and Jian Wang. Changes of brain structure and function in adhd children. *Brain topography*, 24(3-4):243–252, 2011.

[229] Daniele Quercia, Rossano Schifanella, and Luca Maria Aiello. The shortest path to happiness: Recommending beautiful, quiet, and happy routes in the city. In *Proceedings of the 25th ACM conference on Hypertext and social media*, pages 116–125, 2014.

[230] M Ross Quillan. Semantic memory. Technical report, BOLT BERANEK AND NEWMAN INC CAMBRIDGE MA, 1966.

[231] Sebastian Raimondo, Barbara Benigni, and Manlio De Domenico. Environmental conditions and human activity nexus. the case of northern italy during covid-19 lockdown. *arXiv preprint arXiv:2010.07721*, 2020.

[232] Sebastian Raimondo and Manlio De Domenico. Measuring topological descriptors of complex networks under uncertainty. *Physical Review E*, 103(2), February 2021.

[233] Patricia A. Reuter-Lorenz and Katherine A. Cappell. Neurocognitive aging and the compensation hypothesis. *Current Directions in Psychological Science*, 17(3):177–182, 2008.

[234] Barry W Rovner, Jeremy Broadhead, Miriam Spencer, Kathryn Carson, and Marshal F Folstein. Depression and alzheimer's disease. *Am J Psychiatry*, 146(3):350–353, 1989.

[235] Mikail Rubinov et al. Schizophrenia and abnormal brain network hubs. *Dialogues in clinical neuroscience*, 15(3):339, 2013.

[236] Jeffrey D Rudie, JA Brown, D Beck-Pancer, LM Hernandez, EL Dennis, PM Thompson, SY Bookheimer, and MJNC Dapretto. Altered functional and structural brain network organization in autism. *NeuroImage: clinical*, 2:79–94, 2013.

[237] Marco Saerens, Youssef Achbany, Francois Fouss, and Luh Yen. Randomized shortest-path problems: Two related models. *Neural Computation*, 21(8):2363–2404, 2009.

[238] David P Salmon and Mark W Bondi. Neuropsychological assessment of dementia. *Annual review of psychology*, 60:257, 2009.

[239] Silvio Sarubbo, Alessandro De Benedictis, Stefano Merler, Emmanuel Mandonnet, Sergio Balbi, Enrico Granieri, and Hugues Duffau. Towards a functional atlas of human white matter. *Human Brain Mapping*, 36(8):3117–3136, 2015.

[240] Silvio Sarubbo, Matthew Tate, Alessandro De Benedictis, Stefano Merler, Sylvie Moritz-Gasser, Guillaume Herbet, and Hugues Duffau. Mapping critical cortical hubs and white matter pathways by direct electrical stimulation: an original functional atlas of the human brain. *Neuroimage*, 205:116237, 2020.

[241] Silvio Sarubbo, Matthew Tate, Alessandro De Benedictis, Stefano Merler, Sylvie Moritz-Gasser, Guillaume Herbet, and Hugues Duffau. A normalized dataset of 1821 cortical and subcortical functional responses collected during direct electrical stimulation in patients undergoing awake brain surgery. *Data in brief*, 28:104892, 2020.

[242] Michael Schirner, Anthony Randal McIntosh, Viktor Jirsa, Gustavo Deco, and Petra Ritter. Inferring multi-scale neural mechanisms with brain network modelling. *eLife*, 7, January 2018.

[243] David J Schretlen and Anne M Shapiro. A quantitative review of the effects of traumatic brain injury on cognitive functioning. *International review of psychiatry*, 15(4):341–349, 2003.

[244] Caio Seguin, Martijn P van den Heuvel, and Andrew Zalesky. Navigation of brain networks. *Proc Natl Acad Sci*, 115(24):6297–6302, 2018.

[245] Terrence J Sejnowski, Patricia S Churchland, and J Anthony Movshon. Putting big data to good use in neuroscience. *Nature neuroscience*, 17(11):1440–1441, 2014.

[246] Thomas Sellke, MJ Bayarri, and James O Berger. Calibration of ρ values for testing precise null hypotheses. *The American Statistician*, 55(1):62–71, 2001.

[247] Zeshu Shao, Esther Janse, Karina Visser, and Antje S Meyer. What do verbal fluency tasks measure? predictors of verbal fluency performance in older adults. *Frontiers in psychology*, 5:772, 2014.

[248] Xiaoning Sheng, Haifeng Chen, Pengfei Shao, Ruomeng Qin, Hui Zhao, Yun Xu, and Feng Bai. Brain Structural Network Compensation Is Associated With Cognitive Impairment and Alzheimer's Disease Pathology. *Front. Neurosci.*, 15(February):1–13, 2021.

[249] Smadar Shilo, Hagai Rossman, and Eran Segal. Axes of a revolution: challenges and promises of big data in healthcare. *Nature medicine*, 26(1):29–38, 2020.

[250] Cynthia SQ Siew, Dirk U Wulff, Nicole M Beckage, and Yoed N Kenett. Cognitive network science: A review of research on cognition through the lens of network representations, processes, and dynamics. *Complexity*, 2019, 2019.

[251] Roberta Sinatra, Jesús Gómez-Gardenes, Renaud Lambiotte, Vincenzo Nicosia, and Vito Latora. Maximal-entropy random walks in complex networks with limited information. *Physical Review E*, 83(3):030103, 2011.

[252] Steven A Sloman, Bradley C Love, and Woo-Kyoung Ahn. Feature centrality and conceptual coherence. *Cognitive Science*, 22(2):189–228, 1998.

[253] Jan Christiaan Smuts. *Holism and evolution*. Рипол Классик , 1926.

[254] David A Snowdon, Susan J Kemper, James A Mortimer, Lydia H Greiner, David R Wekstein, and William R Markesbery. Linguistic ability in early life and cognitive function and alzheimer's disease in late life: Findings from the nun study. *Jama*, 275(7):528–532, 1996.

[255] Albert Solé-Ribalta, Manlio De Domenico, Sergio Gómez, and Alex Arenas. Random walk centrality in interconnected multilayer networks. *Physica D: Nonlinear Phenomena*, 323:73–79, 2016.

[256] Albert Solé-Ribalta, Sergio Gómez, and Alex Arenas. Decongestion of urban areas with hotspot pricing. *Networks and Spatial Economics*, 18(1):33–50, 2018.

[257] Chaoming Song, Tal Koren, Pu Wang, and Albert-László Barabási. Modelling the scaling properties of human mobility. *Nature physics*, 6(10):818–823, 2010.

[258] Shawn F Sorrells, Mercedes F Paredes, Arantxa Cebrian-Silla, Kadellyn Sandoval, Dashi Qi, Kevin W Kelley, David James, Simone Mayer, Julia Chang, Kurtis I Auguste, et al. Human hippocampal neurogenesis drops sharply in children to undetectable levels in adults. *Nature*, 555(7696):377–381, 2018.

[259] Olaf Sporns. *Networks of the Brain*. MIT press, 2010.

[260] Olaf Sporns and Richard F Betzel. Modular brain networks. *Annual review of psychology*, 67:613–640, 2016.

[261] Olaf Sporns, Dante R Chialvo, Marcus Kaiser, and Claus C Hilgetag. Organization, development and function of complex brain networks. *Trends in cognitive sciences*, 8(9):418–425, 2004.

[262] Olaf Sporns, Dante R. Chialvo, Marcus Kaiser, and Claus C. Hilgetag. Organization, development and function of complex brain networks. *Trends Cogn. Sci.*, 8(9):418–425, 2004.

[263] Olaf Sporns, Giulio Tononi, and Rolf Kötter. The human connectome: a structural description of the human brain. *PLoS computational biology*, 1(4):e42, 2005.

[264] Larry Squire, Darwin Berg, Floyd E Bloom, Sascha Du Lac, Anirvan Ghosh, and Nicholas C Spitzer. *Fundamental neuroscience*. Academic press, 2012.

[265] Massimo Stella and Yoed N Kenett. Viability in multiplex lexical networks and machine learning characterizes human creativity. *Big Data and Cognitive Computing*, 3(3):45, 2019.

[266] Mark Steyvers and Joshua B Tenenbaum. The large-scale structure of semantic networks: Statistical analyses and a model of semantic growth. *Cognitive science*, 29(1):41–78, 2005.

[267] Steven H Strogatz. *Nonlinear dynamics and chaos with student solutions manual: With applications to physics, biology, chemistry, and engineering*. CRC press, 2018.

[268] Housheng Su, Dan Chen, Gui-Jun Pan, and Zhigang Zeng. Identification of network topology variations based on spectral entropy. *IEEE Transactions on Cybernetics*, pages 1–11, 2021.

[269] Richard Suzman, John R Beard, Ties Boerma, and Somnath Chatterji. Health in an ageing world—what do we know? *The Lancet*, 385(9967):484–486, 2015.

[270] Greta Szatloczki, Ildiko Hoffmann, Veronika Vincze, Janos Kalman, and Magdolna Pakaski. Speaking in alzheimer's disease, is that an early sign? importance of changes in language abilities in alzheimer's disease. *Frontiers in aging neuroscience*, 7:195, 2015.

[271] Nassim Nicholas Taleb. *Antifragile: Things that gain from disorder*, volume 3. Random House Incorporated, 2012.

[272] Nassim Nicholas Taleb and Raphael Douady. Mathematical definition, mapping, and detection of (anti) fragility. *Quantitative Finance*, 13(11):1677–1689, 2013.

[273] Vanessa Taler and Natalie A Phillips. Language performance in alzheimer's disease and mild cognitive impairment: a comparative review. *Journal of clinical and experimental neuropsychology*, 30(5):501–556, 2008.

[274] Ziqi Tang, Kangway V Chuang, Charles DeCarli, Lee-Way Jin, Laurel Beckett, Michael J Keiser, and Brittany N Dugger. Interpretable classification of alzheimer's disease pathologies with a convolutional neural network pipeline. *Nature communications*, 10(1):1–14, 2019.

[275] Qawi K Telesford, Sean L Simpson, Jonathan H Burdette, Satoru Hayasaka, and Paul J Laurienti. The brain as a complex system:

using network science as a tool for understanding the brain. *Brain connectivity*, 1(4):295–308, 2011.

[276] Atsushi Tero, Seiji Takagi, Tetsu Saigusa, Kentaro Ito, Dan P Bebber, Mark D Fricker, Kenji Yumiki, Ryo Kobayashi, and Toshiyuki Nakagaki. Rules for biologically inspired adaptive network design. *Science*, 327(5964):439–442, 2010.

[277] Giulio Tononi and Gerald M Edelman. Consciousness and complexity. *science*, 282(5395):1846–1851, 1998.

[278] Thomas Trappenberg. *Fundamentals of computational neuroscience*. OUP Oxford, 2009.

[279] Alexander I Tröster, David P Salmon, Donna McCullough, and Nelson Butters. A comparison of the category fluency deficits associated with alzheimer's and huntington's disease. *Brain and Language*, 37(3):500–513, 1989.

[280] Angela K Troyer, Morris Moscovitch, and Gordon Winocur. Clustering and switching as two components of verbal fluency: evidence from younger and older healthy adults. *neuropsychology*, 11(1):138, 1997.

[281] Peter Turchin. *Quantitative analysis of movement: measuring and modeling population redistribution in animals and plants*. Sinauer Associates, 1998.

[282] Nathalie Tzourio-Mazoyer, Brigitte Landeau, Dimitri Papathanassiou, Fabrice Crivello, Olivier Etard, Nicolas Delcroix, Bernard Mazoyer, and Marc Joliot. Automated anatomical labeling of activations in spm using a macroscopic anatomical parcellation of the mni mri single-subject brain. *Neuroimage*, 15(1):273–289, 2002.

[283] Martijn P. van den Heuvel and Hilleke E. Hulshoff Pol. Exploring the brain network: A review on resting-state fMRI functional connectivity. *European Neuropsychopharmacology*, 20(8):519–534, August 2010.

[284] Martijn P. van den Heuvel and Olaf Sporns. Network hubs in the human brain. *Trends in Cognitive Sciences*, 17(12):683–696, December 2013.

[285] Michiel van Elk, Hein T van Schie, Rolf A Zwaan, and Harold Bekkering. The functional role of motor activation in language processing: Motor cortical oscillations support lexical-semantic retrieval. *Neuroimage*, 50(2):665–677, 2010.

[286] David C Van Essen, Stephen M Smith, Deanna M Barch, Timothy EJ Behrens, Essa Yacoub, Kamil Ugurbil, Wu-Minn HCP Consortium, et al. The wu-minn human connectome project: an overview. *Neuroimage*, 80:62–79, 2013.

[287] Hanneke van Ewijk, Dirk J Heslenfeld, Marcel P Zwiers, Jan K Buitelaar, and Jaap Oosterlaan. Diffusion tensor imaging in attention deficit/hyperactivity disorder: a systematic review and meta-analysis. *Neuroscience & Biobehavioral Reviews*, 36(4):1093–1106, 2012.

[288] Francisco J Varela. Resonant cell assemblies: a new approach to cognitive functions and neuronal synchrony. *Biological research*, 28:81–81, 1995.

[289] Petra E Vértes, Aaron F Alexander-Bloch, Nitin Gogtay, Jay N Giedd, Judith L Rapoport, and Edward T Bullmore. Simple models of human brain functional networks. *Proceedings of the National Academy of Sciences*, 109(15):5868–5873, 2012.

[290] Gandimohan M Viswanathan, Sergey V Buldyrev, Shlomo Havlin, MGE Da Luz, EP Raposo, and H Eugene Stanley. Optimizing the success of random searches. *nature*, 401(6756):911–914, 1999.

[291] Ludwig Von Bertalanffy. The meaning of general system theory. *General system theory: Foundations, development, applications*, pages 30–53, 1973.

[292] Mitchell M Waldrop. *Complexity: The emerging science at the edge of order and chaos*. Simon and Schuster, 1993.

[293] Mark Wardman. Public transport values of time. *Transport policy*, 11(4):363–377, 2004.

[294] Duncan J. Watts and Steven H. Strogatz. Collective dynamics of 'small-world' networks. *Nature*, 393(6684):440–442, June 1998.

[295] Duncan J Watts and Steven H Strogatz. Collective dynamics of 'small-world'networks. *nature*, 393(6684):440–442, 1998.

[296] Brady J Williamson, Manlio De Domenico, and Darren S Kadis. Multilayer connector hub mapping reveals key brain regions supporting expressive language. *Brain Connectivity*, 11(1):45–55, 2021.

[297] Marc Wortmann. Dementia: a global health priority-highlights from an adi and world health organization report. *Alzheimer's research & therapy*, 4(5):1–3, 2012.

[298] Stefan Wuchty. Scale-free behavior in protein domain networks. *Molecular biology and evolution*, 18(9):1694–1702, 2001.

[299] Hideaki Yamamoto, Satoshi Moriya, Katsuya Ide, Takeshi Hayakawa, Hisanao Akima, Shigeo Sato, Shigeru Kubota, Takashi Tanii, Michio Niwano, Sara Teller, Jordi Soriano, and Ayumi Hirano-Iwata. Impact

of modular organization on dynamical richness in cortical networks. *Science Advances*, 4(11):eaau4914, November 2018.

[300] Zhijun Yao, Yuanchao Zhang, Lei Lin, Yuan Zhou, Cunlu Xu, and Tianzi Jiang. Abnormal cortical networks in mild cognitive impairment and alzheimer's disease. *PLoS Comput. Biol.*, 6(11), 2010.

[301] Vasoontara Sbirakos Yiengprugsawan and Colette Joy Browning. Non-communicable diseases and cognitive impairment: Pathways and shared behavioral risk factors among older chinese. *Frontiers in public health*, 7:296, 2019.

[302] Yoshinari Yonehara, Yusuke Goto, Ken Yoda, Yutaka Watanuki, Lindsay C Young, Henri Weimerskirch, Charles-André Bost, and Katsufumi Sato. Flight paths of seabirds soaring over the ocean surface enable measurement of fine-scale wind speed and direction. *Proceedings of the National Academy of Sciences*, 113(32):9039–9044, 2016.

[303] Vasily Zaburdaev, S Denisov, and J Klafter. Lévy walks. *Reviews of Modern Physics*, 87(2):483, 2015.

[304] Wayne W Zachary. An information flow model for conflict and fission in small groups. *Journal of anthropological research*, 33(4):452–473, 1977.

[305] Andrew Zalesky, Alex Fornito, and Edward T Bullmore. Network-based statistic: identifying differences in brain networks. *Neuroimage*, 53(4):1197–1207, 2010.

[306] Jeffrey C Zemla and Joseph L Austerweil. Estimating semantic networks of groups and individuals from fluency data. *Computational brain & behavior*, 1(1):36–58, 2018.

[307] Jeffrey C Zemla, Yoed N Kenett, Kwang-Sung Jun, and Joseph L Austerweil. U-invite: Estimating individual semantic networks from fluency data. In *CogSci*, 2016.

[308] Muhua Zheng, Antoine Allard, Patric Hagmann, Yasser Alemán-Gómez, and M Ángeles Serrano. Geometric renormalization unravels self-similarity of the multiscale human connectome. *Proceedings of the National Academy of Sciences*, 117(33):20244–20253, 2020.

[309] Shanjiang Zhu and David Levinson. Do people use the shortest path? an empirical test of wardrop's first principle. *PloS one*, 10(8):e0134322, 2015.

Appendix A

The latent geometry of mind's plausible semantic space

This appendix is an extension of chapter 2. Part of this appendix has been published as supplementary materials [49] of the corresponding paper [50]. Here we report:

- a statistical analysis on neuropsychological tests used to assess the diagnosis of patients with dementia, in subsec. A.1.1;
- the detailed results of Kolmogorov-Smirnov statistical tests and t-tests for the local metrics, (i.e DOE, ρ_w, Max_J, d, far) for the three geometries Itwac, Twitter and Wikipedia, in subsec. A.1.2. These tests are performed to assess significant differences in the navigation of concepts of Alzheimer's disease (DEM) patients, Mild Cognitive Impairment (MCI) patients and healthy controls (CTR). Similarly, we assess the differences in such a navigation at the mesoscale (hierarchy), in subsec. A.1.3 and at the network scale (steady state distribution and mean first passage time matrices), in subsec. A.1.4;
- a discussion on the choice of teleportation parameter in the PageRank algorithm, when adding a dumping effect in the transition probability matrix, in sec. A.2.

A.1 Extended Results

This section is devoted to the detailed results of statistical tests i) on the neuropshycological assessment and ii) on the metrics used to investigate the navigation of concepts in the human mind.

A.1.1 Statistical analysis on neuropsychological tests

The goal of this statistical analysis is to investigate the differences between different stages of dementia and to assess how dementia evolves over time. To this aims we have submitted 18 different neuropsychological tests to our sample of 185 patients at different stages of dementia, for more than one year, and we have investigated such differences by means of statistical hypothesis tests.

All the patients under study were assessed in the Azienda Provinciale per i Servizi Sanitari (APSS) of Trento, Italy. Our analysis is based on the results of 18 neuropsychological tests performed by 185 patients. Among them 92 patients suffer of dementia (DEM), which includes vascular dementia, frontotemporal dementia, degenerative dementia and Alzheimer's disease (M=40%, F=60%, age=75±7, education=9±4) and 93 patients suffering of Mild Cognitive Impairment (MCI) — a precursor of Alzheimer's disease — (M=48%, F=52%, age=77±6, education=9±4).

The neuropsychological assessment covers the following 18 tests: a global assessment (Mini Mental State exam indicated as MMSE), denomination test (naming test), Verbal Fluency (semantic, categories of cars, animals and fruits, and phonemic, letters F, A, S), memory (Digit Span backwards and forwards, Corsi block-tapping test, story recall test, Modified Figure of Rey/recognition, Modified Figure of Taylor/recognition), frontal test (Frontal Assessment Battery indicated as FAB), attention (attentive matrices test), visuo-spatial working memory (Clock Drawing Test), praxis

assessment tasks (construction of Figure of Rey/recall and construction of Figure of Taylor/recall), depression (Cornell Test), autonomies assessment (Activities of daily living indicated as ADL, Instrumental activities of daily living indicated as IADL) for a total of 18 tests, each one having a cut-off threshold. A test is passed if the score is greater than or equal to the cut-off threshold, except for the depression test, where the score must be less than the cutoff for the test to be passed, and the Mini Mental State exam, where the score must be strictly greater than the cutoff for the test to be passed. For each test, we have adjusted the raw scores according to age and schooling, obtaining the corrected scores. All the analyses have been carried out according to the corrected scores. Patients are examined every six months, after the first visit they attend follow up visits and, according to the disease severity, they can be classified as MCI or DEM. The diagnosis is established after the first visit. It is to be noticed that, each patient performed a total of 16 tests during each visit, in fact the tests Modified Figure of Rey and Modified Figure of Taylor are administered alternately, as well as for the tests construction of Figure of Rey and construction of Figure of Taylor. For the sake of simplicity, we will refer to these tests interchangeably. In fig. A.1 we reports an illustrative example of some test score trends of those patients which performed PV, FU1 and FU2. The trends show how test scores change passing from the first visit (PV) to the first follow up (FU1) after six months and to the second follow (FU2), after another six months. Specifically, we depict a general overview of the neuropsychological test scores distributions over time for the two diagnoses, i.e. MCI (in orange) and DEM (in blue). For each test, a dotted line connects the average score of each diagnosis in each visit, readable on the x-axis. These plots show that apparently there is no constant trend in the performances of the neuropsychological tests, but rather that such test performances can improve, remain the same or worsen both within a spe-

cific diagnosis over time (intra-diagnosis) and between different diagnoses in the same visit (inter-diagnosis).

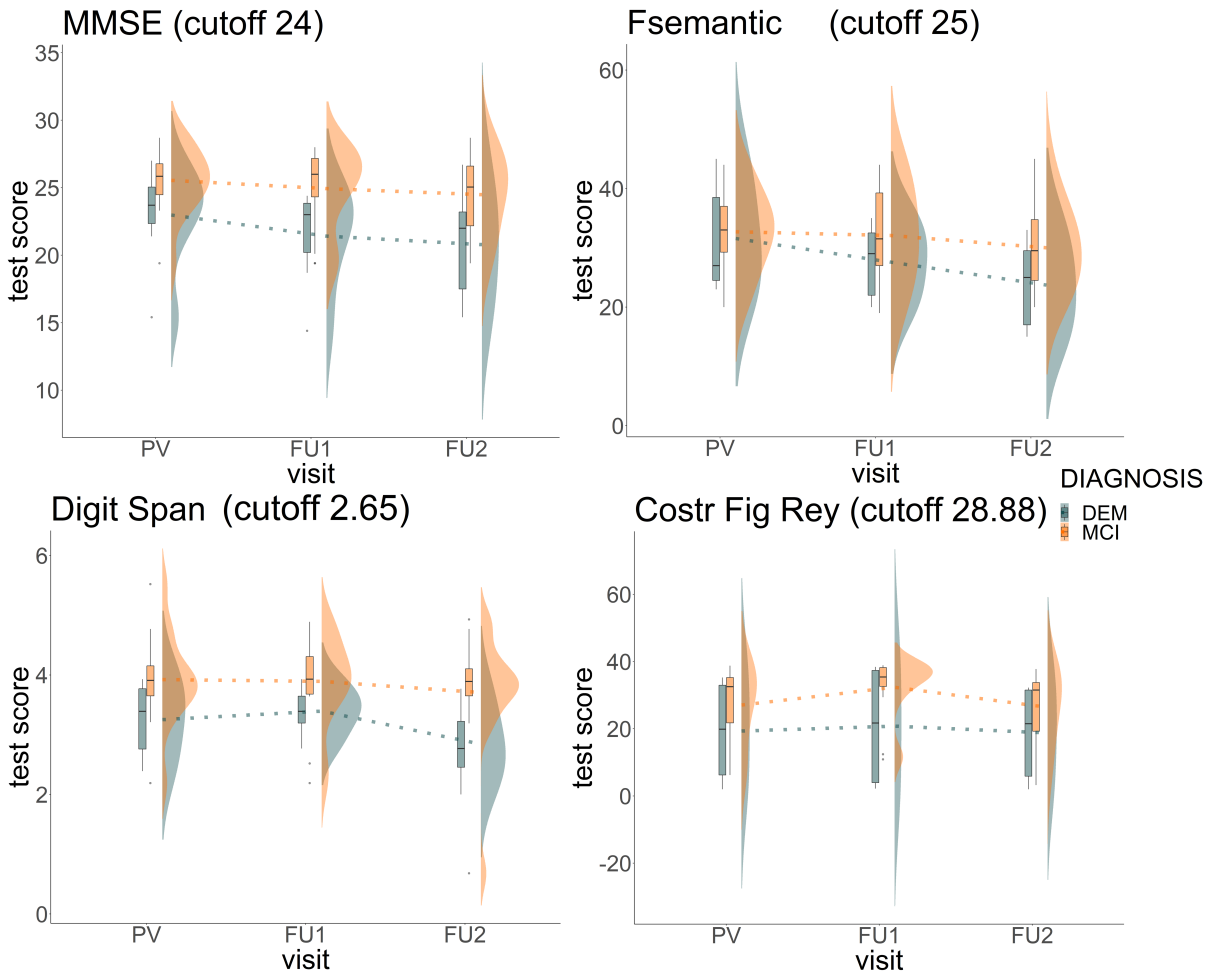

Figure A.1: *Neuropsychological tests scores.* Neuropsychological test score distributions over time for the two diagnoses, i.e. MCI (in orange) and DEM (in blue). For each test, a dotted line connects the average score of each diagnosis in each visit, readable on the x-axis.

Statistical analysis aims to investigate whether there exist significant differences intra-diagnosis and inter-diagnosis, in terms of neuropsychological test scores. The former are the differences in time among patients classified with the same label (e.g. DEM_t , DEM_{t+1}) the latter are the differences among patients classified with different label in the same visit (i.e. MCI_t, DEM_t). To this purpose, we performed statistical hypothesis

Test	$PV - FU1$	$PV - FU2$	$FU1 - FU2$
MMSE	0.903535	0.070312	0.592604
Naming	0.183020	0.577032	0.335561
Semantic	0.050302	0.035555	0.052136
Phonemic	0.917272	0.846521	0.139351
Digit span forward	0.004412	0.130517	0.559837
Digit span backward	0.471220	0.679558	0.384670
Corsi span	0.527144	0.115460	0.057117
Babcock story recall	0.306057	0.070637	0.097838
Rey figure	0.246474	0.279396	0.010120
FAB	0.331737	0.873100	0.935614
Attentional matrices	0.150622	0.504576	0.434077
Clock Drawing Test	0.057730	0.577032	0.164823
Copy of Rey figure	0.000823	0.359292	0.003762
Depression	0.068957	0.532275	0.869225
ADL	1.000000	0.448561	Nan
IADL	0.213373	0.233156	1.000000
All	0.190367	0.68548	0.525223

Table A.1: Intra-diagnosis tests, MCI patients. P-values of paired t-tests on neuropsychological tests, performed by MCI patients during PV, FU1, FU2. Null hypothesis: the difference in group means is zero. "All" indicates all tests, in this case we evaluate if the total number of passed tests is significantly different between two visits.

tests on the mean score of each neuropsychological test and on the averages of the total number of passed tests, with a 95% confidence interval. In particular, we implemented the unpaired two-tiled t-test to evaluate the inter-diagnosis differences, and the paired two-tiled t-test for the intra-diagnosis differences. Given the results of the variance test, we performed the Welch's t-test, for the group of patients in FU2. In this way, we were able to establish the most significant (discriminatory) neuropsychological tests in highlighting differences among the two groups, i.e. MCI and DEM, as well as in defining how a diagnosis evolves over time. Results of statistical tests are shown in tables A.1 to A.3.

Results of statistical hypothesis tests can be summarized as follow.

For what concern MCI patients, the hypothesis tests on intra-diagnosis differences, i.e. paired t-test, show that not all neuropsychological tests are statistically significant in highlighting the differences between MCI at time t and MCI at time t+1, and MCI at time t and MCI at t+2 (table A.1). The most significant tests between the first visit (PV) and the first follow up (FU1) are the ones related to verbal memory (Forward Digit Span) and executive functions (Construction of Rey figure/recall). Surprisingly, these tests improve passing from PV to FU1. The more significant tests between PV and the second follow up (FU2) are the ones related to language (semantic verbal fluency) whose performances worsen with time. Finally, the more significant tests between FU1 and FU2 are the ones related to spatial memory (Rey figure copy/recognition) whose performance improve with time, and the executive functions (Construction of Rey figure/recall) that worsen passing from FU1 to FU2. Analyzing the differences in the average number of passed tests per visit ("All") it turns out that there are no significant differences between one visit and the next.

As for MCI, for DEM patients the hypothesis tests on intra-diagnosis differences, i.e. paired t-test, show that not all neuropsychological tests are statistically significant to highlight the differences between DEM at time t and DEM at time t+1 and DEM at time t and DEM t+2 (table A.2). The most significant tests between PV and FU1 are the ones related to depression and to autonomies, that both decrease over time, resulting in less depressed but less autonomous patients. Passing from PV to FU2 the more significant tests are the ones related to the global assessment (Mini Mental State exam) and to the language (semantic verbal fluency) for both these tests the performances worsen with time. Finally, the more significant tests between FU1 and FU2 are the ones related to the language (semantic verbal fluency) and to the verbal memory (Backward Digit span), again

Test	$PV - FU1$	$PV - FU2$	$FU1 - FU2$
MMSE	0.115357	0.040428	0.670454
Naming	0.205428	0.586299	NaN
Semantic	0.051490	0.012920	0.010684
Phonemic	0.266785	0.435989	0.507418
Digit span forward	0.408460	0.321088	0.706007
Digit span backward	0.379451	0.065282	0.030461
Corsi span	0.168755	0.453427	0.738752
Babcock story recall	0.265088	0.309186	0.950721
Rey figure	0.436871	0.178882	0.502585
FAB	0.513170	0.835258	0.587640
Attentional matrices	0.383022	0.303794	0.359100
Clock Drawing Test	0.095992	0.338801	NaN
Copy of Rey figure	0.310744	0.463681	0.425214
Depression	0.011754	0.225519	0.924900
ADL	0.301079	0.214639	0.174688
IADL	0.009465	0.073507	NaN
All	0.743982	0.454906	0.058201

Table A.2: Intra-diagnosis tests, DEM patients. P-values of paired t-tests on neuropsychological tests, performed by DEM patients during PV, FU1, FU2. Null hypothesis: the difference in group means is zero. "All" indicates all tests, in this case we evaluate if the total number of passed tests is significantly different between two visits.

Test	PV	$FU1$	$FU2$
MMSE	0.000008	0.000398	0.002017
Naming	0.000462	0.019643	0.138464
Semantic	0.002491	0.113263	0.001238
Phonemic	0.115943	0.298696	0.399993
Digit span forward	0.684604	0.016343	0.333250
Digit span backward	0.025307	0.120918	0.001079
Corsi span	0.060874	0.042920	0.070041
Babcock story recall	0.586418	0.441269	0.110941
Rey figure	0.618668	0.340872	0.195626
FAB	0.000301	0.029037	0.002354
Attentional matrices	0.000440	0.044948	0.026988
Clock Drawing Test	0.007502	0.010250	0.002356
Copy of Rey figure	0.048849	0.001110	0.321386
Depression	0.075975	0.466255	0.193832
ADL	0.079525	0.017737	0.041824
IADL	0.00392	0.015806	0.148684
All	1.5e-05	0.000153	0.000816

Table A.3: Inter-diagnosis tests, MCI-DEM patients. P-values of unpaired t-tests on neuropsychological tests, performed by MCI and DEM patients during PV, FU1, FU2. Null hypothesis: the difference in group means is zero. "All" indicated all tests, in this case we evaluate if the total number of passed test is significantly different between two diagnoses.

the performances worsen with time. As well as for MCI, for DEM patients there are no significant differences in the average number of passed tests per visit ("All").

For what concerns differences between MCI and DEM, the hypothesis tests on inter-diagnosis differences, i.e. unpaired t-test, show that not all neuropsychological tests are statistically significant to highlight the differences between DEM and MCI (table A.3) in each visit. The most significant tests during PV are: the global assessment (Mini Mental State exam), the language (denomination and semantic verbal fluency) the verbal memory

(Backward Digit span), the frontal assessment battery, the selective attention (attentive matrices), the clock, executive functions (Construction of Rey figure/recall) and the autonomies. For all these neuropsychological tests, DEM patients' performances are, on average, lower than those of MCI patients. The more significant tests during FU1 are: the global assessment (Mini Mental State exam), the language (denomination), the verbal memory (Forward Digit span), the spatial memory (Corsi test), the frontal assessment battery the selective attention (attentive matrices), the clock, the executive functions (Construction of Rey figure/recall) and the autonomies. As for PV, also in this case DEM patients' performances are, on average, lower than those of MCI patients. Finally, during FU2 the more significant tests in assessing the differences between MCI and DEM are: the global assessment (Mini Mental State exam) the language (semantic verbal fluency) the verbal memory (Backward Digit span), the frontal assessment battery, the selective attention (attentive matrices), the clock and the autonomies. Again, DEM patients perform worse, on average, with respect to MCI patients. Analyzing the differences in the average number of passed tests per visit between the two diagnosis, it turns out that DEM patients pass significantly less tests (in total) than MCI patients ("All") in each considered visit.

A.1.2 Geometry

Tables A.4 and A.5 show respectively the results of Kolmogorov-Smirnov statistical tests and t-tests on the five local metrics related to the exploration of concepts and computed using the cosine distance, for each pair of groups, for the three geometries.

		Itwac		Twitter		Wikipiedia	
Metrics	Pairs	Test statistic	P-val adj	Test statistic	P-val adj	Test statistic	P-val adj
DOE	DEM-MCI	0.198	0.05	0.177	1.10e-01	0.220	2.31e-02
	DEM-CTR	0.601	4.68e-07	0.510	4.62e-05	0.684	3.83e-09
	MCI-CTR	0.559	2.77e-06	0.418	1.43e-03	0.629	6.40e-08
ρ_w	DEM-MCI	0.186	8.20e-02	0.254	5.21e-03	0.219	2.33e-02
	DEM-CTR	0.657	1.95e-08	0.609	3.14e-07	0.791	2.98e-12
	MCI-CTR	0.647	2.22e-08	0.501	4.52e-05	0.720	2.38e-10
Max_J	DEM-MCI	0.110	0.63	0.067	0.99	0.197	5.56e-02
	DEM-CTR	0.323	0.05	0.343	0.03	0.510	4.62e-05
	MCI-CTR	0.303	0.06	0.328	0.03	0.355	1.32e-02
d	DEM-MCI	0.242	9.05e-03	0.222	2.09e-02	0.295	6.43e-04
	DEM-CTR	0.793	1.70e-12	0.760	2.65e-11	0.837	1.03e-13
	MCI-CTR	0.748	1.49e-12	0.686	1.42e-10	0.773	1.03e-13
far	DEM-MCI	0.110	0.63	0.099	0.76	0.187	7.97e-02
	DEM-CTR	0.379	6.00e-03	0.313	0.0712	0.498	5.40e-05
	MCI-CTR	0.385	4.70e-03	0.298	0.07	0.500	3.00e-05

Table A.4: Results of Kolmogorov-Smirnov statistical tests for the three semantic spaces, p-values are adjusted according to Holm–Bonferroni method.

A.1.3 Hierarchy

Figure A.2 reports boxplots within violin plots of the explorative potential distributions, both in terms of visited clusters and in terms of words contained in the visited clusters, for the three categories of subjects in the three geometries. Results of Kolmogorov-Smirnov statistical tests and t-tests for these indicators, for each pair of groups, are shown in tables A.6 and A.7 respectively.

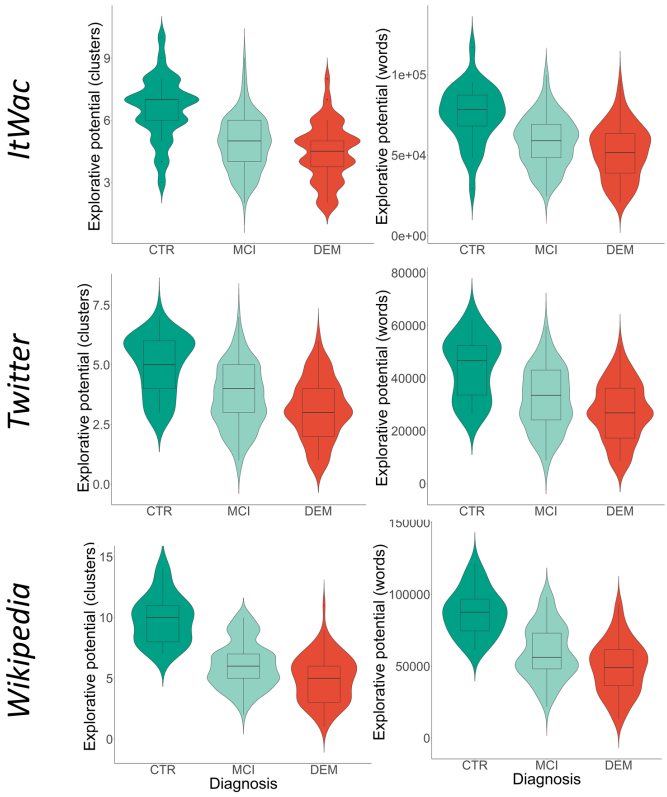

Figure A.2: *Explorative potential.* Boxplots within violin plots of the explorative potential distributions, expressed both in terms of visited clusters and of words contained in the visited clusters for the three categories of subjects in the three semantic spaces.

		Itwac				Twitter				Wikipiedia			
Metrics	Pairs	Test statistic	df	P-val adj	Effect size	Test statistic	df	P-val adj	Effect size	Test statistic	df	P-val adj	Effect size
DOE	DEM-MCI	-1.631	158.6	1.04e-01	0.240	-1.795	170.3	7.44e-02	0.264	-2.930	161.5	3.87e-03	0.432
	DEM-CTR	-6.360	75.7	4.15e-08	1.088	-6.576	115.9	4.34e-09	0.933	-9.786	119.9	1.67e-16	1.320
	MCI-CTR	-5.822	49.9	8.31e-07	1.210	-5.588	97.3	4.20e-07	0.861	-8.648	106.5	1.18e-13	1.282
ρ_w	DEM-MCI	-2.213	173.5	2.81e-02	0.326	-2.517	181.4	1.27e-02	0.370	-2.390	182.4	1.79e-02	0.351
	DEM-CTR	-8.967	71.0	8.06e-13	1.575	-9.790	95.3	1.35e-15	1.528	-13.584	59.0	2.42e-19	2.592
	MCI-CTR	-7.780	55.7	3.69e-10	1.523	-7.619	87.6	5.69e-11	1.224	-11.344	63.2	1.38e-16	2.086
Max_J	DEM-MCI	-1.030	172.7	0.30	0.152	-0.996	174.7	0.32	0.147	-2.828	173.3	5.24e-03	0.416
	DEM-CTR	-4.044	63.191	4e-04	0.747	-3.518	78.9	2.2e-03	0.592	-6.585	90.7	8.70e-09	1.048
	MCI-CTR	-3.515	49.9	1.9e-03	0.731	-2.898	62.4	1.04e-02	0.536	-4.452	70.4	6.24e-05	0.781
d	DEM-MCI	-2.845	182.5	4.95e-03	0.418	-2.701	182.2	7.56e-03	0.397	-3.078	182.0	2.40e-03	0.453
	DEM-CTR	-11.520	44.5	1.79e-14	2.587	-10.584	46.6	1.66e-13	2.306	-11.865	44.8	6.05e-15	2.654
	MCI-CTR	-9.850	43.1	2.69e-12	2.260	-8.953	44.5	3.24e-11	2.004	-10.087	42.8	1.39e-12	2.324
far	DEM-MCI	-0.464	163.4	0.64	0.068	-0.725	171.7	0.4696	0.107	-1.932	165.6	5.50e-02	0.285
	DEM-CTR	-3.473	109.9	1.5e-03	0.509	-2.328	118.8	6.49e-02	0.323	-6.509	87.9	1.35e-08	1.049
	MCI-CTR	-3.666	79.9	1.3e-03	0.611	-1.839	106.0	0.14	0.273	-5.544	61.4	1.32e-06	1.033

Table A.5: Results of t-tests for the three semantic spaces, df stands for degrees of freedom, p-values are adjusted according to Holm–Bonferroni method, the effect size is the value of Cohen's d.

		Itwac		Twitter		Wikipiedia	
Metrics	Pairs	Test statistic	P-val adj	Test statistic	P-val adj	Test statistic	P-val adj
clusters	DEM-MCI	0.116	0.56	0.147	0.27	0.207	3.77e-02
	DEM-CTR	0.560	4.09e-06	0.514	3.7e-05	0.824	2.75e-13
	MCI-CTR	0.444	5.21e-04	0.402	2.6e-03	0.696	1.17e-09
words	DEM-MCI	0.169	0.14	0.193	6.44e-02	0.242	9e-03
	DEM-CTR	0.537	1e-05	0.525	2.34e-05	0.770	1.39e-11
	MCI-CTR	0.420	1.3e-03	0.425	1.12e-03	0.581	9.11e-07

Table A.6: Results of Kolmogorov-Smirnov statistical tests for the three semantic space, p-values are adjusted according to Holm–Bonferroni method.

A.1.4 Network

Tables A.8 to A.10 report the correlation values between the steady state distribution ($\vec{\pi}$) of the three groups (DEM, MCI, CTR) in the three geometries (Itwac, Twitter, Wikipedia). Correlation values of mean first passage time matrices (MFPT) are reported in tables A.11 to A.13. Finally, Frobenius norms of mean first passage time matrices of the three groups, in the three geometries, are shown in table A.14.

		Itwac				Twitter				Wikipiedia			
Metrics	Pairs	Test statistic	df	P-val adj	Effect size	Test statistic	df	P-val adj	Effect size	Test statistic	df	P-val adj	Effect size
clusters	DEM-MCI	-2.255	182.2	2.53e-02	0.332	-2.590	182.8	1.03e-02	0.381	-4.023	182.9	8.40e-05	0.592
	DEM-CTR	-6.489	48.1	1.32e-07	1.385	-7.249	50.6	6.88e-09	1.501	-11.845	48.6	1.85e-15	2.513
	MCI-CTR	-5.057	45.8	1.46e-05	1.110	-5.307	52.3	4.61e-06	1.074	-9.098	48.2	9.81e-12	1.933
words	DEM-MCI	-2.551	182.1	1.15e-02	0.375	-2.602	182.4	1.00e-02	0.382	-3.801	182.9	1.96e-04	0.559
	DEM-CTR	-5.648	50.3	2.25e-06	1.174	-6.923	47.1	3.17e-08	1.498	-10.923	56.6	4.40e-15	2.128
	MCI-CTR	-3.943	47.7	5.24e-04	0.843	-5.041	49.7	1.31e-05	1.051	-7.946	56.7	1.74e-10	1.540

Table A.7: Results of t-tests for the three semantic spaces, df stands for degrees of freedom, p-values are adjusted according to Holm–Bonferroni method, the effect size is the value of Cohen's d.

	$DEM - MCI$	$DEM - CTR$	$MCI - CTR$
Pearson	0.99	0.94	0.95
Spearman	0.88	0.70	0.71
covariance	0.01	0.0086	0.0089
norm	0.04	0.13	0.12

Table A.8: Correlation values between the steady state distributions in *Itwac* semantic space.

	$DEM - MCI$	$DEM - CTR$	$MCI - CTR$
Pearson	0.97	0.96	0.99
Spearman	0.84	0.57	0.57
covariance	0.02	0.01	0.01
norm	0.13	0.14	0.05

Table A.9: Correlation values between the steady state distributions in *Twitter* semantic space.

	$DEM - MCI$	$DEM - CTR$	$MCI - CTR$
Pearson	0.93	0.85	0.86
Spearman	0.64	0.68	0.81
covariance	0.002	0.002	0.002
norm	0.09	0.16	0.15

Table A.10: Correlation values between the steady state distributions in *Wikipedia* semantic space.

	$DEM - MCI$	$DEM - CTR$	$MCI - CTR$
Pearson	0.99	0.89	0.91
Spearman	0.99	0.94	0.94
covariance	371.78	342.85	455.55
norm	59.92	111.06	89.34

Table A.11: Correlation values between the mean first passage time matrices in *Itwac* semantic space.

	$DEM - MCI$	$DEM - CTR$	$MCI - CTR$
$Pearson$	0.98	0.92	0.88
$Spearman$	0.97	0.90	0.82
$covariance$	156.96	192.56	193.67
$norm$	18.45	61.00	63.00

Table A.12: Correlation values between the mean first passage time matrices in *Twitter* semantic space.

	$DEM - MCI$	$DEM - CTR$	$MCI - CTR$
$Pearson$	0.90	0.63	0.63
$Spearman$	0.91	0.77	0.80
$covariance$	2005.85	1639.81	1213.20
$norm$	643.41	921.02	788.58

Table A.13: Correlation values between the mean first passage time matrices in *Wikipedia* semantic space.

	CTR	MCI	DEM
$itWac$	1480.51	635.05	389.04
$Twitter$	1085.24	583.08	280.27
$Wikipedia$	3372.137	2054.467	3066.652

Table A.14: Frobenius norm of mean first passage time matrices of the three groups and for the three geometries.

A.2 Choice of teleportation parameter in the PageRank algorithm

In 2007, Griffiths, Steyvers and Firl, in their paper "Google and the Mind - Predicting Fluency With PageRank" [135] demonstrated how Page Rank algorithm can predict human response in a fluency task. The parallelism between the google search engine – and more in general the World Wide Web – and human mind lies in the ability to retrieve information which is relevant to a particular query. Specifically, information (e.g. concepts) within human mind are retrieved, and thus connected, according to an "order" which is strikingly similar to the way web pages are connected. Thanks to this pair-wise association of concepts in human mind, it is possible to build semantic networks, which have proven to have special properties similar to those of the World Wide Web, such as the "scale-free" degree distribution (Steyvers & Tenenbaum, 2005 [266]). In their work of 2007, Griffiths, Steyvers and Firl [135], with a sort of mimic of the google search engine, aimed to discover which words is most likely to be produced in a fluency task. By comparing Page Rank and other standard predictors computed on a semantic network, they found out that PageRank outperforms other metrics in predicting the words that people produce during a verbal fluency task. For this reason, they claim that PageRank of a word could be use in the design of, or in the model of, memory experiments. Concomitantly, taking inspiration from the process of clustering and switching when retrieving concepts from memory, network scientists provided a new kind of random walk over a graph as a Markov process – i.e. the switcher random walk – (Goñi et al., 2010) [131] to generalize the exploration task on a network.

In this vein and by following the assumption of a semantic network navigated by a random walk (Abbott, Austerweil& Griffiths, 2015 [5]), we

probed the navigation of concepts in terms of its Markov chain representation. The rationale behind this representation is given by a parallelism between a random walker walking on a spatial network and a random memory retriever retrieving concepts from a network of concepts, i.e. from a navigation of concepts on top of a network. As it often happens, here the terms "random walk" and "Markov chain" are used interchangeably.

For each diagnosis and for the healthy controls we have estimated a Markov chain, where each state is represented by a cluster of concepts, previously defined through a clustering algorithm. The Markov chain is represented by a directed graph encoding the semantic network where each state represents a cluster of words, and the probability to transit from one state to another is given by a transition matrix. Since we aim at characterizing the exploration of concepts (at this point, at the macroscale), we have to evaluate the dynamic of such an exploration on the Markov chain. To this aim we consider the steady state distribution and the mean first passage time matrix for each diagnosis. A unique steady-state probability distribution it is guaranteed for any ergodic Markov chain. In order to guarantee the ergodicity – satisfying the conditions of irreducibility and aperiodicity – we modify the transition matrix by adding a damping effect given by the Page Rank algorithm. In formulas, for each category (DEM, MCI, healthy controls) we compute:

$$\widehat{T} = \alpha\widehat{M} + (1-\alpha)\frac{1}{S} \tag{A.1}$$

Where $\widehat{T}$ represents the new (modified) transition matrix, $\widehat{M}$ is the transition matrix estimated according to the frequency of words pronounced by the subjects belonging to that specific category, α is the damping effect and S is the total number of states of the Markov chain. By adding the damping effect, we intend to model the navigation of concepts considering two main components governing the exploration dynamic: a) a word

frequency-based component $\widehat{M}$ and b) a random component, given by the random walk uniformly distributed component $(1-\alpha)\frac{1}{S}$. In this way, the second component acts as a sort of noise, introduced when modelling the exploration of concepts, to avoid possible overfitting of the model to our data. Relying on the parallelism between google search engine and memory retrieval tasks, among all possible values between 0 and 1, the damping factor is usually set at 0.85 (Brin and Page, 1998 [214], and Mihalcea, Tarau, Figa, 2004 [197] in the field of semantic networks), and this is also the value we arbitrary choose to modify the transition matrix, for each of the three categories.

Curiously, in 1995, three years before Page Rank paper was published by Brin and Page, two cognitive and linguistic scientist, Bradley Love and Steven Sloman [252], proposed an algorithm to measure the features centrality of a given node on a graph for human concepts (this is pointed out also by Griffiths, Steyvers and Firl, 2007 [135]). Practically, their algorithm was equivalent to the Page Rank. This last curiosity strengthens the close relationship between the information retrieval processes within human mind and the one of World Wide Web, pointing out that, not surprising, these two different fields of study have proposed equivalent strategies to meet the same purposes, independently.

Appendix B

From the brain to the globe: the changing world during COVID-19 pandemic

The period of my Ph.D. research has been signed by the COVID-19 pandemic. Leaving aside the challenging atmosphere generated by this unprecedented worldwide event, at that time I felt an urgent desire to give my contribution in advancing researches on this matter as a young complex scientist.

In this regards, together with my colleague Sebastian Raimondo and my supervisor Manlio De Domenico, we conducted a parallel work related to the nexus between environmental conditions and the human activity, during the lockdown in Northern Italy due to COVID-19 pandemic. This work is currently in press at *Complexity* journal [231].

Our study aimed at unraveling causal relationships among 16 environmental conditions and human activity variables, taking advantages from the unprecedented setup offered by draconian countermeasures adopted for the Italian lockdown.

Specifically, we capitalized on information theory, network science and Bayesian inference to map the backbone of the complex interplay between

meteorological and socio-economic variables. We have introduced a novel information-theoretic method based on statistical divergence to identify abrupt changes (tipping points) in the system dynamics, caused by a sudden intervention, such as the lockdown. Using this information on tipping point, we build a counterfactual prediction of what would have happen to the pollutant concentration without the intervention.

Our study enabled for testing sustainability policies. What we found out is that, despite a measurable decrease in NO2 concentration due to many human activities stop, locking down a region is insufficient to significantly reduce emissions. In this regard, we argued that policy strategies more effective than lockdowns must be considered for pollution control and climate change mitigation.